Alma Mater Studiorum – Università di Bologna

DOTTORATO DI RICERCA IN

Scienze ambientali: tutela e gestione delle risorse naturali

Ciclo XXVIII

Settore Concorsuale di afferenza: 03/A1 - CHIMICA ANALITICA

Settore Scientifico disciplinare: CHIM/01 - CHIMICA ANALITICA

TITOLO TESI

Analytical pyrolysis and microextraction methods to characterize oil and biochar from thermal and catalytic cracking of biomass

Presentata da: Roberto Conti

Coordinatore di dottorato

Prof. Enrico Dinelli

Tutor

Prof. Daniele Fabbri

Esame finale, anno 2016

Table of contents

Chapter 1

Introduction

1.1 Energy and Climate Change

Energy plays a fundamental role in the economic growth and the World's development being an integral part of almost all human activities: it provides services for heating, lighting, health, industrial production and transportation.

From 1973 to 2012 the World total energy supply has doubled (Fig.1.1.1) [1].

Although a slight decrease of oil supply, the primary energy use is still dominated by fossil fuels (oil, coal and natural gas) that cover more than 80% of total energy.

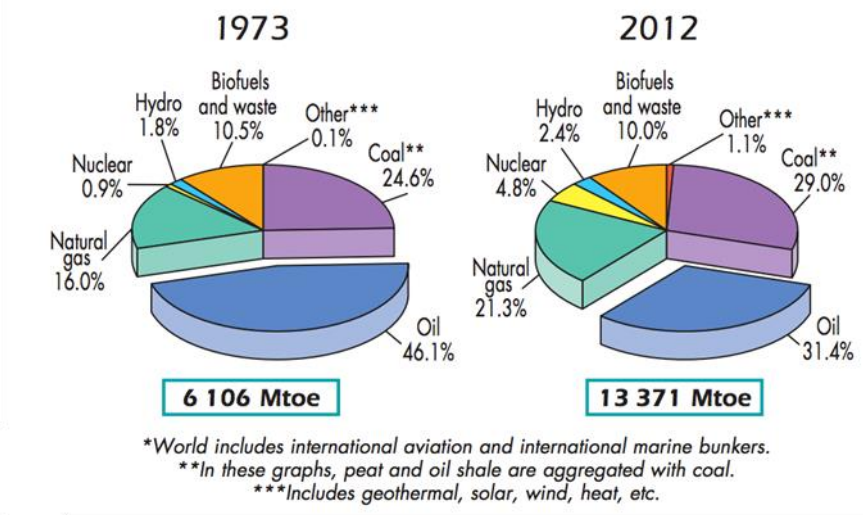

Figure 1.1.1: World total energy supply by fuel (Mtoe) from IEA World Energy Outlook 2014 [1]

Trends reported by IPCC [2] showed that most of the total anthropogenic GHG emissions are associated with energy supply and they rapidly grew from 2000 to 2010 reaching the highest level in human history with 49 $GtCO_2$-eq per year in 2010.

Energy supply sector is the largest contributor (35%) in global greenhouse gas (GHG) emissions.

Furthermore, when taking into account the distribution of total GHG emissions by economical sector it can be seen (Fig. 1.1.2) that direct GHG emissions are mainly dominated by contributions from Industry (21%), Agricolture, Forestry and Other Land Use (AFOLU) (24%), transport (14%) and buildings (6%).

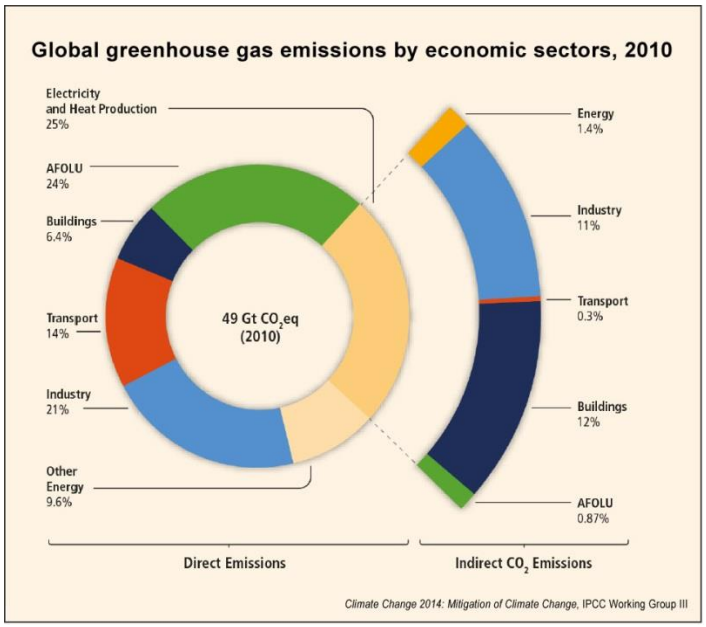

Figure 1.1.2: Global GHG emissions by economic sectors, from IPCC 2014 [2]

In addition, 25% of emissions are classified as indirect GHG emissions from electricity and heat production. Considering an assignment of electricity and heat production by economic sector, the total emissions from industry and buildings reached 31% and 19%, respectively.

According to the Kyoto Protocol (adopted on 1997 and extended to 2020) and lately to the 21st yearly session of the Conference of the Parties (COP21, 2015), developed Countries (which ratified the protocol) that are principally responsible of the current high GHG emissions levels, have to implement stategies in order to reduce GHG emissions levels (per capita by 9% by 2030) and keep the rise in global average temperature below 2°C.

Briefly, the Kyoto mechanisms can be summurized in:

- International Emission Trading
- Clean Development Mechanism (CDM)
- Joint Implementation (JI)

Actions in the energy sector can make efforts to achieve the World's agreed climate goal.

In energy supply sector switching from fossil fuels to low-carbon power (e.g.: solar power, wind power, bio-energy) is needed.

Furthemore, fossil fuels are still the main resource in transport sector. Thus, it becomes essential to develop alternatives and sustainables liquid fuels. In this respect, fuels from biomass can prove to be a winning strategy for the transportation market, being biomass the only potentially renewable source of organic carbon.

Biofuels derived from plant biomass generate significantly less greenhouse gas emissions than do fossil fuels and can even be greenhouse gas neutral if efficient methods for biofuels production are developed [3].
In addition, IEA prevision estimated the worldwide raw biomass energy potential in 2050 between 150 and 450 EJ/ year [4].

1.2 Biofuels

Biofuels represent an interesting alternative to the use of fossil fuels and oil for the production of power, heat and transportation fuels [5]. Biofuels can turn out a promising and environmental friendly option in order to keep the pledges submitted by the Countries to reduce the GHG emissions and the dependence of fossil fuels [6]
Biofuels can be distinguished into three different categories (called generations) depending on the biomass from which they are produced (Tab. 1.2.1).
The first-generation biofuel consists of (1) biodiesel from vegetable oils or animal fats which is made by chemically reacting lipids with methyl alcohol producing fatty acids methyl esters and (2) bioethanol from sugar or starch crops such as sugarcane, corn, wheat.
European Parliament issued Directive 98/70/EC relating to the quality of petrol and diesel fuels and Directive 2009/28/EC on the promotion of the use of energy from renewable sources with which promoted the use of first generation biofuels to ensure that the energy from renewable sources was at least 10% of the final consumption of energy in transport in 2020.
However, the main first-generation biofuels drawback is connected to the land use competition for food production [7]. Indeed, an intensive production of liquid biofuel needs great quantity of arable land shifting the land use away from food to agro-energy [8]
For this reason, European Commission recently issued Directive 2015/1513/EC amending the above-mentioned directives.
Briefly, Directive 2015/1513/EC promoted second-generation and third-generation biofuels
Second-generation biofuels produced from lignocellulosic residues and bio-wastes.
Plant biomass is one of the most abundant (but technologically ill-used) biological resources on the planet [9] and biomass energy accounts for almost 14% of World primary energy consumption [10]. Plant biomass can simply be burned to produce heat and electricity but it shows a great potential to produce technologically advanced liquid biofuels [9]. Thus, second-generation biofuels can be suitable to reduce CO_2 emissions avoiding food crops competition.
However, they are still under development regarding conversion technologies and process operation [11].

Second-generation biofuels are mainly produced through two different conversion routes: thermochemical and biochemical process. Thermochemical conversion that will be following debates in more detail consists of pyrolysis [12], gasification [13] or hydrothermal treatments including both liquefaction [14] and gasification [15].

2^{nd} generation biofuels can be produced from non-food biomass such as lignocellulosic by-products (cereal straw, sugar cane bagasse, forest residues), wastes (organic components of municipal solid wastes), and dedicated feedstock (purpose-grown vegetative grasses, short rotation forests and other energy crops). These dedicated energy-crops will still probably be grown on land in competition with food and fiber production; nevertheless energy yields in terms of GJ/ha are likely to be higher than traditional dedicated to 1st-generation biofuels.

In addition, poorer quality lands and marginal lands could be utilized, but keeping in mind that any crop grown without adequate water and nutrient replenishment cannot maintain high oil yields over the longer term [16, 17].

Finally, third-generation biofuels are produced from plant biomass not requiring soil to grow such as algae and cyanobacteria [18].

Macroalgae and microalgae can be used as feedstock for biofuel production and also for others commercial applications such as wastewater treatment utilizing water contaminants as nutrients for its growth or to produce high-value products such as fine chemicals or simply cosmetics and food additives.

Algae are autotrophic aquatic organisms characterized by a much higher biodiversity (more than 300.000 species) than terrestrial plants [19], also considering our scant knowledge on the species living in the oceans.

Algae have attracted interested for promising attributes in energy production: such as lipid-rich composition of oleaginous species (40-80%), high growth rate, low requirements in water [20].

The harvesting of algaculture for producing vegetable oil, biodiesel, bioethanol, biomethanol, biobutanol and other biofuels is also becoming increasingly commercially viable [21].

In addition to biodiesel production by lipid extraction and trasesterfication, the conversion of algal biomass to drop-in hydrocarbons fuel can be made through thermochemical and biochemical conversion as previously mentioned to second-generation biofuels.

Table 1.2.1: Comparison of different generation biofuels with petroleum products (adapted from Suganya et al., 2016 [18])

	Petroleum products	First generation	Second generation	Third generation
Technology	Petroleum refinery	Chemical and enzymatic transesterification	Hydrolysis, fermentation, thermochemical/biochemical conversion	transesterification, thermochemical/biochemical conversion
Feedstock	Crude petroleum	Vegetable oils, corn/sugar feedstocks	lignocellulosic residues, bio-wastes	Algae
Products	Diesel, gasoline, kerosene, jet fuel	biodiesel, bioethanol	pyrolysis oil, HTL oil, FT oil	biodiesel, bioethanol, Py-oil, HTL oil
Drawbacks	Depletion, environmental pollution, Ecological problems	Food Vs Fuel competition, Land use and limited feedstock	Agricultural land consumption, complicated process	Low product yield at large scale, less biomass production

1.3 Pyrolysis of biomass

Thermochemical processes consist of heating biomass under controlled conditions aiming to convert biomass into energy and materials.

As above-mentioned in section *1.2*, they are divided in several technologies, each one able to provide energy (heat and electricity), liquid and gaseous fuels (bio-oil and syngas) and solid materials (char or chemicals):

- Direct combustion to provide heat for cooking or heating houses and electricity by steam production.
- Gasification that takes place at high temperature (600-1500°C) to produce syngas (mainly CO and H_2)
- Pyrolysis to provide a liquid fuel (bio-oil), a likely substitute of heavy oil, and solid material (char) for several applications, especially soil applications, such as soil amendment or agent for soil remediation [22, 23]

Pyrolysis is thermal decomposition occurring in absence of oxygen or under an inert gas flow [24]. There are different types of pyrolysis carried out on the basis of different process conditions (Table 1.3.1).

Table 1.3.1: different modes of pyrolysis and relative product weight yields (on dry basis biomass)

Mode	Conditions	Liquid	Solid	Gas
Fast	≈ 500°C, short vapour residence time (< 2 s)	75 wt.% (Bio-oil)	12 wt.% (char)	13 wt.%
Intermediate	≈ 500°C, moderate vapour residence time (min.)	50 wt. % (two phases)	25 wt. % (char)	25wt. %
Slow	≈ 400°C, long vapour residence time (h)	30 wt. %	35 wt. % (char)	35 wt. %

Shorter hot-vapour residence times (fast pyrolysis) increase liquid yields, while longer residence times and lower temperatures (slow pyrolysis) favor gas and char production. Then, intermediate pyrolysis having moderate residence times (minutes) shows a well proportionate products distribution with 50 % of liquid (separated in organic phase and aqueous phase) and 25 % of char and gas.

A large range of process and reactor have been patented in the last decades.

A conceptual fast-pyrolysis process is depicted in Figure 1.3.1.

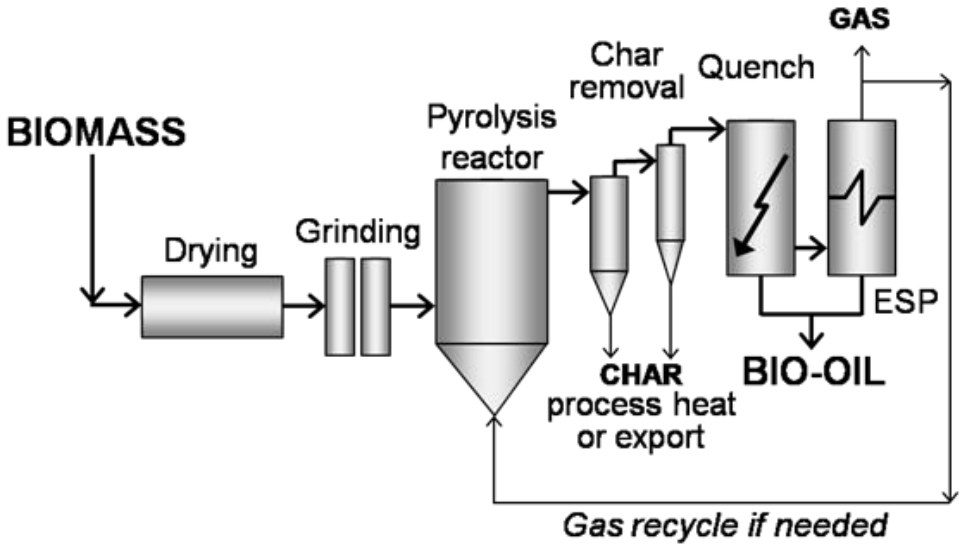

Figure 1.3.1: Typical fast-pyrolysis process [24]

Each process step has many alternatives, such as the reactor and liquid collection, but the underlying principles are similar. Indeed, several configurations have been studied: bubbling fluid bed reactor [25], circulating fluid-bed and transported-bed reactors [26], cyclonic reactors [27], and ablative reactors [28].

In addition, an intermediate pyrolysis reactor has been developed and patented by A. Hornung and co-workers [29]. The reactor consists of two coaxial conveyor screws (an inner screw and a covering screw). The intermediate pyrolysis of biomass produces a bio-oil with low tar yields and viscosity, which is distinctive in intermediate pyrolysis in comparison to fast pyrolysis [29].

1.4 Bio-oil: a feasible renewable liquid fuel

Liquid fraction resulting from pyrolysis, known as bio-oil or pyrolysis oil, is a dark brown complex mixture of hundreds of polar and non-polar compounds [30-33]. It is the result of depolymerization and fragmentation of cellulose, holocellulose, lignin (for lignocellulosic biomass), but also lipids and proteins in case of proteinaceous biomass such as algae or animal waste.

Chemically, bio-oil is a mixture of water (about 25%), phenols, guaiacols, syringols, nitrogen-containing compounds (e.g.: indoles, pyrroles), fatty acids (e.g.: acetic acid, formic acid and long-chain carboxylic acids), aldehydes, ketones, hydrocarbons, sugars, and pyrolytic lignin.

Bio-oil could be considered as a renewable substitute to heavy fuel oil usually used for electricity generation and as source of heat in cement kilns.

However, its chemico-physical properties (Tab. 1.4.1) and the high amount of oxygenated compounds, and sometimes also nitrogen-containing compounds, make it an unsuitable substitute for heavy fuel oil.

Bio-oil is a corrosive (pH around 2.5), viscous, and instable liquid with low high heating value (15-19 MJ/kg) if compared with heavy fuel (40 MJ/kg). Properties like acidity or viscosity can damage engines or turbines in high temperature zones with fast deterioration of materials commonly used in energy generation systems [34]. Although a large number of studies on biomass derived oils as biofuels have been performed [35-39], direct use of bio-oil requires significant adaptations of technology to fuel characteristics and it has not yet been fully proven at demonstration scale.

Table 1.4.1: chemical properties of bio-oil and heavy oil (adapted from [40])

Oil characteristics	bio-oil (from woody biomass)	heavy fuel oil
Water [wt%]	15-30	0.1
pH	2-8-3.8	-
Kinematic viscosity [cP]	40-100	180
HHV [MJ/kg]	16-19	44
ash [%]	0.1-0.2	0.1
C [%]	55-65	83-86
O [%]	28-40	<1
N [%]	<0.4	<0.1

Concerning the use of bio-oil as transportation fuel, it is evident that bio-oil must be catalytically upgraded if it is to be used as a conventional liquid fuel.

Different approaches were employed targeting bio-oil's quality improvement following petroleum refinery and industrial pathways.

- Catalytic steam gasification/reforming of bio-oil for syngas and hydrogen production [41-43]
- Hydrodeoxygenation (HDO) of bio-oil [44,45]
- Catalytic cracking over heterogeneous catalysts (e.g.: metal oxides, zeolites) [40,46-48]

HDO is bio-oil treatment at high hydrogen pressure (30-140 bar) and moderate temperature (200-400°C). HDO is likely the most common route to bio-oil deoxygenation and it is typically carried out in the presence of sulfided nickel-molybdenum and cobalt-molybdenum

catalysts. Non-sulfided catalysts including Pt-SiO_2-Al_2O_3 and Ru have also been used for hydrodeoxygenation.

However, HDO is an expensive treatment because it requires H_2 and expensive catalyst as cobalt, platinum or ruthenium.

Catalytic cracking is a promising method for bio-oil upgrading or for direct conversion of solid biomass into gasoline range aromatic products.

The advantages of catalytic cracking are that no H_2 is required, atmospheric processing reduces operating cost, and the temperatures employed are similar to those used in the production of bio-oil.

Many catalyst have been used including mesoporous catalysts (e.g.: MCM-41, SBA-15) [49-52], microporous zeolites (e.g.: HZSM-5, Y-zeolites, β-zeolites) [48, 53, 54], and metal oxides (e.g.: MgO, CaO, TiO_2, NiO) [55].

1.5. Catalytic cracking over zeolites

Zeolites are crystalline aluminosilicates composed of SiO_4 and AlO_4 tetrahedral, with O atoms connecting neighbouring tetrahedrons, and contain pores and cavities of molecular dimensions [56].

Zeolites have four properties that make them especially interesting for heterogeneous catalysis: 1) Cation exchange capacity allowing the introduction of cations with various catalytic properties; 2) if these cations are exchanged to H^+, they can have high number of strong acid sites; 3) pore diameters are less than 10 Å; 4) they have pores with one or more discreet sizes.

Many zeolites have multi-dimensional microporous structures that permit small molecules of reactants to diffuse into the zeolite structure.

Zeolite is a shape-selective catalyst and various types of shape selectivity can be identified contigent on if pore size restricts the reacting molecules entrance, the product molecules departure, or the creation of certain transition conditions.

Selectivity of the reactants is achieved when, among all the reactant molecules, only molecululles which are small enough diffuse through the catalyst pores. When parts of the products inside the pores are too large to diffuse out, product selectivity occurs [57].

Modification of zeolites with different metals is a widely used practice for making materials with a wide range of applications. Metals can be located in the zeolite pores by ion-exchange or wet impregnation. The majority of metal-loaded zeolites (e.g.: Ga-ZSM5 [54] or Pt [58]) are used in catalytic processes.

Zeolites are the most common catalyst used in petrochemical industry. One of the most important applications of zeolites is in fluid catalytic cracking (FCC) process. It provides about 45% of the global gasoline pool through hydrocarbon cracking into gasoline range molecules [59].

A broad range of zeolites have been investigated, but the shape-selective and acid characteristics of ZSM-5 (MFI framework) showed the best performance for pyrolysis oil valorization [54]. Several studies showed that zeolite ZSM-5 addition in a pyrolysis reactor could significantly increase the formation of gasoline-range aromatics hydrocarbons (mainly BTX) mirrored by decrease of oxygen content [48, 53, 54, 60-64].

However, CO, CO_2, water, and coke were also formed during process.

During catalytic pyrolysis, bio-oil or biomass vapours pass through a series of pyrolysis reactions followed by catalytic conversion of oxygenated compounds available in

pyrolysis vapors. The catalytic pyrolysis reaction pathway (Fig 1.5.1) can be explained through a series of pyrolysis reactions followed by catalytic conversion of biomass-derived oxygenateseffected by catalysts [53].

The three main components of lignocellulosic biomass are cellulose, hemicellulose, and lignin. Each one undergoes a different reaction, but no significant interactions between the three components, during both thermal pyrolysis and catalytic conversion stages, was observed.

The predominant pyrolysis product of cellulose is levoglucosan. During catalytic pyrolysis, levoglucosan goes through dehydration, decarbonylation, or decarboxylation reactions to form smaller furanic compounds with effects from the catalyst.

These furans then undergo a series of acid-catalyzed decarbonylation and oligomerization reactions inside the pores of zeolite to form aromatics and olefins. The major product from pyrolysis of hemicellulose is double-hydrated xylose, which can diffuse into zeolite pores without further reactions, along with other low molecular weight compounds such as formic acid, acetic acid, and furaldehyde.

Pyrolysis of lignin primarily generates monomeric phenolic compounds, which have very low reactivity on HZSM-5 catalyst. Predominant acid-dehydration of phenol leads to large amounts of coke formation, while cracking of phenols produce aromatics, at times. Olefins produced from cracking of alkyl-phenols could be an alternative way to production of aromatics. Recent studies showed that the increased formation of aromatics could be attributed to the preferential occurrence of decarbonylation reactions [65].

In addition, it has been hypothesized that zeolites are also capable of converting protein-derived nitrogenous compounds into aromatic hydrocarbons while releasing the nitrogen as ammonia, which can then be used as a nitrogen fertilizer [66].

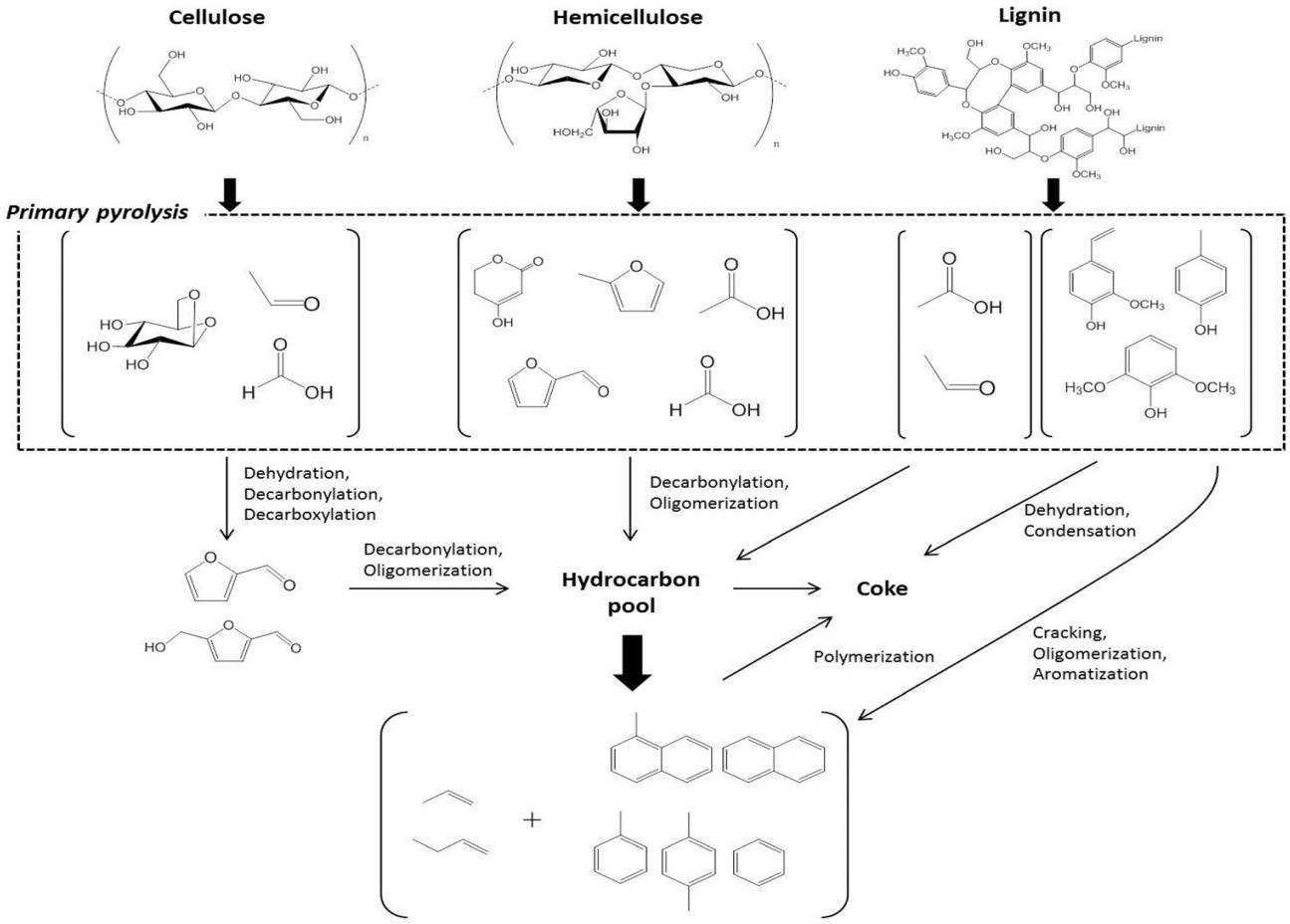

Figure 1.5.1: Reaction pathway for catalytic pyrolysis of lignocellulosic biomass over HZSM-5 [53]

1.6 Chemical characterization methods

As above-mentioned in section 1.4, bio-oil is a complex mixture of chemicals with several functional groups coming from biomolecules (lignin, cellulose, hemicellulose, protein, and other natural products). Pyrolysis causes thermal cracking of these biomolecules into simpler organic compounds obtaining a large number of different products with different polarity, volatility, and molecular weight (e.g.: phenolics species from lignin can have molecular weight as high as ≈5000 amu) [67].

For this reason, in order to obtain a big picture of bio-oil chemical composition several sample preparation methods and analytical techniques are needed.

Determination of the total chemical composition of bio-oil (Fig. 1.6.1) is a large challenge because only 40% of organic matter is quantifiable by conventional GC-MS methods.

In addition, the bio-oil contains polar, nonvolatile components that are only accessible by HPLC [67], comprehensive two-dimensional gas-chromatography time-of-flight mass-spectrometry (GCxGC-TOF-MS)[68], Fourier Transform Infrared (FT-IR) [69], size-exclusion chromatography (SEC) [70, 71], nuclear magnetic resonance (NMR) [69, 72].

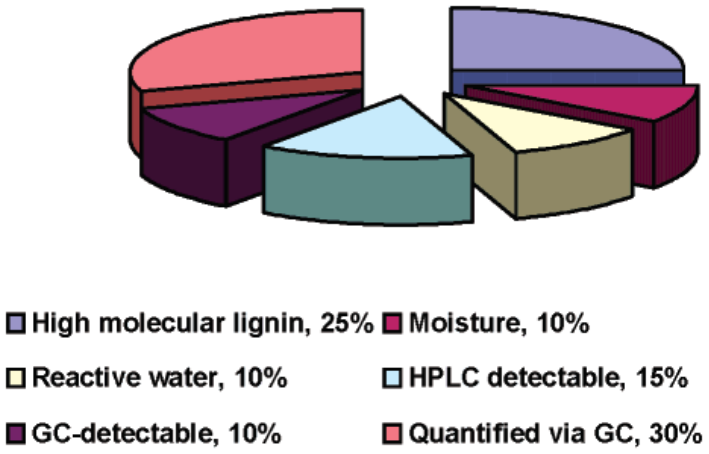

Figure 1.6.1: Typical percentage of chemical composition of bio-oil detected by analytical methods [67]

Nonetheless, studying the effect of pyrolysis parameters onto bio-oil quality, the effects of different reactors or process scale ups on bio-oils, or investigating catalytic pyrolysis with several catalysts, chemical characterization through previously mentioned analytical techniques turns out to be a complex, expensive, and time-consuming method.

Analytical pyrolysis (Py-GC-MS), where a micro pyrolyser is directly interfaced with the GC and the pyrolysate is sent with the career flowing gas to the chromatographic column [73],

could be a fast method able to predict pyrolysis process, both thermal and catalytic, avoiding any sample pretreatment and using a small sample amount [74].

In addition, Py-GC-MS is an interesting method to analyze the solid residue (biochar) obtained from pyrolysis.

Furthermore, Solid Phase Micro Extraction (SPME) is another suitable fast method for bio-oil [75,76] and biochar analysis [77, 78].

SPME is both a sampling and an analytic technique that involves the use of a fiber coating with an extracting phase (PDMS, PEG etc.) which extracts different analytes from the media providing detailed information on the extracted compounds when it is transferred to an injection port of a separating instrument such as a GC.

SPME applications on pyrolysis bio-oil are discussed in more detail in Chapter 4.

1.5 Biochar

The term biochar generally indicates the carbon-rich by-product of thermochemical process (e.g. gasification, pyrolysis, hydrothermal gasification) in an oxygen-limited environment [79].

Production of biochar, in combination with its storage in soils, has been suggested as one possible alternative and promising strategy for CO_2 removal and, at the same time,improve soil quality [79].

Pyrolysis conditions and the biomass source cause the formation of biochars with different chemico-physical characteristics leading to change in agronomic properties such as nutrient concentrations, CSC, pH, and also environmental stability [80, 81].

Biochar is a highly heterogeneous material characterized by stable and labile fractions.

It is mainly characterized by high organic carbon content and shows an aromatic structure made up of six carbon rings linked together [82].

Biochar structure can be defined as graphite-like carbon layers (crystalline) tied to non-graphitic layers [83].

Experimental studies showed that several functional groups can be placed on the graphitic layer surface [84]. These functional groups such as hydroxyl, carbonyl, carboxyl, phenyl, etc. are highly relevant to determining the biochar stability.

The stability of biochar is of fundamental importance in the context of biochar use for environmental management for two primary reasons: first, stability determines how long carbon applied to soil, as biochar, will remain in the soil and contribute to the mitigation of

climate change; second, stability will determine how long biochar will continue to provide benefits to soil, plant, and water quality [85].

During the production of biochar, biomass undergoes to a series of chemical reactions that are highly complicated and depend on both the nature of the biomass and the conditions [86, 87]. Decarboxylation, dehydration, decarbonylation, demethoxylation, intermolecular rearrangement, condensation, aromatization, etc. are some of the proposed chemical reactions that can take place [88].

Understanding the biochar structure, we can make effort to know its stability and its applications.

Several analytical techniques have been applied in order to study the chemical structure of biochar: ^{13}C-NMR [89-92], FT-IR [93, 94], TGA [91, 92, 95], and Py-GC-MS [96-101].

Py-GC-MS has been applied to characterize the molecular structure of biochar by means of molecular markers and its application is discussed in detail in Chapter 5.

References

[1] IEA, 2014. World Energy Outlook 2014, Available from: http://www.worldenergyoutlook.org

[2] IPCC, 2014: Climate Change 2014: Mitigation of Climate Change. Contribution of Working Group III to the Fifth Assessment Report of the Intergovernmental Panel on Climate Change, Cambridge University Press, Cambridge, United Kingdom and New York, NY, USA

[3] Huber G., Iborra S., Corma A., (2006) Synthesis of transportation fuels from biomass: Chemistry,catalysts and engineering. Chem. Rev. 106, 4044-4098]

[4] Biofuels for Transport: An International Perspective. International Energy Agency: Paris, France, 2004

[5] Stocker M. (2008), biofuels and biomass-to-liquid fuels in the biorefinery: catalytic conversion of lignocellulosic biomass using porous materials. Angew. Chem.Int. Ed., 47,

[6] Tilman, D., Socolow, R., Foley, J. A., Hill, J., Larson, E., Lynd, L., Williams, R. (2009). Beneficial biofuels-the food, energy, and environment trilemma. Science, 325, 270

[7] Rathmann, R., Szklo, A., Schaeffer, R. (2010). Land use competition for production of food and liquid biofuels: An analysis of the arguments in the current debate. Renewable Energy, 35, 14-22

[8] Azar C. Emerging scarcities: bioenergy–food competition in a carbon constrained world. In: Simpson D, Toman M, Ayres R, editors. Scarcity and growth in the new millennium. Resources for the future. Baltimore, MD: Johns Hopkins University Press; 2003

[9] Gomez LD., Clare GS., McQueen-Mason J., (2008) Sustainable liquid biofuels from biomass: the writing's on the walls. New Phytol, 178, 473-485

[10] Parikka M.,(2004) Global biomass fuel resources Biomass and Bioenergy 27, 613-620

[11] Damartzis T., Zanabiotou A., (2011) Thermochemical conversion of biomass to second generation biofuels through integrated process design-A review, Renew. Sust Energ Rev, 15, 366-378

[12] Bridgwater, A. V., Peacocke, G. V. C. (2000). Fast pyrolysis processes for biomass. Renewable and sustainable energy reviews, 4, 1-73

[13] Hanaoka, T., Inoue, S., Uno, S., Ogi, T., Minowa, T. (2005). Effect of woody biomass components on air-steam gasification. Biomass and bioenergy, 28, 69-76

[14] Toor, S. S., Rosendahl, L., Rudolf, A. (2011). Hydrothermal liquefaction of biomass: a review of subcritical water technologies. Energy, 36, 2328-2342

[15] Schmieder, H., Abeln, J., Boukis, N., Dinjus, E., Kruse, A., Kluth, M., Schacht, M. (2000). Hydrothermal gasification of biomass and organic wastes. The Journal of Supercritical Fluids, 17, 145-153

[16] Luoma, J.R., 2009. Hailed as a miracle crop, Jatropha falls short of hype. Yale Environment 360, Guardian Environmental Network.
http://www.guardian.co.uk/environment/2009/may/05/jatropha-biofuels-food-crops

[17] Sims, R. E., Mabee, W., Saddler, J. N., Taylor, M. (2010). An overview of second generation biofuel technologies. *Bioresource technology, 101, 1570-1580*

[18] Suganya, T., Varman, M., Masjuki, H. H., Renganathan, S. (2016). Macroalgae and microalgae as a potential source for commercial applications along with biofuels production: A biorefinery approach. *Renew Sust Energ Rev, 55, 909-941*

[19] Scott, S. A., Davey, M. P., Dennis, J. S., Horst, I., Howe, C. J., Lea-Smith, D. J., Smith, A.G. (2010). Biodiesel from algae: challenges and prospects. *Current opinion in biotechnology, 21, 277-286*

[20] Schenk, P. M., Thomas-Hall, S. R., Stephens, E., Marx, U. C., Mussgnug, J. H., Posten, C., Hankamer, B. (2008). Second generation biofuels: high-efficiency microalgae for biodiesel production. *Bioenergy Research, 1, 20-43*

[21] Yeang, K. (2008). Biofuel from algae. Architectural design, 78, 118-119

[22] Lee, J.W.; Kidder, M.; Evans, B.R.; Paik, S.; Buchanan III, A.C.; Garten, C.T.; Brown, R.C. (2010). Characterization of Biochars Produced from Cornstovers for Soil Amendment. *Environ. Sci. Technol., 44, 7970-7974*

[23] Zhang, X.K.; Wang, H.L., He, L.Z., Lu, K.P., Sarmah, A., Li, J.W., Bolan, N.S., Pei, J.C., Huang H.G. (2013). Using biochar for remediation of soils contaminated with heavy metals and organic pollutants. *Environ Sci Pollut Res, 20, 8472-8483.*

[24] Bridgwater A.V., (2015). Pyrolysis of biomass, Biomass Power of the World: Trasformations to Effective Use, Edited by W. van Swaaij, S. Kersten and W. Palz, Pan Stanford Pte. Ltd.

[25] Scott, D.S., Piskorz, J., (1984). The Continuous Flash Pyrolysis of Biomass. *Can. J. Chem. Eng. 62, 404-412*

[26] R.G. Graham, B.A. Freel, M.A Bergougnou (1988). The Production of Pyrolysis Liquids, Gas, and Char from Wood and Cellulose by Fast Pyrolysis. In Research in Thermochemical Biomass Conversion; Bridgwater, A. V., Kuester, J. L., Eds.; Elsevier Applied Science: London, pp 629-641.

[27] Lédé, J., Verzaro, F., Antoine, B., Villermaux, J. (1986). Flash pyrolysis of wood in a cyclone reactor. *Chemical Engineering and Processing: Process Intensification, 20, 309-317*

[28] Peacocke, G. V. (1994). Ablative pyrolysis of biomass (Doctoral dissertation, Aston University)

[29] Hornung, A., Apfelbacher, A., Sagi, S. (2011). Intermediate pyrolysis: A sustainable biomass-to-energy concept-Biothermal valorisation of biomass (BtVB) process. *Journal of scientific and industrial research, 70, 664-667*

[30] A.V. Bridgwater, (2012) Review of fast pyrolysis of biomass and product upgrading, *Biomass Bioenerg. 38, 68-94*

[31] Q. Zang, J. Chan, T. Wang, Y. Xu, (2007) Review of biomass pyrolysis oil properties and upgrading research, *Energ. Convers. Manage. 48, 87-92*

[32] P.K. Kanaujia, Y.K. Sharma, U.C. Agrawal, M.O. Garg, (2013) Analytical approaches to characterizing pyrolysis oil from biomass, *TrACh 42, 125-136*

[33] Meier D., (1999) New methods for chemical and physical cahracterization and round robin testing. Fast pyrolysis of biomass: a handbook, pp. 92-101, A. Bridgwater (Ed), et al., CPL Press, Newbury, UK .

[34] Leech J., (1996) Running a dual fuel engine on pyrolysis oil. In Biomass gasification and pyrolysis: state of the art and future prospects. M. Kaltschmitt, A.V. Bridgwater, Eds. CPL Press, Newbury, UK, 175–85

[35] Lopez-Juste G, SalvYa-Monfort JJ. (2000) Preliminary test on combustion of wood derived fast pyrolysis oils in a gas turbine combustor. *Biomass and Bioenergy 19, 119–128*

[36] Sridhar G, Paul PJ, Mukunda HS. (2001) Biomass derived producer gas as a reciprocating engine fuel—an experimental analysis. *Biomass and Bioenergy 21, 61–72*

[37] Crookes RJ, Kiannejad F, Nazha MAA. (1997) Systematic assessment of combustion characteristics of biofuels and emulsions with water for use as diesel engine fuels. *Energy Conversion and Management 38, 1785–1795.*

[38] Demirbas A. (2000) Conversion of biomass using glycerin to liquid fuel for blending gasoline as alternative engine fuel. *Energy Conversion and Management 41, 1741–1748*

[39] Chiaramonti, D., Bonini, M., Fratini, E., Tondi, G., Gartner, K., Bridgwater, A. V., Baglioni, P. (2003). Development of emulsions from biomass pyrolysis liquid and diesel and their use in engines—Part 1: emulsion production. *Biomass and Bioenergy 25, 85-99*

[40] Mortensen, P. M., Grunwaldt, J. D., Jensen, P. A., Knudsen, K. G., Jensen, A. D. (2011). A review of catalytic upgrading of bio-oil to engine fuels. *Appl. Cat. A: General, 407, 1-19*

[41] Garcia, L., Salvador, M. L., Arauzo, J., Bilbao, R. (1999). Catalytic steam gasification of pine sawdust. Effect of catalyst weight/biomass flow rate and steam/biomass ratios on gas production and composition. *Energy & Fuels, 13, 851-859.*

[42] Wang, D., Czernik, S., Montane, D., Mann, M., Chornet, E. (1997). Biomass to hydrogen via fast pyrolysis and catalytic steam reforming of the pyrolysis oil or its fractions. *Industrial & Engineering Chemistry Research, 36, 1507-1518.*

[43] Garcia, L., French, R., Czernik, S., Chornet, E. (2000). Catalytic steam reforming of bio-oils for the production of hydrogen: effects of catalyst composition. *Applied Catalysis A: General, 201, 225-239*

[44] Wildschut, J., Mahfud, F. H., Venderbosch, R. H., & Heeres, H. J. (2009). Hydrotreatment of fast pyrolysis oil using heterogeneous noble-metal catalysts. *Industrial & Engineering Chemistry Research, 48, 10324-10334.*

[45] de Miguel Mercader, F., Groeneveld, M. J., Kersten, S. R. A., Way, N. W. J., Schaverien, C. J., Hogendoorn, J. A. (2010). Production of advanced biofuels: Co-processing of upgraded pyrolysis oil in standard refinery units. *Applied Catalysis B: Environmental, 96, 57-66*

[46] Vitolo, S., Bresci, B., Seggiani, M., Gallo, M. G. (2001). Catalytic upgrading of pyrolytic oils over HZSM-5 zeolite: behaviour of the catalyst when used in repeated upgrading–regenerating cycles. *Fuel, 80, 17-26.*

[47] Huber, G. W., Corma, A. (2007). Synergies between Bio-and Oil Refineries for the Production of Fuels from Biomass. *Angew. Chem. Int. Ed., 46, 7184-7201*

[48] Carlson, T. R., Jae, J., Lin, Y. C., Tompsett, G. A., Huber, G. W. (2010). Catalytic fast pyrolysis of glucose with HZSM-5: the combined homogeneous and heterogeneous reactions. *Journal of Catalysis, 270, 110-124.*

[49] Iliopoulou E.F., Antonakou E.V., Karakoulia S.A., Vasalos I.A., Lappas A.A., Triantafyllidis K.S., (2007). Catalytic conversion of biomass pyrolysis products by mesoporous materials: Effect of steam stability and acidity of Al-MCM-41 catalysts. *Chemical Engineering J. 134, 51-57*

[50] Adam J., Blazso M., Meszaros E., Stocker M., NIlsen M., Bouzga A., Oye G. (2005). Pyrolysis of biomass in the presence of Al-MCM-41 type catalyst. *Fuel 84, 1494-1502*

[51] Torri C., Lesci I.G., Fabbri D.,(2009) Analytical study on the pyrolytic behavior of cellulose in the presence of MCM-41 mesoporous materials. *J. Anal. Appl. Pyrolysis 85, 192-196*

[52] Stefanidis S., Kalogiannis K., Iliopoulou E.F., Lappas A. A., Triguero J.M., Navarro M.T., Rey F., (2013). Mesopore-modified mordernites as catalysts for catalytic pyrolysis of biomass and cracking of vacuum gasoil processes. *Green Chemistry 15, 1647-1658*

[53] Wang K., Kim, K.H., Brown R. C. (2014). Catalytic pyrolysis of individuals components of lignocellulosic biomass. *Green Chemistry 16, 727-735*

[54] Cheng Y.T., Jae J., Shi J., Fan W., Huber G., (2012). Production of Renewable aromatic compounds by catalytic fast pyrolysis of lignocellulosic biomass with bifunctional Ga/ZSM-5, Catalysts. *Angew. Chem. 124, 1416-1419*

[55] Lu Q., Zhang Z.F., Dong C.Q., Zhu X.F., (2010) Catalytic upgrading of biomass fast pyrolysis vapors with nano metal oxides: an analytical Py-GC-MS study. *Energy 3, 1805-1820*

[56] Breck D.W (1974) Zeolite Molecular Sieves: Structure, Chemestry and Use. J. Wiley & Sons, New York

[57] Asadieraghi, M., Daud, W. M. A. W., Abbas, H. F. (2015). Heterogeneous catalysts for advanced bio-fuel production through catalytic biomass pyrolysis vapor upgrading: a review. *RSC Advances 5, 22234-22255*

[58] Hu H., Zhang Q., Cen J., L X., (2014) High suppression of the formation of ethylbenzene in benzene alkylation with methanol over ZSM-5 catalyst modified by platinum. *Catalysis Communications 57, 129-133*

[59] Ertl H.K.G., Schuth F., Weitkamp J, (2008). Handbook of heterogenous catalysis. Wiley-VCH, 2nd edn.

[60] Iliopoulou, E. F., Stefanidis, S., Kalogiannis, K., Psarras, A. C., Delimitis, A., Triantafyllidis, K. S., Lappas, A. A. (2014). Pilot-scale validation of Co-ZSM-5 catalyst performance in the catalytic upgrading of biomass pyrolysis vapours. *Green Chem., 16, 662-674*.

[61] Thangalazhy-Gopakumar, S., Adhikari, S., Chattanathan, S. A., Gupta, R. B. (2012). Catalytic pyrolysis of green algae for hydrocarbon production using H+ ZSM-5 catalyst. *Bioresour. technol., 118, 150-157.*

[62] Vitolo, S., Bresci, B., Seggiani, M., Gallo, M. G. (2001). Catalytic upgrading of pyrolytic oils over HZSM-5 zeolite: behaviour of the catalyst when used in repeated upgrading–regenerating cycles. *Fuel, 80(1), 17-26.*

[63] Yildiz, G., Pronk, M., Djokic, M., van Geem, K. M., Ronsse, F., Van Duren, R., Prins, W. (2013). Validation of a new set-up for continuous catalytic fast pyrolysis of biomass coupled with vapour phase upgrading. *J. Anal. Appl. Pyrol., 103, 343-351.*

[64] Torri, C., Fabbri, D., Garcia-Alba, L., Brilman, D. W. F. (2013). Upgrading of oils derived from hydrothermal treatment of microalgae by catalytic cracking over H-ZSM-5: A comparative Py–GC–MS study. *J. Anal. Appl. Pyrol, 101, 28-34.*

[65] Puertolas B., Veses A., Callèn MS. Mitchell S., Garcià T., Perez-Ramirez J., (2015) Porosity-acidity interplay in hierarchical ZSM-5 Zeolites for pyrolysis oil valorization to aromatics. *ChemSusChem 8, 3283-3293.*

[66] Wang, K., Brown, R. C. (2013). Catalytic pyrolysis of microalgae for production of aromatics and ammonia. Green Chemistry 15, 675-681

[67] Mohan D., Pittman C. U., Steele P. H.,(2006). Pyrolysis of wood/biomass for bio-oil: a critical review, *Energ. Fuel. 20, 848-889*

[68] Rathstack P., Otto M., (2014). Classification of chemical compound classes in slow pyrolysis liquids from brown coal using comprehensive gas-chromatography mass spectrometry. *Fuel 116, 841-849.*

[69] Putun A.E. Apaydin E., Putun E., (2004). Rice straw as a bio-oil source via pyrolysis and steam pyrolysis. *Energy 29, 2171-2180*

[70] Gerdes C., Simon M., Ollesch T, Meier D., Kaminsky W. (2002) Design, Construction and Operation of Fast pyrolysis Plant for biomass. *Eng. Life Sci. 167-174.*

[71] Bayerbach R., Dy Nguyen V., Schurr U., Meier D. (2006) Characterization of the water-insoluble fraction from fast pyrolysis liquids (pyrolytic lignin): Part III. Molar mass characteristics by SEC, MALDI-TOF-MS, LDI-TOF-MS, and Py-FIMS. *J. Anal. Appl. Pyrolysis 77, 95-101*.

[72] Mullen C.A., Strahan G.D., Boateng A.A. (2009). Characterization of various fast-pyrolysis bio-oils by NMR spectroscopy. *Energ Fuel 23, 2707-2718*

[73] Moldoveanu C.S, Analytical pyrolysis of natural organic polymers (1998). Elsevier

[74] Scholze B., Meier D.. (2001) Characterization of the water-insoluble fraction from pyrolysis oil (pyrolytic lignin). Part I. PY–GC/MS, FTIR, and functional groups. *J. Anal. Appl. Pyrolysis 60, 41-54.*

[75] Torri C., Fabbri D.,(2009) Application of off-line pyrolysis with dynamic solid-phase microextraction to the GC-MS analysis of biomass pyrolysis product, *Microchem. J. 93,133-139*

[76] Tessini C., Muller N., Mardones C., Meier D., Berg A., Von Baer D., (2012) Chromatographic approaches for determination of low-molecular mass aldehydes in bio-oil, *J. Chromatogr. A 1219, 154-160*

[77] Rombolà A.G., Marisi G., Torri C., Fabbri D., Buscaroli A., Ghidotti M, Hornung A., (2015) Relationship between Chemical Characteristics and Phytotoxicity of biochar from poultry litter pyrolysis. *J. Agricultural Food. Chemistry 63, 6660-6667*

[78] Ghidotti, M., Conti, R., Fabbri, D., Hornung A. (2014) Molecular analysis of extractable fraction of biochar. Ecomondo, a mediterranean platform for the sustainable growth. Fabio Fava Ed. Rimini (I) November 5-8, Maggioli, 49-54.

[79] Lehmann, J.; Gaunt, J.; Rondon, M. (2006). Bio-char sequestration in terrestrial ecosystems - a review. *Mitig. Adapt. Strategy Glob. Change 11, 403-427*

[80] Gaskin J.W. Steiner C., Harris K., Das K.C., Bibens B. (2008). Effect of low-temperature pyrolysis conditions on biochar for agricultural use. *American Society of Agricultural and Biological Engineering 51, 2061-2069*

[81] Harris P.J.F. (2007). Solid state growth mechanism for carbon nanotubes. *Carbon 45, 229-239*

[82] Bruun E.W., (2011). Application of fast pyrolysis biochar to a loamy soil-effects on carbon and nitrogen dynamics and potential for carbon sequestration. PhD thesis, Ris DTU, National Laboratory for sustainable energy, Denmark.

[83] Downie, A., Crosky, A., Munroe, P., (2009). Physical Properties of Biochar. In: Lehmann, J., Joseph, S. (Eds.), Biochar for Environmental Management. Earthscan, London, pp. 13-32

[84] Brennan J.K., Bandosz T.J., Thomson K.T., Gubbins K.E. (2001). Water in porous carbons. *Colloid and surface A: physochemical and engineering aspects 187-188, 539-568*

[85] Lehmann, J. and Joseph, S. (2009). Biochar for environmental management: An introduction. In: J. Lehmann and S. Joseph, editors, Biochar for environmental management: Science and technology. Earthscan, London., 1-12

[86] Glaser, B., Lehmann, J., Zech, W. (2002) Ameliorating physical and chemical properties of highly weathered soils in the tropics with charcoal e a review. *Biol. Fertil. Soils 35, 219-230.*

[87] Di Blasi, C. (2008) Modelling chemical and physical processes of wood and biomass pyrolysis. *Prog Energ Combust Sci 34, 47–90*

[88] Funke, A. and Ziegler, F. (2010) Hydrothermal carbonization of biomass: a summary and discussion of chemical mechanisms for process engineering. *Biofuels Bioprod Biorefining, 4, 160–177*

[89] Bruun, S., Jensen, E S., Jensen L S., (2008). Microbial mineralization and assimilation of black carbon: Dependency on degree of thermal alteration. *Organic Geochemistry, 39, 839-845,*

[90] Calvelo Pereira, R., Kaal, J., Camps Arbestain, M., Pardo Lorenzo, R., Aitkenhead, W., Hedley, M., Marcias, F., Hindmarsh, J., Marcià-Agullò, J.A.. (2011). Contribution to characterisation of biochar to estimate the labile fraction of carbon. *Organic Geochemistry, 42, 1331-1342*

[91] Zimmerman, A.R., Gao, B., Ahn M-Y., (2011). Positive and negative carbon mineralization priming effects among a variety of biochar-amended soils. *Soil Biology & Biochemistry, 43, 1169-1179*

[92] Kim, K.H., Kim, J-Y., Cho, T-S., Choio, J.W., (2012). Influence of pyrolysis temperature on physicochemical properties of biochar obtained from the fast pyrolysis of pitch pine (Pinus rigida). *Bioresource Technology 118, 158-162*

[93] Labbè, N., Harper, D., Rials, T., (2006). Chemical Structure of Wood Charcoal by Infrared Spectroscopy and Multivariate Analysis. *Journal of agricultural and food chemistry, 54, 3492-3497*

[94] Novak, J.M., Busscher, W.J., Watts, D.W., Laird, D.A., Ahmedna, M.A., Niandou, M.A.S., (2010). Short-term CO_2 mineralization after additions of biochar and switchgrass to a typic Kandiudult. *Geoderma, 154, 281–288*

[95] Zimmerman, A.R., (2010). Abiotic and microbial oxidation of laboratory-produced black carbon (biochar). Environmental Science & Technology, 44, 1295-1301.

[96] Fabbri D., Torri C., Spokas K.A., (2012) Analytical pyrolysis of synthetic chars derived from biomass with potential agronomic application (biochar). Relationship with impacts on microbial carbon dioxide production. *J. Anal. Appl. Pyrol., 93, 77-84*

[97] Kaal J., Cortizas A.M., Nierop K.G.J., (2009) Characterisation of aged black carbon using a coil pyroprobe pyrolysis-GC/MS method optimized for black carbon. *J. Anal. Appl. Pyrol., 85, 408-416*

[98] Kaal J., Rumpel C., (2009) Can pyrolysis-GC/MS be used to estimate the degree of thermal alteration of black carbon?, *Org. Geochem., 40, 1179-1187*

[99] Kaal J., Schneider M.P.W., Schmidt M.W.I, (2012), Rapid molecular screening of black carbon (biochar) thermosequences obtained from chestnut wood and rice straw: A pyrolysis-GC/MS study. *Biomass Bioenerg., 45,115–129.*

[100] Kaal J., Cortizas A.M., Reyes O., Solino M., (2012), Molecular characterization of Ulex europaeus biochar obtained from laboratory heat treatment experiment - A pyrolysis-GC/MS study. *J. Anal. Appl. Pyrol., 95, 205-212*

[101] Conti R., Rombolà A.G., Modelli A., Torri C., Fabbri D., (2014). Evaluation of the thermal and environmental stability of switchgrass biochars by Py-GC-MS. *J. Anal. Appl. Pyrol. 110, 239–247.*

Chapter 2

Aim of the thesis

As illustrated in the introductive section, pyrolysis of biomass could be an interesting technology for biofuels and biochar production.

However, regarding on biofuel production pyrolysis is still on demonstrative scale because of bio-oil quality, scaling-up, and upgrading issues. For this reason, nowadays a large number of research projects and companies are developing innovative processes to obtain advanced biofuels.

Great interest has been given to the upgrading of pyrolysis by zeolite cracking, especially with HZSM-5. Many studies have dealt with lignocellulosic biomass, but the increasing role of wastes and the interest on algae in the energetic sector are promoting research on these substrates. Algae and some wastes are rich in proteins, biopolymers that have been less investigated in comparison to lignin and cellulose with regards to thermal and catalytic cracking. One of the objectives of this thesis was to gather chemical information on the thermal behavior of proteinaceous substrates in the presence of zeolite and compare with lignocellulosic biomass.

The action of catalyst is on the pyrolysis vapours evolved from the thermal breakdown of biopolymers. The knowledge of the chemical composition of vapours is important to understand the changes before their condensation into bio-oil or the degradation on the surface catalyst. For this aim, a sampling procedure for the direct analysis of pyrolysis vapours based on absorption onto a microfiber was developed.

Char is a product formed upon biomass pyrolysis intentionally as a target material or as secondary product in bio-oil production,

the strong interest given from the potential agricultural use and at the same time as CO_2 sequestration agent. For this reason in some Countries it has been recently commercialized as soil amendment. Its increasing application has implications on its environmental stability and impact that need to be carefully investigated. The environmental properties of biochar are dependent on its chemical characteristics. A molecular approach to characterize the thermal stability and degree of carbonization of biochar recently proposed in the literature was further investigated and scrutinized in this thesis.

Furthermore, the thesis is focused on the development of reliable analytical methods by means of Py-GC-MS and SPME-GC-MS in order to:

1. Selecting optimal pyrolysis conditions
2. Predicting bio-oil composition
3. On-line monitoring pyrolysis vapours to reduce lab working-time and sample treatment for a potential industrial application
4. Investigating biochar structure and its correlation with thermal stability

Results section is split in three chapters, each one of them showed a different application of analytical tools within bio-oil and biochar characterization topic:

In **Chapter 3** two studies on the characterization of catalytic bio-oils from proteinaceous and lignocellulosic biomass were reported.
The first study was focused to the optimization of catalytic pyrolysis conditions in term of catalyst and process parameters by Py-GC-MS. In addition, a comparison between Py-GC-MS and pyrolysis on bench scale reactor was conducted on an interesting microalgae strain (*Desmodesmus communis*).
In the second study a comparison on the effect of catalyst on bio-oils from lignocellulosic (pine sawdust) and different proteinaceous biomass (spirulina, seaweed and fish discharge) was conducted.

In **Chapter 4** SPME-GC-MS as a fast analytical method to characterize pyrolysis vapours was studied. At-line monitoring of pyrolysis vapours was developed on a bench scale pyrolysis reactor in order to demonstrate the applicability of SPME as online monitoring tool able to avoid sample pretreatment, to reduce laboratory working time and useful for industrial applications.

In **Chapter 5** two studies on the molecular composition of different biochars by Py-GC-MS were reported.
In the first study, Py-GC-MS was applied on a thermo sequence of biochar from an herbaceous feedstock (switchgrass). Labile fraction of biochar was classified and the optimal process conditions were investigated utilizing different molecular markers.
In the second study, Py-GC-MS molecular markers previously found were applied to thermo sequence of biochar from a different herbaceous feedstock (cornstalk) in order to validate the preliminary results. Moreover, the effect of different biomass source (lignocellulosic, agricultural/industrial waste and algae) was investigated by Py-GC-MS molecular marker and TGA analysis.

Chapter 3

Characterization of bio-oil from catalytic cracking of proteinaceous biomass

3.1 Analytical and preparative catalytic pyrolysis of microalgae *Desmodesmus communis* for hydrocarbons production: A Py-GC-MS study

3.1.1 Introduction

In biomass-derived fuels, the first generation of biofuels mainly include biodiesel from vegetable oils and bioethanol from starch and sugar cane [1]. They represent the most mature bio/chemical technology into the market; however their sustainability is a matter of concern because of a shift in land use away from food production [2].The second generation biofuels are represented by lignocellulosic biomass, woody crops, and agricultural wastes (no-food crops).

Microalgae is the feedstock for the third-generation biofuels. Microalgae are characterized by rapid growth and high carbon fixing efficiency [3] but nitrogen in the fuel is the major drawback due to the high content of proteins in comparison with lignocellulosic biomass.

Whereas the first generation biofuels is based on well-known technologies, biofuels from lignocellulosic and especially from algal feedstock is rather a new technology.

Several bioenergy conversion processes from algae have been developed: torrefaction [4], hydrothermal liquefaction [5-8] and pyrolysis [9-17]. Pyrolysis is a thermal degradation process widely applied to convert solid biomass into a liquid (bio-oil) for energetic applications. Bio-oil obtained from wood is expected to enter soon the market [18] but microalgae are still in the early stage of research and development.

Heterogeneous catalysts are broadly used in pyrolysis process in order to improve the chemical-physical properties of liquid fractions.

In the past catalytic pyrolysis of lignocellulosic biomass was extensively investigated [19-25]. Recently, catalytic pyrolysis of microalgae has been subject of study by several researchers [9, 11, 12, 14, 15, 17].

Du et al., [9] studied catalytic pyrolysis of *C. vulgaris* and model compounds using H-ZSM5 and found that increasing catalyst biomass ratio from 1:1 to 5:1 the aromatic yields significantly increase. Other studies on *C. vulgaris* showed that it is possible to increase the catalyst-biomass ratio till 9:1 increasing the aromatic yield [15] recovering a maximum carbon yield of aromatic hydrocarbons around 24 % and the possibility to recover ammonia from nitrogen [14].

Babich et al., [11] studied the effect of Na_2CO_3 as catalyst on *Chlorella* showing a decrease of liquid yield respect to non-catalytic pyrolysis but an enhancement of bio-oil properties in term of calorific value, acidity and aromatic content with an energy recovery in bio-oil about 40 %.
Pan and co-workers [16] performed both non-catalytic and catalytic pyrolysis, with H-ZSM5, on *Nannochloropsis* sp. varying the temperature. They found the best temperature to be 400°C to optimize the bio-oil yield. In addition, they observed that increasing the catalyst amount caused an increase in the HHV of bio-oil from 24.6 MJ/kg to 32.7 MJ/kg.
Although several studied on catalytic pyrolysis on microalgae have been conducted, studies on Scenedesmaceae strain are scant [10, 26, 27].
Desmodesmus sp. is of interest because of its resistance, high growth rates and the presence of algeaenan [7, 28, 29].
In addition, few studies have compared Py-GC-MS with preparative pyrolysis and evaluated the predictive potential of Py-GC-MS for protein-rich biomass [10, 30]
Harman-Ware et al., [10] pyrolyzed *Desmodesmus* sp. at two different rector scales in order to compare the origin and the formation of products from fast pyrolysis. Pyrolysis at 480°C both in an isothermal spouted bed reactor and a dynamic Py-GC-MS were carried out. Although Py-GC-MS results agreed with GC-MS results obtained from bio-oil fractions, they found some difference between large scale pyrolysis and analytical pyrolysis on distribution and type of products detected. Analytical pyrolysis showed larger amount of nitrogen-containing compounds such as amines, while from the spouted bed reactor the compounds appeared to be mostly amides. The authors ascribe it likely the results of secondary reactions during pyrolysis or in bio-oil during condensation. Difference between analytical and bench scale pyrolysis was also observed from zeolite cracking of other algae [31].
In this study, catalytic pyrolysis of microalgae *Desmodesmus communis* with different catalyst and different catalyst-biomass ratio by Py-GC-MS was investigated.
The aim of this work is to use Py-GC-MS as a screening technique in order to gather preliminary information on the cracking process and selecting the optimal parameters. The original biomass and the corresponding thermal bio-oil obtained after pyrolysis were utilized as substrate.
The influence of MCM-41containing titanium or tin as additional metals and zeolite H-ZSM5 has been investigated by Py-GC-MS.
MCM-41 catalysts have been selected as they were usefully used in field of catalysis [32, 33] due to their larger pores and mild-to-moderate acidity. In addition, an in-depth literature review revealed there are no studies about pyrolysis of microalgae using this kind of catalyst.

Finally, zeolite H-ZSM5 was selected due to its wide use in catalytic pyrolysis but the results showed in literature are heterogeneous because of sharp range in term of amount and weight-ratio used in literature.

After Py-GC-MS screening, bench scale pyrolysis tests at the optimal catalytic conditions were carried out.

3.1.2. Experimental

3.1.2.1 Materials

In this study *Desmodesmus communis* algal strain was used.

D. communis was isolated by G. Samorí and co-workers and the isolation procedure is given elsewhere [29].

Before pyrolysis experiments a sample of algal biomass was filtered on Whatman® glass fiber filters grade GF/C which ensures almost complete elimination of free water (water remains associated with the biomass, about 90% by weight) and the material obtained was subjected to freeze-drying. The biomass was stored at -20 ° C before being analyzed and used for the pyrolysis experiments.

The zeolite used is commercial H-ZSM-5 (MFI SiO_2/Al_2O_3 = 45, Zeolite Soconomy Mobil – Five, Clariant). Diameter of pores = 6 Å; surface area > 300 m^2 g^{-1}, orthorhombic structure made by tridimensional net of interconnected pores).

The synthesis of MCM-41 Ti- or Sn-containing mesoporous materials was carried out at CIRSA-University of Bologna and described elsewhere [34].

All the solvents and materials (e.g.: Amberlite® XAD-2 and Tedlar® bag) used were obtained from Sigma-Aldrich.

3.1.2.2 Preparative pyrolysis: production of thermal bio-oil

Thermal bio-oil sample was obtained using a fixed bed tubular quartz reactor (length: 650 mm, internal diameter 37 mm) placed into a refractory furnace. *D. communis* sample (approximately 12 g for each batch test , in total 48.6 g of algal biomass were pyrolysed) was placed onto a quartz boat and pyrolysed under a nitrogen flow of 1000 cm^3 min^{-1}. When the temperature inside the reactor, measured with a thermocouple, reached the selected value, the boat was pushed into the oven. Pyrolysis runs were performed at 420°C for 30 min. The pyrolyser was connected downstream to two cold traps (-15°C with ice/NaCl mixture) for trapping the condensable vapours. The combined liquid fraction from four sequential

pyrolysis was centrifuged and phases could be separated: the upper phase was named as thermal bio-oil, the bottom phase as the aqueous phase [31].

3.1.2.3 Preparative catalytic pyrolysis

Catalytic pyrolysis (7 batch pyrolysis, 3 g per batch) was performed in a quartz tubular reactor of height 60 cm, ID 4.5 cm which inserted vertically into an electrically-heated tubular furnace (Fig 3.1.1). The pyrolysis apparatus included a change-sample vessel in which the sample was placed in a quartz basket hung on a quartz rod, which could easily move vertically inside the reactor tube.

In a typical run, the catalyst was placed in the reactor and then it was heated under nitrogen flow with a flow rate of 100 mL min^{-1}. After the system reached steady state at 460 °C, the basket containing feedstock was introduced into the reactor, just above the catalyst, thus only the vapors of pyrolysis are in contact with catalyst.

The generated pyrolysis vapors were passed directly over the catalyst surface, before leaving through the bottom of the reactor. The volatiles leaving the reactor passed sequentially through a condensation trap cooled at -15 °C, a dissolution trap containing n-heptane cooled with dry ice and finally an adsorption trap packed with XAD-2 resin.. The exhaust gas was collected in a 1 L Tedlar® gas sampling bag for GC-TCD analysis. In each experiment, char (in basket) and liquid (oil and aqueous fraction) yields were determined by weight. The liquid fractions from each trap were collected by Pasteur pipette and the XAD-2 resin was washed out with cyclohexane, then analyzed by GC-MS.

The non-condensable gases and aerosols trapped were calculated by difference. In catalytic experiments, used catalyst was regenerated by heating in a muffle furnace for 6 h at 550 °C (weight loss provided coke yield).

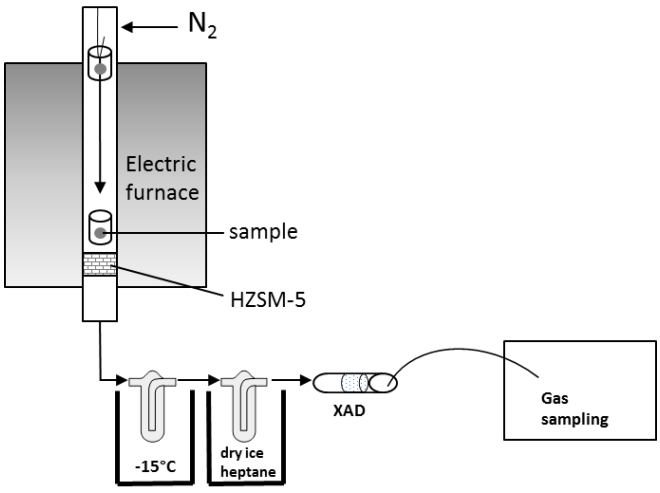

Figure 3.1.1: Experimental configuration of the reactor for catalytic pyrolysis

3.1.2.4 Elemental analysis

Elemental analyses (CHNS) of biomass and bio-oil sample were performed by combustion using a Thermo Scientific Flash 2000 series analyser. Ash content was calculated according to ASTM method (ASTM E1755 – 01, 2015) as the mass percent of residue remaining after dry oxidation at 575 ± 25°C for 5h using a muffle oven. Then oxygen content was calculated by difference.

3.1.2.5 GC-MS analysis

A sample of bio-oil was dissolved in cyclohexane solution to a 1% w/v concentration spiked with 0.1 mL internal standard solution (100 mg/L 1,3,5-tri-terz-butylbenzene in cyclohexane). Bio-oil direct analysis was performed with a 6850 Agilent HP gas chromatograph connected to a 5975 Agilent HP quadrupole mass spectrometer (EI 70 eV, at a frequency of 1.55 scan s^{-1} within the 10-450 m/z range). Analytes were separated by a HP-5 fused-silica capillary column (stationary phase poly [5% diphenyl/95% dimethyl] siloxane, 30 m, 0.25 mm i.d., 0.25 mm film thickness) using helium as carrier gas with the following thermal program: 50°C with a hold for 5 min, then ramping up with a heating rate of 10°C min-1 until 325 °C followed by a column cleaning at 325 °C for 10 min.

Bio-oil solution was analysed after silylation using the following thermal program: 100 °C with a hold for 5 min, then ramping up with a heating rate of 5°C min^{-1} until 310°C. As silylation procedure an aliquot of the prior solution (100 µl) was combined with internal standard (sorbitol 10 mg/L in ACN), silylated with BSTFA/TMCS/pyridine for 2 h at 60 °C, and analysed by GC–MS.

Aqueous phase GC-MS analysis were performed by means of solid phase microextraction (SPME) using a 85 µm polyacrylate (PA) fiber by Sigma-Aldrich. An aliquot of aqueous phase (1 mL) was placed in a 1.5 mL clean vial, then a conditioned SPME fiber was immersed into the vial for a direct-immersion extraction (DI-SPME) with an extraction time of 30 min. After extraction, fiber was thermally desorbed at 280°C into the injection port of the Agilent GC-MS in splitless mode. GC-MS analysis was performed using the thermal program previously used for bio-oil analysis.

3.1.2.6 Analytical pyrolysis (Py-GC-MS)

Py-GC-MS analyses were performed using an electrically heated platinum filament CDS 5250 pyroprobe interfaced to a Varian 3400 GC equipped with a GC column (HP-5-MS; Agilent

Technologies 30 m × 0.25 mm, 0.25 μm) and a mass spectrometer (Saturn 2000 ion trap, Varian Instruments). GC thermal program: 35°C to 310°C at 5°C min^{-1}; MS conditions: electron ionisation at 70 eV, full scans acquisition in the 10–450 m/z interval. A quartz sample tube containing approximately 10 mg of mixture with different sample (biomass or thermal bio-oil) to catalyst ratio (1:5, 1:10, 1:20 by weight) was inserted into the Py–GC interface (300 °C) and then pyrolysed at 600 °C (set temperature) for 100 s with helium as carrier gas (100 mL min^{-1}).

3.1.3. Results and discussion

3.1.3.1 Bio-oil composition: proximate and GC-MS analysis

Thermal bio-oil was obtained from the combined liquid fractions from four sequential batch pyrolysis of *D. communis* in the absence of catalyst. . The liquid fraction was collected in the condensation traps with an overall percentage yield of 33%. After centrifugation, thermal bio-oil and aqueous phase could be separated with 18% and 15% yields, respectively. In addition, char and non-condensable gas (this latter estimated by difference) showed yields of 25% and 42%, respectively.

Table 3.1.1 shows the elemental composition of *D. communis* feedstock and the relative thermal bio-oil.

It can be seen that carbon content into the bio-oil increases to 60.3% and the hydrogen content increases to 8.7%, while the oxygen content decreases to 24.2% in comparison to the initial biomass.

Table 3.1.2 shows the compounds identified in the bio-oil sample after silylation. Over a hundred compounds could be tentatively identified.

The most of the pyrolysis products identified can be attributed to the thermal degradation of carbohydrates, proteins and lipids or to Maillard reaction between sugars and amino acids.

A detailed attribution of the pyrolysis products can be done on the basis of a classification of chemical classes and the original biopolymers.

Pyrolysis of proteins generates N-containing compounds called “black nitrogen” which comprise pyrroles-type N, some amides N and less extent pyridine-type N [8, 35].

However, pyrroles derivatives can be generate also by degradation of chlorophyll, while pyridine and methylpyridine are also typical pyrolysis products formed by the reaction between amino groups and sugars (Maillard reaction) [36].

Indoles and phenols as produced by side chains of tyrosine and triptophane amino acid residues of proteins[37].

Finally, thermal degradation of amino acids, peptides or proteins can give 2,5-diketopiperazines (DKPs) (e.g. Cyclo (Gly-Gly), Cyclo (Ala-Ala) by condensation, depolymerization and cyclization reactions [38].The suite of N-containing compounds detected in *D. communis* bio-oil are in accordance with the results obtained by Harman-Ware and co-workers using a spouted bed reactor [10].

Pyrolysis of lipids gives fatty acids and hydrocarbons (alkane and alkenes) produced by fatty acids pyrolysis/decarboxylation or β-cleavage [39]. Furthermore, from pyrolysis of lipids several phytosterols are produced [40].Pyrolysis of carbohydrates gives rise to anhydrosugars, such as levoglusocan, galactosan, and furans that are identified as silylated derivatives in the *D. communis* bio-oil.

The compounds observed in bio-oil constitute the composition of pyrolysis vapours that flow through the zeolite bed in catalytic bench scale pyrolysis. The effect of catalysts on pyrolysis vapour was investigated by Py-GC-MS of bio-oil/catalyst mixtures.

Table 3.1.1: Elemental analysis (* Oxygen was calculated by difference)

Sample	**N**	**C**	**H**	**S**	**Ash**	**O***
D. communis	5.8	34.7	5.6	0.1	19.7	34.1
Bio-oil	6.8	60.3	8.7	n.d.	n.d	24.2

Table 3.1.2: GC-MS analysis of silylated, TMS (trimethylsilyl), bio-oil sample. RT, retention time, *m/z*, mass to charge ratio. (*) C, carbohydrates; Ch, Chlorophyl; L, lipids; M, Maillard reaction, P, protein, U, Unknown

#	**RT**	***m/z***	**Compound**	**Origin***
1	7.96	75, 116	alanine bisTMS	P
2	8.12	94, 107	dimethyl pyrroles	P, Ch
3	8.25	75, 143	hydroxybutenone TMS	U
4	9.42	73, 116, 130	aminobutyric acid TMS	?
5	9.65	81, 155, 170	2-hydroxymethylfuran TMS	C
6	9.85	80, 94, 109	C3-pyrrole	P, Ch
7	9.85	94, 108, 109	2,3,4-trimethylpyrrole	P, Ch
8	10.2	91, 117, 118	Propenylbenzene	?
9	10.28	113, 143, 157	pentenoic acid TMS	L
10	10.44	75, 117, 173	exanoic acid TMS	L
11	10.7	151, 166	phenol TMS	P
12	11.53	73, 125, 140	imidazole TMS	^
13	11.63	167, 182	1,3-dihydroxybenzene bisTMS	^
14	11.69	116, 131, 158	ND	^
15	12.09	135, 165, 180	2-methylphenol TMS	P
16	12.18	73, 152, 167	hydroxypyridine TMS	M
17	12.27	91, 165, 180	3-methyphenol TMS	P
18	12.29	51, 90, 117	Benzilnitrile	P
19	12.36	100, 142, 157	2-pyrrolidone TMS	P

20	12.46	91, 165, 180	4-methylphenol TMS	P
21	12.7	73, 152, 167	hydroxypyridine TMS	M
22	12.8	73, 149, 164	ND	^
23	12.96	168, 151	ND	^
24	13.08	166, 181	methyl hydroxypyridine TMS	M
25	13.28	166, 181	methyl hydroxypyridine TMS	M
26	13.62	105, 179, 194	ethylphenol TMS	^
27	13.82	105, 179, 194	dimethylphenol TMS	^
28	13.89	180, 195	ND	^
29	13.91	65, 91, 131	Benzenepropanenitrile	P
30	14.31	75, 182	ND	^
31	14.46	73, 205, 218	glycerol triTMS	L
32	14.54	177, 193, 208	ND	^
33	14.58	183	ND	^
34	14.81	89, 90, 117	Indole	P
35	15	73, 239, 254	1,2-dihydroxybenzene bisTMS	C
36	15.12	196	ND	^
37	15.29	255, 271, 286	Cyclo (Ala-Ala) diTMS	P
38	15.46	255, 271, 286	Cyclo (Ala-Ala) diTMS	P
39	15.84	73, 197, 212	ND	
40	15.93	241, 257, 272	Cyclo (Gly-Ala) diTMS	P
41	16.07	77, 130, 131	3-methylindole	P
42	16.15	73, 239, 254	1,4-dihydroxybenzene bisTMS	^
43	16.16	170, 285, 300	cyclodipeptide TMS	P
44	16.19	243, 255, 270	dehydro cyclo (Gly-Ala) diTMS	P
45	16.2	100, 243, 258	Cyclo (Gly-Gly) diTMS	P
46	16.57	197, 211, 226	ND	
47	16.61	170, 285, 300	cyclodipeptide TMS	P
48	16.67	73, 174, 189	indole TMS	P
49	16.67	271, 299, 314	cyclodipeptide TMS	P
50	16.68	181, 224	ND	^
51	16.74	80, 171, 211	ND	^
52	16.83	43, 57, 71	Alkane	L
53	16.84	43, 57, 71	Alkane	L
54	16.9	271, 299, 314	cyclodipeptide TMS	P
55	17.21	55, 69, 83	n-pentadec-1-ene	L
56	17.31	43, 57, 71	n-pentadecane	L
57	18.27	130, 160, 204	ftalamide TMS	^
58	18.41	55, 69, 83	n-exadec-1-ene	L
59	18.49	43, 57, 71	n-exadecane	L
60	18.96	73, 191, 217	anhydrosugar xTMS	C
61	19.06	43, 57, 71	Alkane	L
62	19.45	117, 257	dodecanoic acid TMS	^
63	19.45	73, 217, 204	galactosan triTMS	C
64	19.64	57, 71, 240	n-heptadecane	Ch
65	19.71	73, 204, 217	mannosan triTMS	C
66	19.95	73, 204, 217	levoglucosan triTMS	C

67	19.97	55, 69, 266	Pristene	Ch
68	20.09	55, 69, 266	pristene isomer	Ch
69	20.15	70, 97, 168	Cyclo (Pro-Ala)	P
70	20.41	70, 97, 168	Cyclo (Pro-Ala)	P
71	20.72	43, 57, 71	n-octadecane	L
72	21.08	55, 70, 280	2-exadecene, 3,7,11,15-tetramethyl	Ch
73	21.11	70,125, 154	Cyclo (Pro-Val)	P
74	21.15	95, 123, 278	Phytadiene	^
75	21.22	55, 70, 280	2-exadecene, 3,7,11,15-tetramethyl	Ch
76	21.31	70,125, 154	Cyclo (Pro-Val)	P
77	21.38	95, 123, 278	Phytadiene	^
78	21.59	95, 123, 278	Phytadiene	^
79	21.8	95, 123, 278	Phytadiene	^
80	22.15	70,125, 154	Cyclo (Pro-Ile)	P
81	22.24	70,125, 154	Cyclo (Pro-Ile)	P
82	22.34	70,125, 154	Cyclo (Pro-Leu)	P
83	22.41	70, 96, 194	Cyclo (Pro-Pro)	P
84	22.47	70,125, 154	Cyclo (Pro-Leu)	P
85	23.19	117, 313	palmitic acid TMS	L
86	23.68	43, 57, 71	Heneicosene	L
87	24.39	73, 143	phytol TMS	L
88	24.56	43, 57, 71	C22-alkene	L
89	24.74	117, 339, 354	oleic acidTMS	L
90	24.95	117, 341, 356	stearic acid TMS	L
91	25.42	43, 57, 71	C23-alkene	L
92	26.24	43, 57, 71	C24-alkene	L
93	26.27	379, 394	ND	L
94	27.04	43, 57, 71	C25-alkene	L
95	27.22	57, 250, 292	Eicosanenitrile	L+P
96	27.58	147, 371, 459	1-monopalmitin bisTMS	L
97	27.81	43, 57, 71	C26-alkene	L
98	27.82	239, 371, 459	monopalmitin bisTMS	L
99	28.12	117, 397, 412	docosanoic acid TMS	L
100	28.53	43, 57, 71	C27-alkene	
101	29.23	147, 399, 487	monostearin bisTMS	L
102	29.25	43, 57, 71	C28-alkene	^
103	29.33	117, 425, 440	tetracosanoic acid TMS	^
104	29.96	43, 57, 71	C29-alkene	^
105	30.55	223, 488	tocopherol TMS	^
106	30.8	255, 379, 394	Sterene	L
107	30.84	253, 379, 394	Steratriene	L
108	30.95	55, 255, 351, 379, 394	Stigmastantriene	L
109	31.19	253, 379, 394	Sterene	L
110	31.32	467	C31 alkanole TMS	^
111	31.5	73, 237, 502	alpha-tocopherol (Vit. E) TMS	^
112	32.54	495	C33 alkanole TMS	^
113	32.69	255, 457, 472	ergosterene TMS	^

114	32.76	255, 343, 484	sterol TMS	L
115	32.77	495	ND	L
116	32.89	255, 469, 484	stigmasterol TMS	L
117	33.14	117, 509, 524	sterol TMS	
118	33.15	363, 469, 484	sterol TMS	L
119	33.26	255, 471, 486	Sterol (hydro)	
120	33.84	523	C35 alkanole TMS	L
121	37.68	371, 385, 625	1,3-dipalmitin TMS	L

3.1.3.2 Py-GC-MS

Pyrograms of bio-oil sample and bio-oil-catalysts mixture with 1:20 ratio are depicted in Figure 3.1.2.

Catalytic pyrolysis by zeolite H-ZSM5 showed the best results for bio-oil upgrading comparing to Ti- and Sn- mesophases in terms of hydrocarbons production.

On the basis of the most abundant pyrolysis products detected by Py-GC-MS (Table 3.1.3) using H-ZSM5 at ratio 1:20 as catalyst a sharp increase of monoaromatic hydrocarbons such as toluene, m/p-xylene and C3-benzenes and a decrease of oxygenated compounds (phenol and palmitic acid) and also a partial decrease of nitrogen-containing compounds were observed.

Ti and Sn MCM-41 showed pyrograms similar to the non-catalytic bio-oil. Comparing the relative abundance of non-catalytic bio-oil and bio-oil with MCM-41 (Table 3.1.3), a slight increase of aromatic hydrocarbons such as toluene and C2-benzenes and a decrease of nitrogen-containing compounds and oxygenated was observed.

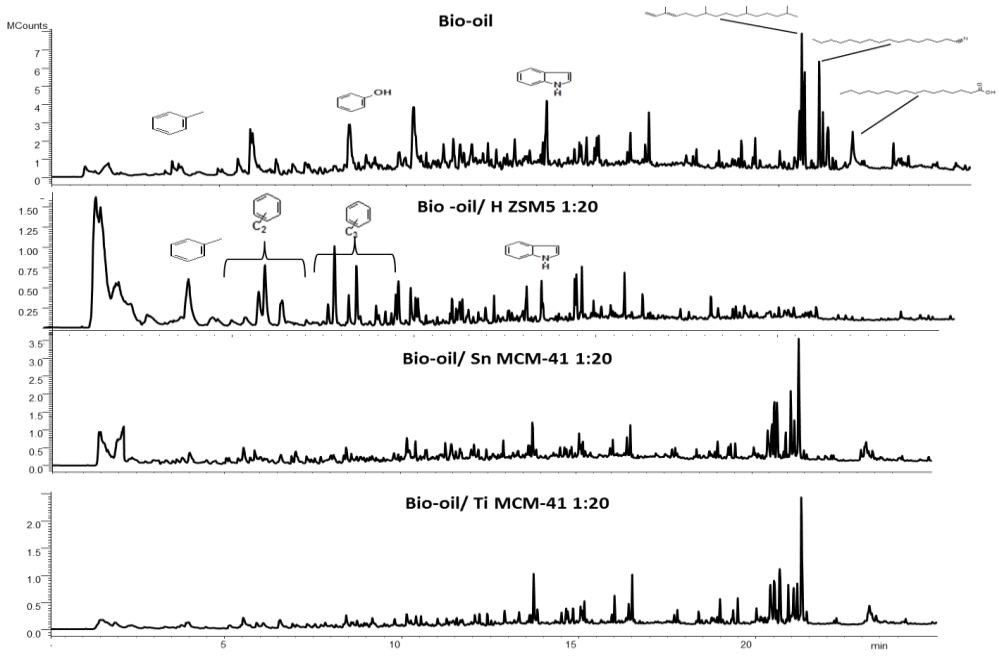

Figure 3.1.2: Py-GC-MS of bio-oil/catalyst mixture with 1:20 ratio (wt/wt) at 600°C.

Table 3.1.3: Py-GC-MS of bio-oil/catalyst mixture with 1:20 ratio (wt/wt) at 600°C. Relative abundance (% peak area) of pyrolysis products with % RSD (n=3)

#	*Compound*	*bio-oil*	*H-ZSM-5*	*RSD %*	*Ti MCM-41*	*RSD %*	*Sn MCM-41*	*RSD %*
1	Benzene	0.33	4.9	89	1	141	1.8	20
2	Pyrrole	8.58	0	0	6.1	55	7.9	0
3	Toluene	2.6	26	18	16.8	61	10.8	22
4	Ethyl benzene	1.27	8	21	4.8	11	1.4	68
5	m-xylene	1.17	14.8	11	2.1	27	1.6	7
6	p-xylene	0.66	3.5	50	2.4	67	1.4	26
7	C3 benzene (1)	0.68	7.8	139	2.1	48	1.2	13
8	Phenol	28.48	2.1	39	4	33	7.4	10
9	C3 benzene (2)	0.67	8.1	4	1.7	29	0.7	5
10	Indole	19	4.2	44	10.3	45	11.7	12
11	1-methyl indole	4.26	0.7	32	4.6	41	4.5	23
12	Phytadiene (1)	5.7	-	-	-	-	4.2	11
13	Phytadiene (2)	4.15	-	-	-	-	4.6	3
14	Exadecanenitrile	1.21	0.6	141	7.3	47	7.6	21
15	Palmitic acid	0.82	-	-	-	-	-	-

Comparable results have been observed using the mixture algae-catalyst in place of bio-oil (Fig.3.1.3). High percentages of aromatic hydrocarbons (Table 3.1.4) were obtained with H-ZSM5 but MCM-41 even showed pyrograms similar to the non-catalytic pyrolysis. In addition, only slight differences in terms of hydrocarbons production were observed when biomass was used in the mixture with respect to the non-catalytic bio-oil.

These results confirm that the catalytic cracking of the pyrolysis vapors of algae can be investigated by Py-GC-MS of biomass/catalyst mixtures. In addition, the superior cracking efficiency of HZSM5 over MCM-41 was demonstrated. Therefore, zeolite H-ZSM5 was selected for detailed Py-GC-MS and bench scale experiments.

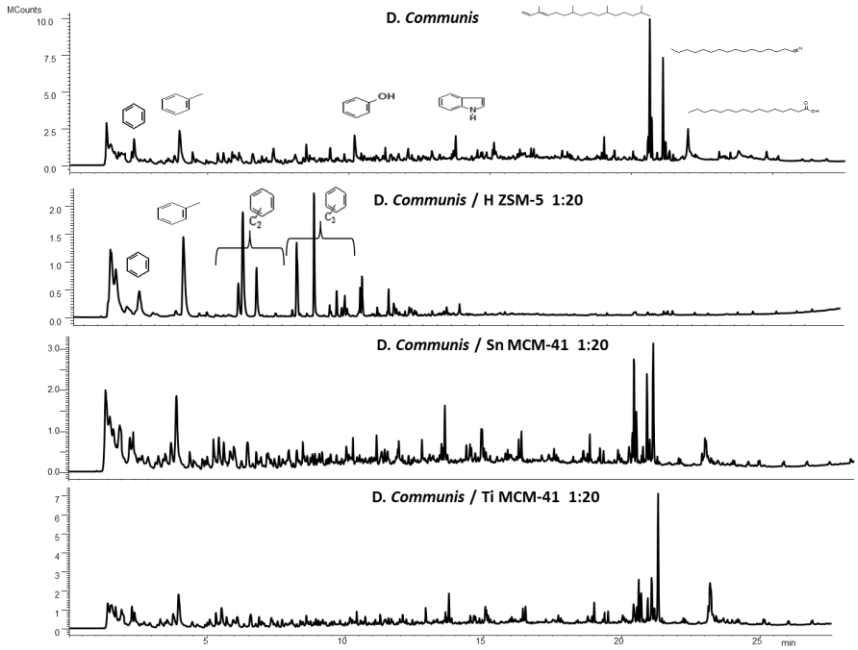

Figure 3.1.3: Py-GC-MS of biomass/catalyst mixture with 1:20 ratio (wt/wt) at 600°C

Table 3.1.4: Py-GC-MS of biomass/catalyst mixture with 1:20 ratio (wt/wt) at 600°C. Relative abundance (% peak area) of pyrolysis products with % RSD (n=3)

#	*Compound*	*algae %*	*ZSM-5*	*RSD %*	*Ti MCM-41*	*RSD %*	*Sn MCM 41*
1	Benzene	1.3	7.2	15	2.4	63	4.1
2	Pyrrole	6.3	0.4	141	11	9	10.1
3	Toluene	29.5	25.7	3	33.2	12	35.7
4	Ethyl benzene	2.7	6.3	26	3	3	3.4
5	m-xylene	4.1	16.9	15	5.7	14	5.3
6	p-xylene	0.9	5.7	13	1.8	4	2
7	C3 benzene (1)	0	11.5	4	1.5	3	1.3
8	Phenol	7.2	0.2	92	0.8	141	0.8
9	C3 benzene (2)	0.3	11	11	1.2	31	0.8
10	Indole	7.6	0.3	56	8.4	8	8.3
11	1-methyl indole	4.3	0.7	130	3.5	7	3.6
12	Phytadiene (1)	12.5	-	-	1.3	141	3.6
13	Phytadiene (2)	6.2	-	-	1.9	72	2.4
14	Exadecanenitrile	0.4	0.2	105	4.9	79	3.3
15	Palmitic acid	1.6	-	-	-	-	-

The effect of lower levels of catalyst was studied by pyrolysing samples with biomass/catalyst ratios1:5 and 1:10 (Fig. 3.1.3). The results are reported in Table 3.1.5 and compared with those relative to the 1:20 ratio. The %RSD were relatively high probably due to sample small amount and inhomogeneity, however, trends could be evidenced.

The results obtained by means of Py-GC-MS showed the best efficiency of H-ZSM5 for catalytic pyrolysis of microalgae in accordance with other studies in literature [9, 11, 14-16]. A biomass/zeolite ratio of 1:5 was sufficient to promote a pyrolysate dominated by hydrocarbons (58% relative abundance). These results can be compared with those reported by Thangalazhy-Gopakumar et al. [15] and Du et al. [9] showing that more significant change in composition of bio-oil from when HZSM5 cracking of green algae was performed with at least 1:4 biomass/catalyst ratio.

The relative content of nitrogen/oxygen containing compounds decreased from 21% to 13% and 2% with increasing zeolite load. The 1:20 biomass to catalyst guaranteed an efficient denitrogenation/deoxygenation and cracking of phytadienes, while the 1:5 ratio resulted in a pyrolysate with important levels of indoles, phenol, pyrrole and phyadienes.

A ten-fold excess of zeolite could represent a good balance between significant cracking and defunctionalisation and zeolite load. Therefore, catalytic pyrolysis experiments on bench scale were performed with a 1:10 biomass to catalyst ratio.

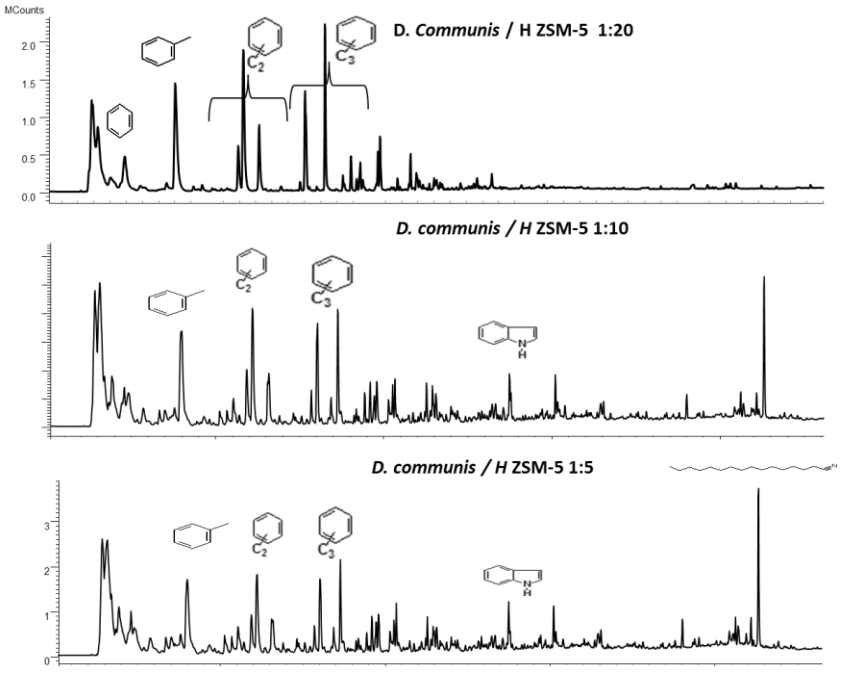

Figure 3.1.4: Py-GC-MS of biomass/H-ZSM5 mixture with 1:20, 1:10 and 1:5 ratios (wt/wt) at 600°C

Table 3.1.5: Py-GC-MS of biomass/H-ZSM5 mixture with 1:20, 1:10 and 1:5 ratios (wt/wt) at 600°C. Relative abundance (% peak area) of the main pyrolysis products with % RSD (n=3).

#	*Compound*	1:5	RSD %	1:10	RSD %	1:20	RSD%
1	Benzene	3.1	49	5	14	7.2	15
2	Pyrrole	4.7	64	2.3	33	0.4	141
3	Toluene	23.1	7	25.6	6	25.7	3
4	Ethyl benzene	4.5	41	6.3	10	6.3	26
5	m-xylene	10.8	29	12.9	9	16.9	15
6	p-xylene	2.2	54	3.4	15	5.7	13
7	C3 benzene (1)	8.7	35	10.4	4	11.5	4
8	Phenol	3	51	1.7	2	0.2	92
9	C3 benzene (2)	5.4	54	7.1	11	11	11
10	Indole	5.6	52	3	12	0.3	56
11	1-methyl indole	4.3	29	3.1	21	0.7	130
12	Phytadiene (1)	1.6	107	0.2	141	-	-
13	Phytadiene (2)	1.5	110	0.1	25	-	-
14	Exadecanenitrile	4.3	59	2.7	55	0.2	105
15	Palmitic acid	0.3	141	-	-	-	-

3.1.3.3 Catalytic pyrolysis on bench scale reactor

The yields of the different fractions obtained after each batch of catalytic pyrolysis with HZSM5 are reported in Table 3.1.6.

Overall, the sum of different fractions shows an average value of 73.5 ± 4.5 % (18% RSD) with a maximum of 84% on the 6th batch and a minimum of 66 % on the 3rd batch.

Non-condensable gas average yield is 26.5 % (by difference).

The first trap showed two phases: an aqueous phase (AP_{T1}) with a thin layer of organic phase (OP_{T1}) suspended on the top. The second trap was a yellowish solution of n-heptane (OP_{T2}) with a visible of aqueous phase at bottom (AP_{T2}). In Table 3.1.7 are shown the percentage yield for each separated fraction.

Table 3.1.6: Yield % of condensation trap 1 (T1), heptane dissolution trap (T2), adsorption trap (XAD), char and coke for each batch experiment; Average values and SD and RSD%

Batch	1	2	3	4	5	6	7	Average	SD
T1	24.67	23	15.59	21.67	23.33	31	22.67	23.1	4.5
T2 (heptane)	4.33	3.33	6.1	6.33	7.33	3.67	2.67	4.8	1.6
XAD	2.23	1.86	1.26	1.21	1.42	0.51	0.96	1.3	0.5
CHAR	32.3	31.3	31.5	30.3	30.3	30.3	30.0	30.9	0.8
COKE	8.67	14.0	11.2	13.0	10.7	18.7	16.7	13.3	3.2

Table 3.1.7: % Yield of separated fractions (AP aqueous phases and OP organic phase in T1 and T2 raps).

	%
AP_{T1}	19.7
OP_{T1}	1.1
AP_{T2}	1.7
OP_{T2}	4.6
XAD	1.3
gas	28.5

The overall yield of the organic phases in the three trap systems was around 8%. Apparently, the solubilisation trap was more efficient; however, the corresponding organic phase could not be isolated. Moreover, a significant fraction of the organic phase was trapped onto the resin.
Less than yields from catalytic cracking of microalgae reported in literature [12, 14, 16, 17]. However, published studies reported catalytic bio-oil with a higher content of oxygenated and nitrogen-containing compounds.
The elemental composition of the fractions is reported in Table 3.1.8. In the case of OP_{T2} and XAD, the fractions could not be isolated for the elemental analysis, elemental composition was estimated by molecular composition obtained by GC-MS analysis. The OP_{T1} showed a high percentage of carbon (77.6%) and rather low oxygen content (7.8%) comparing to the thermal bio-oil (27.9%). The OP_{T2} presented a high carbon content of 91.2 % associated with the GC-MS composition featured by the presence of aromatic hydrocarbons, while oxygenated compounds were not detected.

Table 3.1.8: Elemental analysis of different fractions obtained after catalytic pyrolysis with HZSM5 (AP aqueous phases and OP organic phase in T1 and T2 raps).

	N	**C**	**H**	**O**	**Ash**
CHAR	6.59	51.3	1.92	8.13	32
COKE	0.15	2.67	0.26	0.93	96
AP_{T1}	11.3	4.44	17.5	66.7	-
OP_{T1}	6.1	77.6	8.51	7.8	-
AP_{T2}	15.1	29.4	15.6	39.9	-
OP_{T2}*	n.d.	91.2	8.83	n.d.	-
XAD*	n.d.	91.1	8.93	0.04	-
gas*	n.d.	38.4	6.09	55.5	-

(*estimated values by GC-MS analysis)

3.1.3.4 GC-MS of liquid fractions

An aliquot of organic fraction solubilized in heptane s (OPT_2) was analyzed by GC-MS.

Because of the low organic phase yield obtained from trap 1 (see Tab. 3.1.7), OPT_1 was solubilized with heptanic OPT_2 solution to the end of performing GC-MS analysis. Chromatograms of OPT_2 and combined OPT_1 and OPT_2 are depicted in Figure 3.1.5.

Table 3.1.9 showed the percentage relative abundance of the main detected peaks.

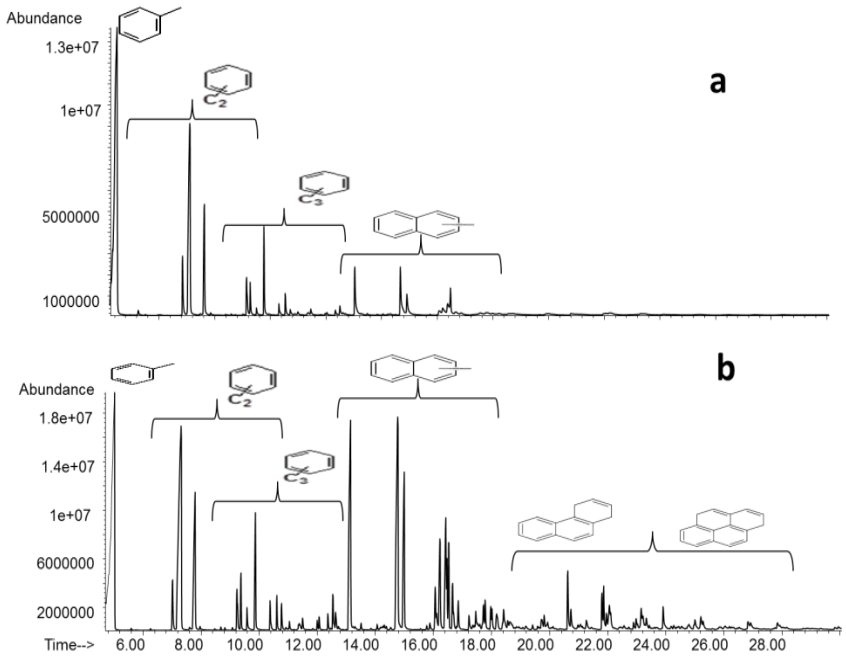

Figure 3.1.5:chromatogram of organic liquid fractions : heptane solution (OPT_2) (a) and combined organic fractions (OPT_1+OPT_2) (b).

OPT_2 chromatogram (Fig. 3.1.5a) was mainly characterized by C7-C9 aromatic hydrocarbons that totally accounted for 88 % of the total relative abundance while the other 12% of total relative abundance (Table 3.1.9) was due by naphthalene and alkyl naphthalenes (C1- and C2-naphthalenes). Interestingly, N- and O-containing compounds were not detected.

In comparison, the GC-MS analysis of the combined organic phases (Fig. 3.1.5b) showed a significant presence of polyaromatic hydrocarbons (naphthalenes , phenanthrenes) and pyrenes) deriving from the organic phase condensed in the first trap (OPT_1) were observed in accordance with Wang et al. who observed the same compounds in the catalytic pyrolysis of *Chlorella vulgaris* over H-ZSM5 [14].The formation of naphthalenes from zeolite cracking of algae was observed by Py-GC-MS in other studies [9, 30].

The presence of 3- and 4-ring polyaromatic hydrocarbons (PAHs), after catalytic cracking is interesting taking into account that pores diameter of HZSM5 is 6 Å which is equivalent to kinematic diameter of naphthalene, so larger molecules should not pass out of H-ZSM5 [16]

but remain in the pores going to form coke [41]. Moreover, 3- and 4-rings PAHs were not detected in Py-GC-MS analysis (Tab. 3.1.5).

However, PAHs may form by secondary reactions on the catalyst surface either directly or via reaction of the smaller aromatics [42].

Table 3.1.9: Main compounds and relative abundance (% of tot. peak area) from organic fractions (OPT_1 and OPT_2)

Compound	***OPT_1+OPT_2***	***OPT_2***
Toluene	22.5	49.3
Ethyl benzene	1.2	3.1
m-xylene	13.6	19.6
p-xylene	4.9	6.7
C3-benzenes	6.5	9.1
Naphthalene	8.4	3.1
C1-naphthalenes	14.3	5.5
C2-naphthalenes	10.7	3.6
C3-naphthalenes	3.6	-
Fluorene	0.8	-
Phenanthrenes	8.0	-
Pyrenes	2.7	-

The composition of the organic phases obtained from preparative catalytic pyrolysis showed similarities with the pyrograms resulting from analytical pyrolysis (Py-GC-MS). The principal difference was the occurrence of N-and O-containing compounds in the pyrograms of the samples with 1:10 biomass/zeolite ratio. These compounds could be distributed preferentially in the water phase of the first trap (APT_1). To gather some information on its molecular composition, this phase was sampled by SPME and analysed by GC-MS. Nitrogenated compounds could be identified (indoles, benzenamines) at proportions comparable to those of hydrocarbons (Tab.3.1.10). Phenols could also be identified. However, the content of carbon in APT_1 was rather low (4%, table 3.1.8) and probably mostly in the form of inorganic ions. It is presumable that organic compounds were present in the water phase at trace levels. When comparing the GC-MS traces of the organic phase (Fig.3.15) with MS-pyrograms relative to different biomass/zeolite ratios (Fig. 3.1.4) it is apparent that the stronger resemblance was found for the 1:20 ratio. This finding would indicate that a higher load of zeolite is required when Py-GC-MS is utilized in order to predict the cracking behavior of biomass in preparative pyrolysis with a catalytic bed. Probably the effect is due to the fact that Py-GC-MS is a faster process.

Table 3.1.10: Main compounds and relative abundance (% of tot. peak area) detected by SPME-GC-MS into APT_1 fraction.

#	Compound	A%	#	Compound	A%
1	Methyl isonitrile	7.09	16	Dialin	0.38
2	Propan-nitrile	1.74	17	C2-phenol	0.56
3	Toluene	4.7	18	C2-benzenamine	0.21
4	Ethyl benzene	1.0	19	Naphthalene	14.4
5	m-xylene	4.2	20	Trimethylstyrene	0.25
6	p-xylene	2.8	21	C2-indane	0.34
7	C3-benzene	1.4	22	C2-indane	0.24
8	C3-benzene	4.6	23	2-methyl naphthalene	16.4
9	Aniline	3.40	24	Indole	6.8
10	Phenol	2.1	25	Methyl indole	0.72
11	C3-benzene	1.5	26	C2-naphthalene	2.6
12	C3-benzene	0.48	27	C2-naphthalene	8.7
13	Methyl phenol	2.2	28	Azulene derivative	0.40
14	Methylbenzenamine	5.5	29	C3-naphthalene	3.08
15	Dimethyl styrene	1.6	30	Fluorene	0.30
				TOT.	**100**

3.1.4 Conclusions

In this study catalytic screening by Py-GC-MS using mesoporous materials (MCM-41) and HZSM-5 zeolite was investigated on *D. communis*. Similar results were obtained when the original algal biomass or the bio-oil obtained after pyrolysis were utilized as substrates. Therefore, Py-GC-MS of biomass/catalyst mixture can be used as simple substrate to mimic the catalytic cracking of the pyrolysis vapours.

HZSM-5 showed the best results in terms cracking efficiency (aromatic hydrocarbons production) in comparison with MCM-41 catalysts. Probably the role of acid groups is more important than the accessibility of rather large molecules (pyrolysis products) into the pores. Py-GC-MS showed that the denitrogenation/deoxygenation increased with increasing zeolite load. N- and O-containing compounds were relatively abundant in the pyrograms from 1:5 catalyst biomass/zeolite ratio, but became insignificant using the 1:20 ratio. The composition of the pyrograms obtained with the 1:20 biomass/zeolite ratio was similar to that of the organic phase obtained by the zeolite pyrolysis with a bench scale reactor using a 1:10 ratio. The composition observed form analytical and preparative zeolite pyrolysis was featured by the predominance of alkylated monoaromatic hydrocarbons similar to that found in gasoline. The yield of the organic phase was rather low (around 8%) in accordance to the severe cracking and defunctionalisation of the pyrolysis vapours.

Although the small proportion of polycyclic aromatic hydrocarbons detected in the catalytic oil, the scale-up to bench scale confirmed the results obtained with analytical pyrolysis in terms of monoaromatic hydrocarbons highlighting the good performance of Py-GC-MS as a suitable and fast screening technique to studying catalytic pyrolysis process and bio-oil composition.

References

[1] Naik, S. N., Goud, V. V., Rout, P. K., Dalai, A. K. (2010). Production of first and second generation biofuels: a comprehensive review. Renewable and Sustainable Energy Reviews, 14(2), 578-597

[2] Rathmann, R., Szklo, A., Schaeffer, R. (2010). Land use competition for production of food and liquid biofuels: An analysis of the arguments in the current debate. Renewable Energy, 35, 14-22

[3] Chen, W. H., Lin, B. J., Huang, M. Y., Chang, J. S. (2015). Thermochemical conversion of microalgal biomass into biofuels: A review. Bioresource Technology, 184, 314-327

[4] Chen, W.H., Huang, M.Y., Chang, J.S., Chen, C.Y., (2014). Thermal decomposition dynamics and severity of microalgae residues in torrefaction. Bioresour. Technol. 169, 258–264.

[5] Peterson A., Vogel F., Lachance R., Fröling M., Antal M., Tester, J., (2008) Thermochemical biofuel production in hydrothermal media: a review of sub- and supercritical water technologies, Energy & Enviromental Science, 1, 32-65

[6] Lopez Barreiro D., Prins W., Ronsee F., Brilman W., (2013), Hydrothermal liquefaction (HTL) of microalgae for biofuel production: state of art review and future prospects, Biomass Bioenergy, 53, 113-127

[7] Garcia Alba L., Torri C., Samori C., van der Spek J., Fabbri D., Kersten S.R.A., Brilman, W., (2012), Hydrothermal treatment (HTT) of microalgae: evaluation of the process as conversion method in an algae biorefinery concept, Energy Fuels, 26, 642-657

[8] Torri C., Garcia Alba, L., Samorì, C., Fabbri, D., Brilman, W., (2012). Hydrothermal treatment (HTT) of microalgae: detailed molecular characterization of HTT oil in view of HTT mechanism elucidation. Energy Fuels, 26, 658-671.

[9] Du, Z., Hu, B., Ma, X., Cheng, Y., Liu, Y., Lin, X., Wan, Y., Lei, H., Chen, P., Ruan, R., (2013), Catalytic pyrolysis of microalgae and their three major components: carbohydrates, proteins, and lipids. Bioresour. Technol. 130, 777–782.

[10] Harman-Ware, A.E., Morgan, T., Wilson, M., Crocker, M., Zhang, J., Liu, K., Stork, J., Debolt, S., (2013). Microalgae as a renewable fuel source: fast pyrolysis of Scenedesmus sp. Renewable Energy 60, 625–632.

[11] Babich, I.V., Hulst, M.V.D., Lefferts, L., Moulijn, J.A., O'Connor, P., Seshan, K., (2011). Catalytic pyrolysis of microalgae to high-quality liquid bio-fuels. Biomass Bioenergy 35, 3199–3207.

[12] Campanella, A., Harold, M.P., (2012). Fast pyrolysis of microalgae in a falling solids

reactor: effects of process variables and zeolite catalysts. Biomass Bioenergy 46, 218–232.

[13] Kim, S.W., Koo, B.S., Le, D.H., (2014). A comparative study of bio-oils from pyrolysis of microalgae and oil seed waste in a fluidized bed. Bioresour. Technol. 162, 96–102

[14] Wang, K., Brown, R.C., (2013). Catalytic pyrolysis of microalgae for production of aromatics and ammonia. Green Chemistry, 15, 675-681

[15] Thangalazhy-Gopakumar, S., Adhikari, S., Chattanathan, S. A., Gupta, R. B. (2012). Catalytic pyrolysis of green algae for hydrocarbon production using H+ ZSM-5 catalyst. Bioresource technology, 118, 150-157.

[16] Pan, P., Hu, C., Yang, W., Li, Y., Dong, L., Zhu, L., Tong, D., Qing, R., Fan, Y., (2010). The direct pyrolysis and catalytic pyrolysis of Nannochloropsis sp. residue for renewable bio-oils. Bioresour. Technol. 101, 4593–4599.

[17] Tran, N.H , Bartlett, J.R, Kannangara, G.S.K., Milev, A.S., Volk, H., Wilson. M.A., (2010) Catalytic upgrading of biorefinery oil from micro-algae, Fuel 89, 265–274

[18] Chen, Y., Wu, Y., Hua, D., Li, C., Harold, M. P., Wang, J., Yang, M. (2015). Thermochemical conversion of low-lipid microalgae for the production of liquid fuels: challenges and opportunities. RSC Advances, 5, 18673-18701

[19] Williams P.T., Horne P.A., (1994). Characterisation of oils from the fluidised bed pyrolysis of biomass with zeolite catalyst upgrading. Biomass Bioenerg. 7, 223-236

[20] Vitolo S., Seggiani M., Frediani P., Ambrosini G., Polit L., (1999). Catalytic upgrading of pyrolytic oils to fuel over different zeolites, Fuel 78, 1147-1159,

[21] Torri C., Reinikainen M., Lindfors C., Fabbri D., Oasmaa A., Kuoppala E., (2010). Investigation on catalytic pyrolysis of pine sawdust: catalyst screening by Py-GC-MIP-AED. J. Anal. Appl. Pyrolysis 88, 7-13.

[22] Carlson T., Vispute T.P., Huber G., (2008). Green gasoline by catalytic fast pyrolysis of solid biomass derived compounds. ChemSusChem 1, 397-400

[23] French R., Czernik S., (2010). Catalytic pyrolysis of biomass for biofuels production. Fuel Processing Technology 91, 25-32

[24] Mullen CA, Boateng AA., (2010). Catalytic pyrolysis-GC-MS of lignin from several sources. Fuel Processing Technology 91, 1446-1458.

[25] Aho A., Kumar N., Eranen K., Salmi T., Hupa M., Murzin D.Y. (2008). Catalytic pyrolysis of woody biomass in a fluidized bed reactor: influence of of the zeolite structure. Fuel 87, 2493-2501

[26] Díaz-Rey, M. R., Cortés-Reyes, M., Herrera, C., Larrubia, M. A., Amadeo, N., Laborde, M., Alemany, L.J., (2014). Hydrogen-rich gas production from algae-biomass by low temperature catalytic gasification. Catalysis Today, 257, 177-184

[27] Obeid, W., Salmon, E., Lewan, M. D., Hatcher, P. G. (2015). Hydrous pyrolysis of Scenedesmus algae and algaenan-like residue. Organic Geochemistry, 85, 89-101

[28] Blokker, P., Schouten, S., van den Ende, H., de Leeuw, J. W., Hatcher, P. G., Damsté, J. S. S. (1998). Chemical structure of algaenans from the fresh water algae Tetraedron minimum, Scenedesmus communis and Pediastrum boryanum. Organic Geochemistry, 29, 1453-1468.

[29] Samorì, G., Samorì, C., Guerrini, F., Pistocchi, R. (2013). Growth and nitrogen removal capacity of Desmodesmus communis and of a natural microalgae consortium in a batch culture system in view of urban wastewater treatment: Part I. Water research, 47, 791-801.

[30] Mante, O.D., Agblevor F.A., (2014) Catalytic pyrolysis for the production of refinery-ready biocrude oils from six different biomass sources. Green Chemistry, 16, 3364-3377

[31] Lorenzetti, C., Conti, R., Fabbri, D., Yanik, J. (2016). A comparative study on the catalytic effect of H-ZSM5 on upgrading of pyrolysis vapors derived from lignocellulosic and proteinaceous biomass. Fuel, 166, 446-452.

[32] Corma, A. (1997). From microporous to mesoporous molecular sieve materials and their use in catalysis. Chemical reviews, 97, 2373-2420.

[33] Iliopoulou, E. F., Antonakou, E. V., Karakoulia, S. A., Vasalos, I. A., Lappas, A. A., Triantafyllidis, K. S. (2007). Catalytic conversion of biomass pyrolysis products by mesoporous materials: Effect of steam stability and acidity of Al-MCM-41 catalysts. Chemical Engineering Journal, 134, 51-57.

[34] Torri, C., Lesci, I. G., Fabbri, D. (2009). Analytical study on the pyrolytic behaviour of cellulose in the presence of MCM-41 mesoporous materials. Journal of Analytical and Applied Pyrolysis, 85, 192-196.

[35] Knicker H., (2010). “Black Nitrogen”- an important fraction in determining the recalcitrance of charcoal. Organic Geochemistry 41, 947-950

[36] Du Z., Mohr M., ma X., Cheng Y., Lin X., Liu Y., Zhou W., Chen P., Ruan R., (2012). Hydrothermal pretreatment of microalgae for production of pyrolytic bio-oil with low nitrogen content. Bioresource Technology 120, 13-18

[37] Chiavari G, Galletti G.C. (1992). Pyrolysis-gas chromatography/mass spectrometry of amino acids. J. Anal. Appl Pyrol. 24, 123-137

[38] Fabbri, D., Adamiano, A., Falini, G., De Marco, R., Mancini, I. (2012). Analytical pyrolysis of dipeptides containing proline and amino acids with polar side chains. Novel 2, 5-diketopiperazine markers in the pyrolysates of proteins. Journal of Analytical and Applied Pyrolysis, 95, 145-155.

[39] Fabbri D., Bevoni V., Notari M., Rivetti F., (2007) Properties of a potential biofuel obtained from soybean oil by transmethylation with dimethyl carbonate. Fuel 86, 690-697 Furthermore, from pyrolysis of lipids several phytosterols are produced

[40] Patterson G.W., (1971). The distribution of sterols in algae. Lipids 6, 120-127

[41] Marcilla A., Gomez-Siurana A., Valdes F.J. (2008) Influence of the temperature on the composition of the coke obtained in the catalytic cracking of low density polyethylene in the presence of USY and HZSM-5 zeolites. Microporous and Mesoporous Materials, 109, 420-428

[42] Jae J., Tompsett G., Foster A., Hammond K., Auerbach S., Lobo R., Huber G., (2011). Investigation into the shape selectivity of zeolite catalysts for biomass conversion. J. Catal. 279, 257-268

3.2 A comparative study on the catalytic effect of H-ZSM5 on upgrading of pyrolysis vapours derived from lignocellulosic and proteinaceous biomass

3.2.1 Introduction

Energy consumption is continuously increased in the last decades due to the worldwide demographic growth and our way of living always more energy-consumptive.

Transportation and industrial sectors are the main energy end-users representing approximately two-third of total delivered energy [1]. Fossil fuel depletion as well as environment issues related to CO_2 emissions leads scientific research to find out alternative and renewable energies. Biomass is considered the most abundant renewable energy source carbon based which can substitute fossil fuels [2].

Pyrolysis can represent a promising technology converting woody and no woody biomass to liquid, solid and gaseous fuels. However, the bio-oil derived from pyrolysis is a complex mixture of hundreds of oxygenated compounds which cause bio-oil low end fuel properties, especially a low heating value, corrosiveness and instability [3-5]. Upgrading processes are then required in order to improve the bio-oil quality. A wide number of studies have investigated bio-oil quality enhancement using different approaches: high pressure hydro-treatment (HDO) [6,7], reactive pyrolysis [8], bio-oil distillation [9] and pyrolysis vapours upgrading through catalysts.

Among the catalysts used, zeolites have received much attention because of their ability to convert biomass-derived oxygenates into aromatic hydrocarbons [10-22,] and for being relatively inexpensive materials. The best results were obtained with H-ZSM-5. Catalytic upgrading over zeolite H-ZSM-5 of lignocellulosic biomass, model compounds and biomass main components (cellulose, hemicellulose and lignin) has been widely investigated by several researchers.

Catalytic pyrolysis over zeolite has been mainly studied by Py-GC-MS [18, 14, 22, 23, 24] and in pilot scale pyrolysis reactor [13, 23]. The upgrading process over zeolite produced primarily monoaromatics such as benzene and alkylbenzenes and polyaromatics (mainly naphthalenes). Mihalcik et al., [18] have studied the catalytic pyrolysis of different type of biomasses and main lignocellulosic components (cellulose, hemicellulose and lignin) by Py-GC-MS. They tested the different zeolites (H-Mordenite, H-ZSM-5, H-Y, H-Beta, and H-Ferrierite) and suggested that H-ZSM-5 was most effective at producing aromatic hydrocarbons. To determine the effect of crystal sizes of ZSM-5 and feedstock species on aromatic yield and selectivity, Zheng et al. studied the fast pyrolysis of different feedstock species (cellulose, hemicellulose, lignin, pine, corncob and straw) over ZSM-5 with varying

crystal size in a Pyroprobe pyrolyser [22]. They reported that the aromatic yield and aromatic selectivity were significantly affected by crystal size of ZSM-5 catalysts. Besides crystal size of catalyst, feedstock species also affected aromatic yield. Thus; cellulose exhibited the maximum aromatic yield of 38.4% and lignin showed the lowest aromatic yield of 10.2%. Similar result was observed by Wang et al., [19], who carried the catalytic pyrolysis of main lignocellulosic components (cellulose, hemicellulose and lignin) over H-ZSM5 catalyst in a micro pyrolyser. The yield of aromatic hydrocarbons decreased in the following order: cellulose > hemicellulose > lignin. Besides analytical pyrolysis experiments, the experiments carried out in pilot scale fluidized bed reactor have also showed that source of biomass plays an important role in product distribution and selectivity to aromatic hydrocarbons [23].

The deactivation of zeolite catalysts have been also investigated. Jae et al. studied the catalytic fast pyrolysis of wood using a spray-dried ZSM-5 catalyst in a lab-scale fluidized bed reactor [21]. ZSM-5 catalyst was stable in a series of 30 reaction/regeneration cycles. In contrast, catalyst deactivation was observed in the pilot plant's continuous operation process, relating to mainly accumulative ash deposition on the catalyst and partial framework dealumination of the fresh zeolite catalyst [13].

Although there is lesser number of studies in literature, the H-ZSM-5 upgrading on algae has also been investigated. Most of studies, focused on *Chlorella vulgaris* [14, 24, 25] and *Nannochloropsis* sp. [26] have showed that the catalytic pyrolysis of microalgae can be an attractive method to convert algal biomass in aromatic hydrocarbons. In addition, it was also reported that the negative properties of algal oil, such as high nitrogen and oxygen content, could be reduced by using high amount of ZSM-5 catalyst [14, 24]. Besides lignocellulosic and algal biomass, waste oils/fats have also been studied for production of new biofuels by pyrolysis [27-29]. In a study carried out by Varuvel et al., [27], waste fish fat was conducted to catalytic pyrolysis. The quality of bio-oils was tested from the point of combustion performance and emission parameters to investigate the suitability in diesel engines. In another study, catalytic pyrolysis of beef tallow and waste cooking oil was studied in closed system in presence of Pd/C catalyst [28]. In addition, Wisniewski Jr. et al., [29] studied the upgrading of pyrolysis oil obtained from waste wish oil by reactive distillation. But at the best of our knowledge, upgrading of pyrolysis oil obtained from fish discard with zeolite has not been studied yet.

Our work is a comparative study on the H-ZSM-5 effect on pine wood (lignocellulosic), two algal biomass, specifically Spirulina (*A. platensis*) (microalgae) and *Ulva lactuca* (seaweed)

and fish discard to better understand the role of the catalyst and of the biomass type on the aromatic hydrocarbon yield and distribution.

3.2.2 Experimental

3.2.2.1 Materials

In this study, two algal biomass, animal waste and lignocellulosic waste were used. Specifically, these were microalgae (Spirulina, *A. platensis*), seaweed (*Ulva lactuca*), fish discard and pine sawdust. Ulva lactuca was collected from Izmir coast on the Aegean Sea, Turkey. It was washed in water, dried in oven at 60 °C. Pine sawdust was provided by a local company in Bologna. Spirulina was cultivated in laboratory. Cells of Spirulina were collected by centrifugation and washed with distilled water, and then dried at 80 °C for 16 h under vacuum. The fish discard investigated in this study was provided by a local fishery vessel in Izmir bay. They was pre-dried at 105°C overnight and milled with a blender. The grounded discards were further dried at 80 °C under vacuum for 24 h. The main characteristics of biomass feedstocks are shown in Table 1.

The catalyst used is commercial H-ZSM-5 previously described in *paragraph 3.1*.

The resin used for trapping of volatiles was XAD-2 resin Amberlite (Supelco, Sigma Aldrich).

3.2.2.2 Analytical pyrolysis (Py-GC-MS)

Py-GC-MS analyses were performed using an electrically heated platinum filament CDS 5000 pyroprobe interfaced to a Varian 3400 GC equipped with a GC column (HP-5-MS; Agilent Technologies 30 m × 0.25 mm, 0.25 μm) and a mass spectrometer (Saturn 2000 ion trap, Varian Instruments). GC thermal program: 35°C to 310°C at 5°C min^{-1}; MS conditions: electron ionisation at 70 eV, full scans acquisition in the 10–450 m/z interval. A quartz sample tube containing around 10 mg of mixture with catalyst to feedstock ratio of 10 was inserted into the Py–GC interface (300°C) and then pyrolysed at 600°C (set temperature) for 100 s with helium as carrier gas (100 mL min^{-1}).

A set of 28 compounds were identified and the relative distribution (% peak area) of the main compounds was calculated. Py-GC-MS analyses were carried out in duplicate. Min-max %RSD and mean %RSD have been calculated for those compounds with % peak area largest than 1%. RSD values are following reported: *Pine*: min-max RSD (0-23 %) and mean RSD

(6%); *Fish*: min-max RSD (2-55 %) and mean RSD (26%); *Spirulina*: min-max RSD (0-47 %) and mean RSD (18%); *Seaweed*: min-max RSD (7-90 %) and mean RSD (31%).

3.2.2.3 Bench scale pyrolysis experiments

The experimental runs were performed in a same reactor previously described in *paragraph 3.1* but with a slightly modified experimental configuration (Fig 3.2.1). The reactor was heated under nitrogen flow with a flow rate of 100 mL min-1. After the system reached steady state at 460 °C, the basket containing feedstock was introduced into the reactor, just above the catalyst, thus only the vapors of pyrolysis are in contact with catalyst.

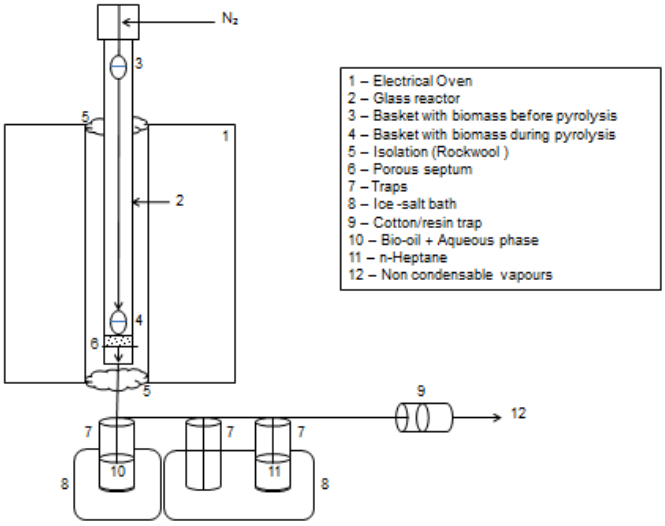

Figure 3.2.1: Experimental configuration of the reactor for thermal and catalytic pyrolysis. In catalytic pyrolysis, zeolite bed was placed between the basket (4) and the porous (6), and a third trap (7 with heptane) was added

The generated pyrolysis vapors were passed directly over the catalyst surface, before leaving through the bottom of the reactor. The volatiles leaving the reactor passed through two ice-salt cooled condensers at -14 °C, where liquid products were collected. In catalytic experiments, a third trap containing heptane solution was used to catch aerosols compounds. The rest of the flow from traps was passed through a filter packed with resin or cotton, which effectively trapped any remaining aerosols. The exhaust gas was vented. The liquid fraction obtained from non- catalytic pyrolysis was centrifuged at 3500 rpm for 15 min to separate aqueous and organic phase. The thermal bio-oil appears to be a dark-brown fluid, viscous and non-homogeneous at sight. On the other hand, catalytic pyrolysis produced liquid product containing less amount bio-oil which was clear and easy to separate from the aqueous phase.

In each experiment, char (in basket) and liquid (oil and aqueous fraction) yields were determined by weight. The non-condensable gases and aerosols trapped were calculated by

difference. The resin was washed out with cyclohexane and washing solution was bottled for GC-MS analysis. In catalytic experiments, used catalyst was regenerated by heating in a muffle furnace for 6 h at 550 °C (weight loss provided coke yield).

3.2.2.4 Feedstock analysis

Moisture content of biomass was calculated by weight loss after heating in an oven at 105°C for about 6 h. Volatile matter (VM) was determined as the mass loss from 1 g of dried sample in covered crucible held at 550 °C for 5 min. Ash was determined as the residual mass left after oxidation at 550 °C for 6 h (NREL/TP-510-42622). Fixed carbon (FC) was calculated by difference from mass balance (FC = 100-VM-ash).

Ultimate analysis was performed using a CHNS-O analyzer (Flash 2000, Thermo Scientific), oxygen content was calculated by difference ($O= 100- \Sigma_{CHNS+Ash}$).

The higher heating value (HHV) of biomasses was calculated according to formula developed by Channiwala and Parikh [30]. The protein content was determined using a protein analyzer (INKJEL M). Determination of the total lipid content of fish and algal biomass was carried out with soxhlet extraction using n-hexane.

3.2.2.5. Product Analysis

Gas chromatography mass spectroscopy (GC/MS) analysis of bio-oil was performed on a gas chromatograph (HP 6850, Agilent) coupled with a mass spectrometer (Agilent HP 5975). equipped with a non-polar column HP-5MS (stationary phase poly[5% difenil/95% dimethyl]siloxane, 30 m x 0.25 mm i.d., 0.25 μm film thickness), using helium as gas carrier (constant pressure 33 cm /s, linear velocity at 200 °C). The GC oven temperature program was 50 °C for 5 min, then 325°C at 10°C/min, hold for 7.5 min. Samples (1 μl) are injected in splitless conditions at injector temperature 280°C. The mass spectrometer operates in electronic ionization (70 eV) in full-scan acquisition, range m/z 29-1000, in elution time between 3.6 and 44.0 min.

GC-MS sample preparation; for the bio-oil obtained from non-catalytic pyrolysis, a solution of bio-oil in 1:1 acetone:cyclohexane (10 % concentration) containing internal standard was prepared. The phenolic compounds, sterols and sugars were determined by GC–MS analysis after trimethylsilylation. The 50 μl sample (10% diluition in cyclohexane:acetone 1:1) was added with 100 μl internal standard (sorbitol) and reacted with a solution containing 50 μl N,O-bis-trimethylsilyl-trifluoroacetamide and 20 μl pyridine for 2 h at 60 °C.

In case of catalytic pyrolysis, the cyclohexane solutions of 10 % concentration were prepared with bio-oil from first trap and heptane solution taken from the third trap using internal standard.

The water contents of bio-oils and water-soluble fractions were determined by Karl Fischer Volumetric Titrator (Mettler Toledo DL31). Fuel properties of chars and bio-oils (elemental composition, ash and HHV) were determined as described in *section 3.2.2.4.*

3.2.3. Results and Discussion

3.2.3.1 Analytical pyrolysis (Py-GC-MS)

Preliminary experiments by Py-GC-MS showed that cracking with the production of hydrocarbons became significant at zeolite/biomass ratio greater than 1:5 and temperatures higher than 350 °C. The results of Py-GC-MS at 600 °C and 1:10 biomass: catalyst ratio are reported in Table 2. The pyrograms of the biomass (Fig. 3.2.2) were dominated by hydrocarbons, mostly monoaromatics. The relative abundance of benzene was rather low (<6% for pine sawdust and seaweed, < 2 % for other biomass), while alkylated benzenes (75% for pine sawdust, 66 % for seaweed, 56 % for fish residue and 44 % for spirulina) accounted for most part of the pyrolysates. The relative content of PAHs, composed of (alkylated) naphthalenes, was < 9 % for pine sawdust and seaweed and ≈ 1 % for the other biomass. The relative content of nitrogen-containing compounds (indole, alkylated pyrroles, aromatic and aliphatic nitriles) increased with the content of proteins in the biomass (see Tab 3.2.1). The percentages were around 5 % for seaweed (16.3 % proteins) and < 30 % for fish and spirulina that showed high percentage of protein with 55% and 49.5 %, respectively. The oxygenated compounds (phenols and benzofurans) were < 5 % for pine sawdust and seaweed while percentage ≤ 10 % for fish residue and spirulina have been detected. No acetic acid and other volatile fatty acids were detected by conducting Py-GC-MS with a polar column targeted for the analysis of carboxylic acids (data not shown). Altogether, these results confirmed that the conditions were adequate for substantial cracking.

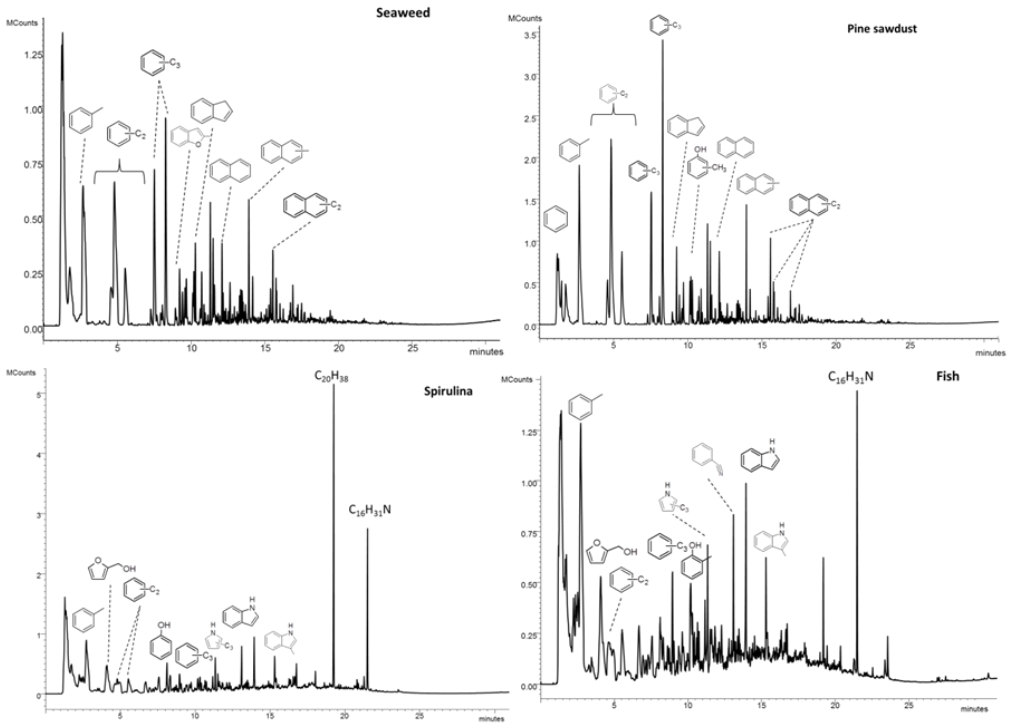

Figure 3.2.2 Total Ion chromatograms from Py-GC-MS at 600 °C of different biomass mixed with ZSM-5 in 1:10 ratio.

Table 3.2.1: Feedstock properties(db: dry basis).

	Seaweed	Spirulina	Fish discard	Pine sawdust
Moisture, %	8.0	7.3	1.5	7.7
Protein, % (db)	16.3	49.5	54.9	n.d
Ash, % (db)	21.9	10.8	13.1	0.17
Volatiles, %(db)	54.2	52.2	68.9	72.4
Fixed carbon, %(db)	23.9	36.9	17.9	27.4
Lipid, % (db)	1.0	2.6	10.8	n.d
HHV , MJ/kg	11.8	19.9	18.2	18.9
Ultimate Analysis, wt %(db)				
C	29.9	43.3	40.4	47.2
H	5.05	7.04	6.30	6.19
N	1.95	9.06	10.98	n.d.
S	1.74	0.42	0.63	0.00
O	41.2	30.1	28.7	46.5

Table 3.2.2: Relative distribution in terms of percentage peak area of main compounds detected in catalytic pyrolysis by Py-GC-MS. (*m/z*: quantitation ion)

			Pine		Fish		Spirulina		Seaweed	
#	Compound	*m/z*	1st run	2nd run	1st run	2nd run	1st run	2nd run	1st run	2nd run
1	benzene	78	6.0	6.6	0.9	2.0	1.8	1.2	4.6	5.1
2	toluene	91	24.0	24.0	43.7	40.6	32.3	22.1	21.2	6.8
3	ethyl benzene	91	4.6	4.6	3.7	2.5	2.2	4.4	6.8	7.6
4	m,p xylene	106	16.0	16.8	1.0	0.8	1.3	2.4	9.6	5.0
5	o-xylene	91	6.4	6.7	0.9	2.7	1.1	1.4	7.5	8.8
6	C3 benzene	105	10.8	9.2	4.2	6.3	5.6	5.6	14.5	16.0
7	phenol	94	1.5	1.1	5.6	2.9	6.9	8.8	1.0	2.2
8	C3 benzene	105	12.9	12.9	2.3	3.8	4.0	4.7	12.7	14.2
9	C3 pyrrole	108	-	-	5.4	6.9	2.8	3.8	-	-
10	indane	117	3.0	3.1	0.7	1.0	0.7	0.9	3.0	3.8
11	2-methyl phenol	107	0.7	0.5	-	-	0.3	0.4	0.5	1.0
12	3-methyl phenol	107	1.2	1.0	5.3	3.9	1.7	2.3	0.9	2.0
13	benzofuran, 1-methyl	131	0.9	0.8	-	-	-	-	2.0	3.4
14	C4 benzene	119	0.9	0.8	-	-	0.3	0.3	0.7	0.8
15	C4 pyrrole	122	-	-	2.1	3.8	1.1	1.5	-	-
16	indane, 1-methyl	117	2.4	2.3	3.3	3.5	2.8	2.7	2.8	3.9
17	benzonitrile 2-methyl	117	0.0	0.0	3.3	3.5	2.8	2.7	2.8	3.9
18	Naphthalene	128	1.9	2.1	0.3	0.5	0.4	0.6	1.7	2.6
19	C5 pyrrole	122	-	-	1.6	2.2	0.9	1.6	-	-
20	benzofuran, 4,7 dimethyl	145	0.7	0.6	-	-	-	-	1.4	2.4
21	Indole	117	-	-	10.0	9.7	8.4	10.1	0.4	1.2
22	methyl naphthalene	141	2.8	3.1	-	-	-	-	2.7	3.8
23	indole, 2methyl	130	-	-	4.1	3.8	4.4	4.2	0.4	1.6
24	C2 naphthalene	141	0.5	0.6	0.1	0.2	0.1	0.2	0.2	0.2
25	C2 naphthalene (2)	156	2.4	2.5	0.1	0.3	0.3	0.4	2.0	2.6
26	C3 naphthalene	170	0.5	0.7	0.0	0.1	0.1	0.0	0.6	1.0
27	phytadiene	71	-	-	0.2	0.1	14.5	15.3	-	-
28	hexadecanenitrile	110	-	-	1.5	0.7	3.3	2.2	-	-

3.2.3.2 Bench scale experiments: pyrolysis yields

Table 3.2.3 showed the product yields from the catalytic and thermal pyrolysis of biomass at 460°C. The volatiles refer the compounds trapped on resin or cotton traps. Since quantitation of compounds trapped in heptane trap could not be done, gas + loss yield shows both their amount and gas compounds. The bio-oil yields significantly changed with the biomass types. In thermal runs, the bio-oil yields of Spirulina and fish discard were higher than yields from Ulva sp. and pine sawdust. The reason might be their high oil and protein contents. Although, the bio-oil yield obtained from seaweed was lowest, the value is reasonable comparing to literature. In literature, reported bio-oil yields were ranging between 10- and 14 wt. % from pyrolysis of different seaweed species [31-33]. The low oil and high char yields from Ulva sp. pyrolysis are due to its high ash content. Seaweed ash contains many alkali metals substances, such as potassium and sodium, lowering oil yield [34] and acting as catalysts for char formation [31].

Table 3.2.3: Product yields from duplicate experiments of thermal (T) and catalytic C) pyrolysis, wt % (Gas + loss, by difference, comprehensive of losses in sample taking, e.g. the thin film remaining on the bottom of the traps).

		Bio-oil		**Aqueous phase**		**Volatiles**		**Char**		**Coke**		**Gas+loss**	
		1st run	2nd run	1st run	2nd run	1st run	2ndrun	1st run	2nd run	1st run	2nd run	1st run	2nd run
Pine	**T**	17.4	16.7	38.3	39.8	0.0	1.1	24.0	23.2	-	-	17.2	19.2
	C	7.6	6.9	24.7	28.1	10.4	9.6	24.4	23.2	9.3	7.4	23.7	24.8
Fish	**T**	40.9	38.9	10.6	11.1	1.1	0.0	32.7	33.3	-	-	12.8	16.7
	C	11.8	9.7	16.8	18.8	6.7	7.3	32.6	32.8	15.2	14.2	16.9	17.2
Spirulina	**T**	32.2	37.4	15.8	12.6	0.4	0.7	26.4	27.0	-	-	22.1	22.3
	C	6.1	7.4	23.9	22.4	7.0	6.6	26.3	26.5	13.3	14.3	23.4	22.8
Seaweed	**T**	10.0	11.0	23.7	22.2	1.1	0.7	42.6	42.1	-	-	19.9	24.0
	C	3.2	7.2	22.5	19.1	7.0	4.4	42.6	42.2	7.0	5.6	17.7	21.5

It is clearly seen that there was a marked reduction in oil yield in the catalytic runs compared to the non-catalytic experiments for all biomasses. This result is in agreement with previous pyrolysis studies in presence of HZSM-5 [14, 35, 36]. Except pine sawdust, using of HZSM-5 led to formation water and water soluble compounds and volatile aromatics which led to a decrease of oil phase yield and an increase of volatiles and aqueous phase yield. In case of pine sawdust, catalyst generates small molecule non-condensable gases, as well as volatile aromatics and water, leading to an increase in gas yield. The comparison of water content of aqueous phases from catalytic pyrolysis with that of thermal run shows the dehydration effect of catalyst (Table 3.2.4).

Table 3.2.4: Water content of aqueous phases, wt%

	Spirulina	*Ulva* sp.	Fish discard	Pine sawdust
Thermal run	57.3	76.9	49.6	45.2
Catalytic run	66.7	97.8	55.1	98.8

As mentioned in Section 3.2.2.3, in contrast to thermal run, the oils obtained using HZSM-5 were clear and light yellow in color, whereas the aqueous phase was colorless. It is noted that distinguishing aromatic odor similar to that of gasoline was detected in resin traps. GC-MS analysis also showed that the compounds trapped in resin/cotton and heptane consisted of mainly aromatics such as toluene, benzene derivatives, naphthalene and its derivatives, and hexadecanenitrile (in case of fish).

One of the main challenges in upgrading of pyrolysis vapors over HZSM-5 is coke formation on catalyst. Coke causes the deactivation of catalyst, besides its formation lowers the yields of desired products. Coke formation depends on catalyst properties, such as pore size and Brønsted acid sites, operating conditions, like temperature, space time, and chemical composition of feedstock [37]. The reported coke amounts from upgrading of pyrolysis vapors from lignocellulosic materials over HZSM-5 [36] were higher than the current study. The fact that coke yields from Spirulina and fish discard were higher than from Ulva sp. and pine sawdust might be due to their high protein and lipid content.

3.2.3.3 Fuel properties of pyrolysis products

The key fuel characteristics of bio-oils collected in first trap are given in Table 3.2.5.

The higher heating value of bio-oils was calculated from the following equation [30].

$$HHV\ (MJ\ kg^{-1}) = 0.3491C+1.1783H+0.1005S0.1034O-0.0151N-0.0211A$$

Table 3.2.5: Fuel characteristics of bio-oil from thermal and ZSM-5 catalytic pyrolysis

Sample		Ultimate Analysis, wt%					O/C	H/C	N/C	HHV
		C	H	N	S	O				MJ kg^{-1}
Spiruline	Cat.	71.4	7.98	2.95	n.d.	17.71	0.19	1.34	0.04	33.87
	Ther.	59.80	7.66	9.22	0.10	23.21	0.29	1.54	0.13	27.00
Fish	Cat.	72.62	8.22	4.38	n.d.	14.77	0.15	1.36	0.05	35.29
	Ther.	56.79	7.51	10.87	0.36	24.47	0.32	1.59	0.16	25.39
Seaweed	Ther.	46.37	5.16	2.45	0.34	45.68	0.74	1.33	0.04	18.54
Pine	Cat.	76.88	7.86	0.18	n.d.	15.08	0.15	1.23	-	37.18
	Ther.	55.98	6.02	0.00	n.d.	38.01	0.51	1.29	-	22.56

It is noted that, for Ulva sp., a few drops of bio-oil (which could not be separated from aqueous phase) were obtained from catalytic pyrolysis. Because of this, bio-oil from catalytic pyrolysis of Ulva sp., could not be analyzed.

Table 3.2.5 shows the significant effect of HZSM-5 on bio-oil properties. It is clearly seen that the quality of bio-oil in terms of heating value was improved by upgrading of pyrolysis vapor.

It is also apparent that bio-oil upgrading includes the removal of nitrogen in addition to the removal of oxygen. The low values for O/C and N/C molar ratios indicate that small amounts of nitrogen and oxygen compounds were present in the catalytic bio-oil. It is noted that the catalytic bio-oil from Spirulina and Ulva sp. contained no sulphur. In summary, HZSM-5 shows denitrogenation and deoxygenation effects besides desulphurization effect. The results obtained confirm that HZSM-5 has catalytic effect on pyrolysis of algal biomass, proteins and fats.

Besides bio-oil, the solid product of pyrolysis (biochar) is one of the useful products which can be used as fuel, soil improver and for obtaining activated carbon. The characteristic of chars is mainly dependent on the composition of the biomass besides the pyrolysis conditions such as temperature and heating rate. Some properties of chars obtained from pyrolysis are given in Table 3.2.6 (average values).

Since catalyst used was only in contact with volatiles products, there was no catalytic effect on char properties. Because of this, biochars obtained from both thermal and catalytic pyrolysis had similar properties.

The difference observed in the biochar properties is due to the different origin and structure of the biomass. As expected, the char obtained from pyrolysis of lignocellulosic material (pine sawdust) had low ash content and high calorific value which is a favorite solid fuel. In addition, due to the low sulphur and nitrogen content, it can be burned with emission problem. In contrary, the chars obtained from algal biomasses and fish discard cannot be used as solid fuel due to their high ash content and low calorific value. It may be used as fertilizer due to the high inorganic content.

Table 3.2.6: Properties of chars from catalytic pyrolysis

Sample	Ultimate analysis, wt%					Ash, wt%	HHV, MJ kg^{-1}
	C	H	N	S	O		
Spiruline	51.4	2.49	7.71	n.d.	-	40.5	20.1
Fish	38.6	1.78	6.73	n.d.	5.20	47.6	13.9
Seaweed	35.2	1.66	2.25	3.1	0.19	51.6	14.0
Pine	80.1	3.47	0.13	0.00	15.55	0.74	30.4

3.2.3.4 Chemical composition of the bio-oils

The bio-oils obtained in the thermal and catalytic pyrolysis were analyzed comparatively by mean of GC–MS analysis (Table 3.2.7 and 3.2.8)

Table 3.2.7: The main compounds detected and quantified (mg g^{-1}) by GC/MS in thermal bio-oil

#	Compounds	Spirulina	Fish	Ulva	Pine
1	Pirazole + derivatives	-	2.5	-	-
2	Pyridine + derivatives	-	0.3	-	-
3	Furaldehyde	-	-	3.5	1.1
4	Furan, dimethyl	-	-	0.6	-
5	Diacetonamine	-	2.9	-	-
6	Hexanenitrile	0.4	-	-	-
7	Pentanenitrile	0.6	-	-	-
8	Styrene	-	0.1	-	-
9	Furaldehyde, methyl	-	-	10.7	0.3
10	(Butilamino)acetonitrile	-	0.1	-	-
11	4-(etilammino)-phenol	-	0.3	-	-
12	Phenols (group)	2.3	-	-	0.7
13	Methylphenol	0.9	1.2	0.8	0.3
14	Triacetone amine	-	0.4	-	-
15	Indole	0.5	1.4	-	-
16	Benzonitrile, methyl	-	0.3	-	-
17	Guaiacols	-	-	-	18.8
18	Benzene propanenitrile	1.3	0.6	-	-
19	Indolizine	2.7	-	-	-
20	Alkanes & Alkenes	4.9	0.1	4.2	1.0
21	Hexadecanenitrile	-	0.7	-	-
22	Eiscosanenitrile	-	0.2	-	-
23	Palmitonitrile	0.8	-	-	-
24	Palmitic acid	0.8	-	0.6	-
25	Palmitamide	5.4	-	0.2	-
26	1-Monopalmitin	-	-	0.1	-
27	Stigmasterol acetate	-	-	1.3	-
28	Cholesterol	-	3.0	0.2	-
	Total	24.2	25.3	24.2	32.5

Table 3.2.8: The main compounds detected and quantified (mg g^{-1}) by GC/MS in catalytic bio-oil

#	**Compound**	Spirulina	Fish	Pine
1	Toluene	35.3	38.4	45.4
2	C2-benzenes	73.3	59.2	104.0
3	C3-benzenes	53.2	44.8	51.2
4	C4-benzenes	29.6	23.5	16.0
5	Indane (H)	4.0	2.8	9.0
6	Indene	0.1	0.4	0.7
7	Indole (N)	2.3	-	-
8	Phenol	-	-	0.1
9	C1-phenols	-	-	0.3
10	C2-phenols	-	-	0.1
11	Benzofuran (O)	-	-	4.3
12	C1-benzofurans	0.4	0.3	0.1
13	C2-benzofurans	-	-	0.1
14	Naphthalene	12.2	9.1	30.8
15	C1-naphthalenes	19.8	12.8	42.9
16	C2-naphthalenes	13.8	12.5	26.7
17	C3-naphthalenes	12.0	11.0	12.9
18	C4-naphthalenes	1.7	1.4	1.4
19	Fluorene	0.6	0.6	0.4
20	Carbazole (N)	0.8	7.0	-
21	C1-carbazoles	1.4	13.9	-
22	C2-carbazoles	0.1	2.0	-
23	C3-carbazoles	0.2	4.7	-
24	Phenanthrene	1.9	2.3	3.2
25	C1-phenanthrenes	2.6	3.8	4.6
26	C2-phenanthrenes	1.1	2.9	1.7
27	C3-phenanthrenes	1.2	1.0	0.9
28	Pyrene	0.2	0.3	0.5
29	C1-pyrenes	0.6	1.2	0.8
30	C2-pyrenes	0.4	1.4	0.5
31	Benzo[a]anthracene	0.5	2.1	0.6
32	Alkanes	3.3	2.3	0.0
33	Other N-compounds	6.4	3.8	0.0
	Total	278.9	265.4	359.2

Main constituents of the thermal bio-oils evaluated using GC-MS analysis are shown in Fig. 3.2.3.

Bio-oil derived from lignocellulosic biomass consisted mainly of oxygenated compounds. Phenols, mainly guaiacols, and furaldehyde represent the main oxygenated compounds in pine sawdust bio-oil. It is interestingly, bio-oil derived from algal biomass contained phenol and its

derivatives attributed to lignin pyrolysis. These compounds might be derived from polyphenolic molecules such as phlorotannins [38] as algal biomass does not contain lignin. It was observed that, Ulva sp. bio-oil contained stigmasterol acetate as phytosterol, whereas cholesterol was found as animal derived sterol in fish residue bio-oil. The nitrogen compounds in fish and spirulina bio-oils could be derived from decomposition of proteins in microalgae and fish discard. Fatty nitriles/amid such as hexadecanenitrile, eiscosanenitrile, palmitonitrile, palmitamide, might be derived from the fats in proteinaceous biomasses [39]. The indole, which is produced by bacteria as a degradation product of the tryptophan amino acids [40], might be produced from thermal decomposition of tryptophan amino acids [41]. Most of compounds observed in fish oil are similar to in oil derived pyrolysis of the meat and bone meal [42].

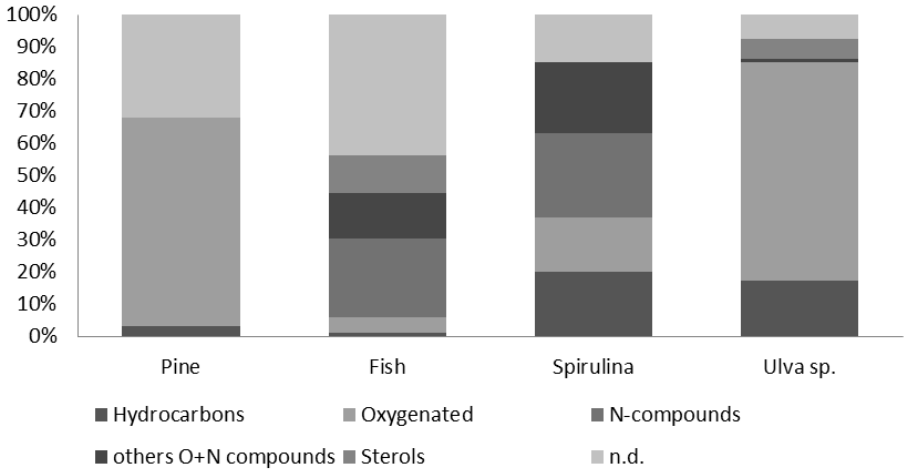

Figure 3.2.3: The major groups in bio-oil from thermal pyrolysis, % relative GC-MS peak area.

The results of GC–MS analysis of catalytic pyrolysis showed large difference between the catalytic bio-oil and the thermal bio-oil in chemical components. The relative content of the hydrocarbons in the catalytic bio-oil (Fig 3.2.4) was much higher than that in the thermal bio-oil (Fig. 3.2.3).

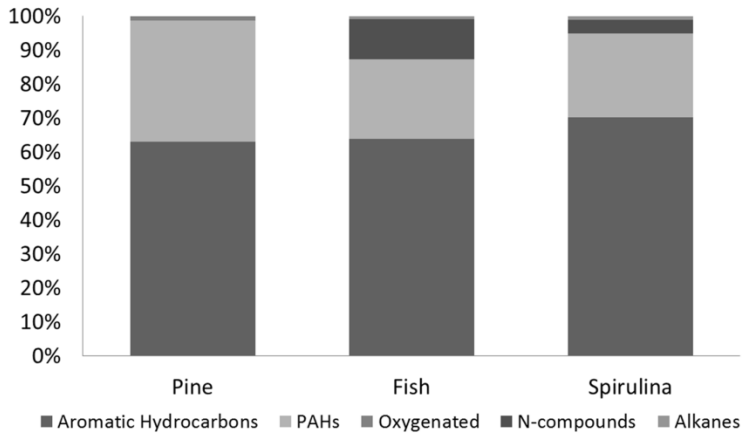

Figure 3.2.4: The major groups in bio-oil from catalytic pyrolysis, % GC-MS peak area (aromatic hydrocarbons: alkylated benzenes, indane, indenes).

As mentioned above, the yield of bio-oil from Ulva sp. was an extremely low amount, hence it was not analyzed by GC-MS. Here, in contrast to thermal bio-oil, hydrocarbons represent benzene derivatives and indane. The increase in aromatic contents was also observed in previous studies on pyrolysis of terrestrial and algal biomass in presence of HZSM-5 [14, 24, 34, 35].

HZSM-5 showed excellent deoxygenation effect on phenols and guaiacols. The significant amount of PAH was formed by upgrading of pyrolysis vapors over HZSM-5. Their relative contents were 36 %, 24 % and 25 % for pine sawdust, fish, and spirulina, respectively.

Although HZSM-5 showed denitrogenation effect for nitriles, amines and amides, it provided the formation of new aromatics containing nitrogen, like carbazoles. The carbazoles might be formed by an intermolecular amination and an intramolecular direct arylation reactions [43].

3.2.3.5 Pyrolysis products distribution: comparison between Py-GC-MS and collected bio-oil

Figure 3.2.5 shows the pyrolysis products distribution, grouped in chemical families, obtained on the basis of the Py-GC-MS results described in section 3.2.3.1.

Comparing the pyrolysis products distribution from Py-GC-MS to that from bench scale pyrolysis reactor (Fig. 3.2.4) it is possible to observe that Py-GC-MS discriminate the products distribution on the basis of biomass more than bench scale pyrolysis. Indeed, the percentage of aromatic hydrocarbons in pine sawdust (87% of total peak area) is higher than in proteinaceous biomass (64% and 62% in spirulina and fish, respectively. *Ulva* sp. data are not reported as missing in bench scale reactor results).

On the other hand, condensed bio-oil shows a much higher amount of PAHs with respect to Py-GC-MS while oxygenated and N-compounds were detected with lower amount in bio-oil

because of the preferential distribution into the aqueous fraction during the condensation step as previously mentioned in chapter 3.1.

The higher amount of PAHs produced from pine suggests that lignocellulosic feedstock are more selectively converted to polycyclic aromatic compounds probably because of the cellulosic component [44].

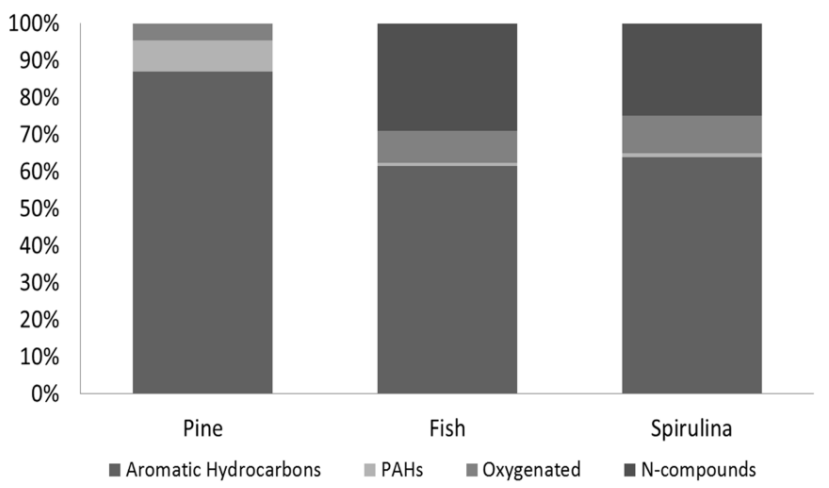

Figure 3.2.5: The major groups in Py-GC-MS , % relative abundance peak area (aromatic hydrocarbons: alkylated benzenes, indane, indenes).

Thus, the pyrolysis products distribution varies between analytical pyrolysis and bench scale process with the following trends:

Hydrocarbons: Py-GC-MS >> Bench scale (Pine); Py-GC-MS ≈ Bench scale (fish, spirulina)

PAHs: Py-GC-MS << Bench scale

O-compounds: Py-GC-MS > Bench scale

N-compounds: Py-GC-MS >> Bench scale

Finally, using Py-GC-MS as screening method is important taking into account that some slight differences can be observed with respect to preparative pyrolysis.

Nonetheless, Py-GC-MS was confirmed a suitable screening method to studying pyrolysis process as also described in the previous paragraph *3.1*.

3.2.4 Conclusions

The effect of H-ZSM-5 on the pyrolysis of four different type of biomass was investigated by means of analytical pyrolysis and preparative pyrolysis to better understand the role of the catalyst and of the biomass type on the product yields and composition.

The main interest was the formation of aromatic hydrocarbons. The following results were derived:

- The effect of catalyst on the yields of pyrolysis products significantly changed with the biomass types.
- The significant amounts of monoaromatic hydrocarbons and PAHs were formed by upgrading of pyrolysis vapors. catalyst was most effective at producing aromatic hydrocarbons and PAHs from pyrolysis vapours from lignocellulosic biomass. A significant fraction of monoaromatic could not be condensed indicating that yields of gasoline fraction could be increased with ameliorations of the trapping system
- Although HZSM-5 showed good denitrogenation effect for nitriles, amines and amides, it led to formation of carbazoles.
- The presence of nitrogen compounds in pyrolysis vapours led to more formation of coke on HZSM-5 surface.
- Products distribution by means of Py-GC-MS was slightly different comparing to the condensed bio-oil. Py-GC-MS led to higher amount both of monoaromatics hydrocarbons and oxygenated compounds

References

[1] U.S Energy Information Administration Indipendent Statistics & Analysis, AEO2014: Early release report 2014, http://www.eia.gov/analysis.

[2] Khanal, S. K., Surampalli, R. Y., Zhang, T. C., Lamsal, B. P., Tyagi, R. D., Kao, C. M. (2010). Bioenergy and biofuel from biowastes and biomass. American Society of Civil Engineers (ASCE).

[3] Bridgwater, A.V., (2012). Review of fast pyrolysis of biomass and product upgrading, *Biomass. Bioenerg., 38, 68-94*

[4] Mohan, D., Pittman, C. U., Steele, P. H., (2006). Pyrolysis of wood/biomass for bio-oil: a critical review, *Energ. Fuel., 20, 848-889.*

[5] Zang, Q., Chan, J., Wang, T., Xu, Y., (2007). Review of biomass pyrolysis oil properties and upgrading research, *Energ Convers Manage, 48, 87-92*

[6] de Miguel Mercader, F., Groeneveld, M. J., Kersten, S. R. A., Way, N. W. J., Schaverien, C. J., & Hogendoorn, J. A. (2010). Production of advanced biofuels: Co-processing of upgraded pyrolysis oil in standard refinery units. *Appl. Catal. B: Environ., 96, 57-66.*

[7] Fogassy, G., Thegarid, N., Toussaint, G., van Veen, A. C., Schuurman, Y., Mirodatos, C. (2010). Biomass derived feedstock co-processing with vacuum gas oil for second-generation fuel production in FCC units. *Appl. Catal. B: Environ., 96, 476-485.*

[8] Marker, T. L., Felix, L. G., Linck, M. B. (2010). U.S. Patent No. 20,100,251,600. Washington, DC: U.S. Patent and Trademark Office.

[9] Elkasabi, Y., Mullen, C. A., Boateng, A. A. (2014). Distillation and Isolation of Commodity Chemicals from Bio-Oil Made by Tail-Gas Reactive Pyrolysis. *ACS Sustainable Chem. Eng., 2, 2042-2052.*

[10] Huber, G. W., Corma, A. (2007). Synergies between Bio-and Oil Refineries for the Production of Fuels from Biomass. *Angew. Chem. Int. Ed.*, 46, 7184-7201.

[11] Carlson, T. R., Cheng, Y-T., Jae, J., Huber, G. W. (2011). Production of green aromatics and olefins by catalytic fast pyrolysis of wood sawdust. *Energy Environ. Sci., 4, 145-161*

[12] Wang, K., Brown, R. C. (2014). Catalytic pyrolysis of corn dried distillers grains with solubles to produce hydrocarbons. *ACS Sustainable Chem. Eng., 2, 2142-2148.*

[13] Iliopoulou, E. F., Stefanidis, S., Kalogiannis, K., Psarras, A. C., Delimitis, A., Triantafyllidis, K. S., Lappas, A. A. (2014). Pilot-scale validation of Co-ZSM-5 catalyst performance in the catalytic upgrading of biomass pyrolysis vapours. *Green Chem., 16, 662-674.*

[14] Thangalazhy-Gopakumar, S., Adhikari, S., Chattanathan, S. A., Gupta, R. B. (2012). Catalytic pyrolysis of green algae for hydrocarbon production using H+ ZSM-5 catalyst. *Bioresour. technol., 118, 150-157.*

[15] Vitolo, S., Bresci, B., Seggiani, M., Gallo, M. G. (2001). Catalytic upgrading of pyrolytic oils over HZSM-5 zeolite: behaviour of the catalyst when used in repeated upgrading–regenerating cycles. *Fuel, 80(1), 17-26.*

[16] Yildiz, G., Pronk, M., Djokic, M., van Geem, K. M., Ronsse, F., Van Duren, R., Prins, W. (2013). Validation of a new set-up for continuous catalytic fast pyrolysis of biomass coupled with vapour phase upgrading. *J. Anal. Appl. Pyrol., 103, 343-351.*

[17] Torri, C., Fabbri, D., Garcia-Alba, L., Brilman, D. W. F. (2013). Upgrading of oils derived from hydrothermal treatment of microalgae by catalytic cracking over H-ZSM-5: A comparative Py–GC–MS study. *J. Anal. Appl. Pyrol, 101, 28-34.*

[18] Mihalcik, D. J., Mullen, C. A., Boateng, A. A. (2011). Screening acidic zeolites for catalytic fast pyrolysis of biomass and its components. *J. Anal. Appl. Pyrol, 92, 224-232.*

[19] Wang, K., Kim, K. H. Brown, R. C. (2014). Catalytic pyrolysis of individual components of lignocellulosic biomass. *Green Chem., 16, 727-735.*

[20] Cheng Y-T, Jae, J., Shi, J., Fan,. Huber W. G., (2012). Production of Renewable Aromatic Compounds by Catalytic Fast Pyrolysis of Lignocellulosic Biomass with Bifunctional Ga/ZSM-5
Catalysts, Angew. Chem. 2012, 124, 1416 –1419

[21] Jae, J., Coolman, R., Mountziaris, T. J., Huber, G. W. (2014). Catalytic fast pyrolysis of lignocellulosic biomass in a process development unit with continual catalyst addition and removal. *Chem. Eng. Sci., 108, 33-46.*

[22] Zheng, A., Zhao, Z., Chang, S., Huang, Z., Wu, H., Wang, X., .Li, H. (2014). Effect of crystal size of ZSM-5 on the aromatic yield and selectivity from catalytic fast pyrolysis of biomass. *J. Mol. Catal. A: Chem., 383, 23-30.*

[23] Mante, O.D, Agblevor, F.A., (2014) Catalytic pyrolysis for the production of refinery-ready biocrude oils from six different biomass sources, *Green Chem., 16, 3364, 3377*

[24] Du, Z., Ma, X., Li, Y., Chen, P., Liu, Y., Lin, X., Lei, H., Ruan, R. (2013). Production of aromatic hydrocarbons by catalytic pyrolysis of microalgae with zeolites: Catalyst screening in a pyroprobe. *Bioresour. Technol, 139, 397-401.*

[25] Wang, K., Brown, R. C. (2013). Catalytic pyrolysis of microalgae for production of aromatics and ammonia. Green Chemistry, 15, 675-681.

[26] Pan, P., Hu, C., Yang, W., Li, Y., Dong, L., Zhu, L., Tong, D., Qing, R., Fan, Y. (2010). The direct pyrolysis and catalytic pyrolysis of *Nannochloropsis sp*. residue for renewable bio-oils. *Bioresour. Technol, 101, 4593-4599.*

[27] Varuvel, E. G., Mrad, N., Tazerout, M., Aloui, F. (2012). Assessment of liquid fuel (bio-oil) production from waste fish fat and utilization in diesel engine. *Appl. Energy, 100, 249-257.*

[28] Ito, T., Sakurai, Y., Kakuta, Y., Sugano, M., Hirano, K. (2012). Biodiesel production from waste animal fats using pyrolysis method. *Fuel Process. Technol., 94, 47-52.*

[29] Wisniewski Jr, A., Wosniak, L., Scharf, D. R., Wiggers, V. R. (2015) Upgrade of Biofuels Obtained from Waste Fish Oil Pyrolysis by Reactive Distillation. *J. Braz. Chem. Soc., 26, 224-232.*

[30] Channiwala, S. A., Parikh, P. P. (2002). A unified correlation for estimating HHV of solid, liquid and gaseous fuels. *Fuel, 81,1051-1063.*

[31] Yanik, J., Stahl, R., Troeger, N., Sinag. A., (2013) Pyrolysis of algal biomass, *J. Anal. Appl. Pyrol., 103, 134–141*

[32] Choi, J., Choi, J. W., Suh, D. J., Ha, J. M., Hwang, J. W., Jung, H. W., Lee, K-Y., Woo, H. C. (2014). Production of brown algae pyrolysis oils for liquid biofuels depending on the chemical pretreatment methods. *Energy Convers. Manage., 86, 371-378.*

[33] Li, J., Wang, G., Chen, M., Li, J., Yang, Y., Zhu, Q., .Jiang, X., Wang, Z., Liu, H. (2014). Deoxy-liquefaction of three different species of macroalgae to high-quality liquid oil. *Bioresour. Technol. 169, 110-118.*

[34] Wang, S., Wang, Q., Jiang, X., Han, X., Ji, H., (2013) Compositional analysis of bio-oil derived from pyrolysis of seaweed, *Energy Convers. Manage., 68, 273–280.*

[35] Li, B., Lv, W., Zhang, Q., Wang, T., Ma, L. (2014). Pyrolysis and catalytic upgrading of pine wood in a combination of auger reactor and fixed bed. *Fuel, 129, 61-67.*

[36] Thilakaratne, R., Wright, M. M., Brown, R. C. (2014). A techno-economic analysis of microalgae remnant catalytic pyrolysis and upgrading to fuels. Fuel, 128, 104-112.

[37] Rezaei, P. S., Shafaghat, H., Daud, W. M. A. W. (2014). Production of green aromatics and olefins by catalytic cracking of oxygenate compounds derived from biomass pyrolysis: A review. *Appl. Catal. A: Gen., 469, 490-511.*

[38] Ross, A. B., Jones, J. M., Kubacki, M. L., Bridgeman, T. (2008). Classification of macroalgae as fuel and its thermochemical behaviour. *Bioresour. Technol., 99, 6494-6504.*

[39] Berruti, F. M., Ferrante, L., Briens, C. L., Berruti, F. (2012). Pyrolysis of cohesive meat and bone meal in a bubbling fluidized bed with an intermittent solid slug feeder. *J. Anal. Appl. Pyrol., 94, 153-162.*

[40] Sasaki-Imamura, T., Yano, A., Yoshida, Y. (2010). Production of indole from L-tryptophan and effects of these compounds on biofilm formation by Fusobacterium nucleatum ATCC 25586. *Appl. Eviron. Microb., 76(13), 4260-4268.*

[41] Harman-Ware, A. E., Morgan, T., Wilson, M., Crocker, M., Zhang, J., Liu, K., Debolt, S. (2013) Microalgae as a renewable fuel source: Fast pyrolysis of Scenedesmus sp. *Renew. Energy, 60,* 625-632.

[42] Chaala, A., Roy, C. (2003). Recycling of meat and bone meal animal feed by vacuum pyrolysis. *Environ. Sci. Technol., 37*(19), 4517-4522.

[43] Ackermann, L., Althammer, A., Mayer, P. (2009). Palladium-Catalyzed Direct Arylation-Based Domino Synthesis of Annulated N-HeterocyclesUsing Alkenyl or (Hetero) Aryl 1, 2-Dihalides. *Synthesis, 2009(20), 3493-3503.*

[44] Du Z., Hu, B., Ma X., Cheng Y., Liu Y., Lin X., Wan Y., Lei H., Chen P., Ruan R., (2013). Catalytic pyrolysis of microalgae and their major components: carbohydrates, proteins and lipids. *Bioresour. Technol., 130, 777-782*

Chapter 4

Characterization of pyrolysis vapours of biomass

4.1 At-line characterization of compounds evolved during biomass pyrolysis by solid-phase microextraction and GC-MS

4.1.1 Introduction

Pyrolysis oil also known as bio-oil is a complex mixture of hundreds of polar and non-polar compounds formed during the thermal degradation of the main biomass components. Bio-oil composition varies depending on feedstock and process conditions [1-3].

Bio-oil contains approximately 20% water, 40% GC-detectable compounds, approximately 15% non-volatile HPLC-detectable compounds and 25% high molecular lignin [4-7]. Bio-oil from lignocellulosic biomass is mainly constituted by pyrolysis products originated from plant biomolecules (cellulose, hemicellulose, and lignin). Pyrolysis of lignin produces phenols and methoxyphenols (guaiacyl and syringyl moieities) while cellulose and hemicellulose give furans, aldehydes, ketones and anhydrous sugars (i.e. levoglucosan and anhydro xylopyranose, from cellulose and hemicellulose, respectively). This mixture of polar and non-polar compounds makes the chemical characterisation extremely difficult and laborious and requires the use of several analytical techniques (i.e. GC-MS, HPLC-MS, and GPC) and chemical procedures (e.g. derivatisation [8, 9], solvent fractionation [10]).

The chemical characterisation at a molecular level is often accomplished by direct GC-MS of the oil (condensed organic fraction) dissolved in an appropriate solvent after pyrolysis has occurred. However, the large variety of constituents ranging from polar hydrophilic to highly hydrophobic compounds may render the choice of the appropriate solvent difficult as certain solvents are immiscible with certain constituents of the bio-oil. Moreover, the distribution of the pyrolysis products in different liquid fractions, generally a bio-oil and an aqueous solution is an additional analytical complication. This leads to inefficiencies in the spectrum of detectable compounds during GC-MS analysis. Therefore, knowledge of hot pyrolysis vapours could be useful to obtain information on the complete composition of the liquids before their condensation in the cold traps. A solvent-less technique capable of hot gas phase analysis such as solid phase microextraction (SPME) is ideally suited for this purpose.

Solid phase microextraction is a sample preparation and sampling technique developed by Pawlizny in 1990 [11,12] which has been employed on a wide range of analytes and for several applications in various research fields, such as environmental chemistry, forensic

chemistry and pharmaceutical and food industries [13-17]. It allows a fast and solvent-free sampling and it is mainly applied coupled with GC-MS or other chromatographic techniques [18].

Previous works have shown SPME can be applied downstream of pyrolysis (Py-SPME) evolved by thermal desorption and pyrolysis, which de-couples the thermal conversion process and the GC-MS analysis, thus providing information on the actual composition of native vapours with simple and solventless technique [9, 16]. Other works showed SPME application by derivatisation headspace SPME (D-HS-SPME) followed by GC-MS for determination of low molecular mass aldehydes in bio-oil [8].

Several studies investigated the application of SPME for direct sampling of gaseous streams from thermochemical conversions, showing the potential of this technique for the on-line monitoring of plant operations [19-23]. This could be quite useful in the case of a distributed biomass/waste conversion schemes based on small scale intermediate pyrolysis where continuous quality control checks are necessary to ensure consistent final product.

Then, SPME sampling turns out to be a useful method as it is fast, solventless and able to give detailed information on the chemical composition of bio-oil. In addition, SPME could be coupled with several analytical techniques. Direct SPME-GC-MS analysis can gives information on the volatiles and semi volatiles compounds. However, by proper derivatisation on headspace, SPME is also able to detect polar compounds (e.g. anhydrous sugars) [9].

Finally, being the fiber reusable, the costs can be reduced in high sample throughput [24].

The aim of this study is to evaluate the SPME sampling directly within the bench scale pyrolysis reactor in order to apply the SPME as *at-line* fast method for the characterisation of several pyrolysis products evolved during the pyrolysis process.

An in-depth literature review revealed that there are no studies using SPME-GC-MS as an analytical technique applied to a bench scale pyrolysis in order to evaluate the pyrolysis in order to obtain a comprehensive spectrum of pyrolysis vapours formed with detailed comparisons made condensate bio-oil post pyrolysis.

Furthermore, the storage capacity has been tested to evaluate its ability to accurately analyse products post experimentation.

In this study, captured products were stored for periods of 48 and 96 hours in order to determine the accuracy of analysis after extended periods of time in storage, determined on a qualitative and quantitative basis.

4.1.2 Experimental

4.1.2.1 Feedstock

A pelletized solid digestate deriving from an anaerobic digestion plant operated by Neue Energie Steinfurt GmbH, Germany (NESt) using a mixture of maize silage (62%), cattle slurry (17%), pig slurry (17%) and cereals (4%) was used as a feedstock [25].

Other biomass samples were from woody (pine sawdust), herbaceous (switchgrass, cornstalk) [26], microalgae (Spirulina, *Arthrospira platensis*), animal residues (poultry litter) from a local poultry farm and agricultural wastes (olive residues).

4.1.2.2 At-line SPME sampling in a bench scale reactor

The SPME fiber tested was a 75 μm Carboxen/polidimethylsiloxane (CAR/PDMS) coated fiber (Supelco) used in retracted fiber configuration. Biomass samples (approximately 6-7 g) were pyrolysed using a fixed bed tubular quartz reactor previously described [27] modified with the addition of a quartz T-junction for the SPME sampling (Fig. 4.1.1).

The SPME fiber was placed through a tee-joint in quartz upstream of the cold salt-ice trap (ca. - 15°C) where the oil was condensed. The pyrolysis experiments were performed at 500°C for 5 min under nitrogen flow set a 1000 mL min^{-1}. At the end of the pyrolysis run the SPME fiber was promptly subjected to GC-MS analysis.

The pyrolysis liquid collected in the cold trap was centrifuged at 3000 rpm for 15 minutes to separate the low viscous aqueous phase (AP) from the tarry dark brown bio-oil (BO). The yields of the various fractions (char, aqueous phase and bio-oil) were determined by weight difference.

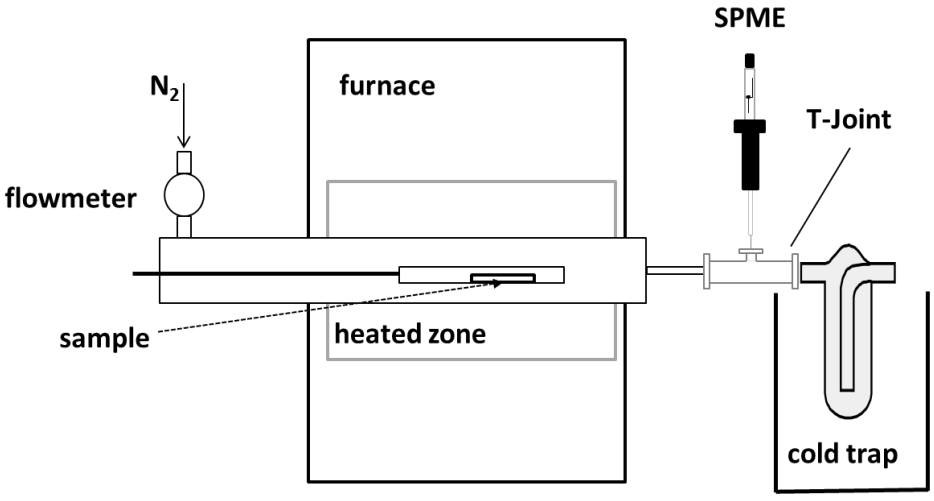

Figure 4.1.1: Bench scale reactor with the addition of a quartz T-junction for the SPME sampling

4.1.2.3 Analysis of pyrolysis liquid

The chemical composition of pyrolysis liquid was determined by solvent fractionation according to the method by Oasmaa and E. Kuoppala [28] slightly modified (ethyl acetate in place of ethyl ethers and lower sample amount).

After the separation into aqueous phase and bio-oil, 1 mL of aqueous phase was taken and added 9 mL of water. Then, the mixture was placed in the centrifuge at 3000 rpm for 10 min. The water insoluble fraction was determined by weight of the formed precipitate after centrifuge. The water soluble fraction was further extracted with 10 mL of ethyl acetate (1:1 v/v) in a separation funnel and let the solution to settle. The ethyl acetate solution was decanted from the bottom and evaporated in a rotary-evaporator at 40°C. Concentration of the water soluble-ethyl acetate insoluble fraction was determined by BRIX method [10]. The same procedure was applied to the bio-oil using 1 g diluted into 10 mL of water.

The following fractions were quantified: water solubles, WS, divided into ethyl acetate soluble, EAS, (furans, phenols etc.) and insoluble, EAI, (sugars determined by the Brix method) and water insoluble, WIS, (pyrolytic lignin, extractives). The water content was determined by Karl Fischer titration.

Bio-oil elemental analysis was performed by combustion using a Thermo Scientific Flash 2000 series analyzer.

For bio-oil, GC-MS analysis was performed on 1% solution w/v in acetone/cyclohexane 1/1 v/v spiked with 0.1 mL internal standard solution (100 mg/L 1,3,5-tri-*terz*-butylbenzene), for the aqueous phase a 10 % solution v/v in acetonitrile spiked with 0.05 mL internal standard solution (5000 mg/L butanoic acid, 2-ethyl).

4.1.2.4 GC-MS analysis

SPME and bio-oil analysis were performed with a 6850 Agilent HP gas chromatograph connected to a 5975 Agilent HP quadrupole mass spectrometer (EI 70 eV, at a frequency of 1.55 scan s^{-1} within the 10-450 *m/z* range). Analytes were separated by a HP-5 fused-silica capillary column (stationary phase poly [5% diphenyl/95% dimethyl] siloxane, 30 m, 0.25 mm i.d., 0.25 mm film thickness) using helium as carrier gas with the following thermal program: 50°C with a hold for 5 min, then ramping up with a heating rate of 10°C min^{-1} until 325 °C followed by a column cleaning at 325 °C for 10 min. SPME desorption was performed at 280°C in the injection port in splitless mode.

The total sum area of GC detectable compounds was quantified in terms of absolute concentration using the internal standard.

A set of 27 compounds was quantified in terms of percentage relative abundance (% peak area to the total area).

All the experiments were run in duplicate. The precision was assessed by triplicate runs of SPME and bio-oil analysis of digestate sample and assumed to be representative of all biomass feedstock.

Percentage relative standard deviations (%RSD) were calculated for each pyrolysis product.

Aqueous phase analyses were performed with a Varian 3400 gas chromatograph equipped with a polar GC column (Agilent Q7221 J&W nitroterephthalic-acid-modified polyethylene glycol DB-FFAP 222 30 m, 0.25mm, 0.2 μm) and connected to a Saturn 2000 ion trap mass spectrometer (Varian Instruments) using an incident electron energy of 70 eV, in full scan acquisition (10-650 *m/z*). The following thermal program was used: 50°C with a hold for 5 min, then ramping up with a heating rate of 10 °C min^{-1} until 250 °C followed by a column cleaning at 250 °C for 5 min.

A set of 21 compounds was quantified (% peak area to the total area).

The precision was assessed by triplicate runs of aqueous phase analysis of digestate sample.

4.1.2.5 Ageing tests

For storage investigations, ageing tests on the SPME fiber were performed after sampling the vapours from the pyrolysis of digestate. The experiments were carried out by storing the fiber, after sampling, for 48 hours or 96 hours at room temperature (20±1°C) under two different storage conditions: under air atmosphere or in vacuum. To get the vacuum the needle containing the fiber was placed (without holder) in a plastic bag and vacuum sealed with a commercial vacuum sealer system for food (Krups Vacuum sealer Type 383) and finally placed into a drawer.

After the storage period, thermal desorption was applied by GC-MS.

The GC-MS analyses were performed with the apparatus used for SPME and bio-oil analysis previously described in section 4.1.*2.4*. The precision was assessed by triplicate runs for each condition.

4.1.3 Results and discussion

4.1.3.1. Bulk analysis of pyrolysis liquids

Bio-oils from several biomass were obtained by means of intermediate pyrolysis at 500 °C for 5 minutes.

Elemental analysis, GC-MS and solvent fractionation procedure (Table 4.1.1) were performed on both the aqueous phase (AP) and bio-oil (BO). Under the pyrolysis conditions, phase separation was observed with all tested samples, yielding an organic product with minimal water content and a aqueous product characterized by high water content (>40 %).

Furthermore, the yields of the bio-oil showed high variations between 49 % (Spirulina) and 7 % (Bark) depending on the original feedstock [29].

Table 4.1.1: Pyrolysis at 500 °C/5 min of different biomass feedstock. Yield of the total liquid and the bio-oil (BO). GC-MS (absolute concentration of total sum detectable areas). Elemental analysis, water content and composition by solvent fractionation of the liquid WS: water solubles, divided into: EAS (ethyl acetate soluble) and EAI (ethyl acetate insoluble); WIS: water insoluble

									WS		WIS
parameters →	Yield (wt%)	Yield BO (wt%)	GC ∑area BO (µg mg^{-1})	GC ∑area AP (µg mg^{-1})	C	H	N	Water %	EAS	EAI	
biomass ↓											
digestate	40.2	10.1	194	17	67.2	7.8	2.8	74.7	1.1	14.5	9.3
pine sawdust	42.2	18.1	83	48	55.6	6.1	0.1	32.8	6.9	32.1	14.8
cornstalk	34.7	19.2	206	41	53.8	6.1	1.5	38.5	5.4	30.0	10.5
switchgrass	33.4	9.1	143	43	51.2	6.5	1.1	50.8	4.7	26.4	1.5
bark	35.1	7.0	222	74	61.5	6.5	0.5	43.3	6.5	31.8	2.0
olive residues	38.9	28.3	161	24	71.8	2.4	0.9	35.8	4.0	17.5	22.5
poultry litter	31.0	35.9	131	n.d.	63.4	8.9	11.4	33.5	2.7	19.6	23.2
spirulina	26.7	48.5	112	24	64.1	8.3	9.4	16.6	4.1	25.6	41.8

The digestate sample showed a liquid composition and liquid yield in accordance with that obtained by Neumann and coworkers [25] processing the same feedstock on a 2 kg/h laboratory scale thermo-catalytic reforming (TCR®) reactor [30].

It can be observed that the bio-oil contained high carbon percentage comprising between 50.3% and 71.8%. Concerning nitrogen, bio-oil from woody feedstock showed low N percentage (less than 1.5%), Olive residues and digestate had a N percentage of 0.9% and 2.8%, respectively. OP from poultry litter and spirulina showed highest N percentage with 11.4 and 9.4%, respectively, according to others works [31, 32].

The aqueous phases were characterized by high water content, especially the digestate sample with 75%.

The lower water content was found in spirulina (17%).

Results from solvent fractionation showed that the water insoluble percentage fraction (WIS) is similar to the yield to bio-oil (correlated with R = + 0.97). This suggests that separation of organic and a water phase is almost complete in the sample as produced from pyrolysis. [33].

4.1.3.2 GC-MS analysis (Bio-oil)

Table 4.1.2 shows the GC-MS qualitative and quantitative results obtained from the direct GC-MS analysis of several bio-oils from different biomass. Chromatograms of bio-oils (Figs. 4.1.2 and 4.1.3) from lignocellulosic biomass (pine sawdust, switchgrass, cornstalk and bark) showed many similarities due to the preponderant lignocellulosic matrix and differences cause by the different lignin structure. Chromatograms were meanly featured by lignin pyrolysis products such as phenols, methoxy phenols (guaiacols) and dimethoxy phenols (syringols) and by cellulose pyrolysis products such as furaldehyde, 1-methyl cyclopente-1-one and 3-methyl cyclopentane-1, 2-dione. Switchgrass and cornstalk chromatograms are characterized by high relative abundance of phenolic moieties, with 4-vinyl phenol as the most abundant compound, in accordance to lignin composition of herbaceous biomass [34]. Instead, pine sawdust (softwood) bio-oil shows a preponderance of guaiacyl moieties with low levels of syringyl moieities. Bio-oil from bark (hardwood) is dominated by both the moieties, in accordance to lignin composition of softwood and hardwood biomasses [35, 36].

Poultry litter bio-oil is mainly characterized by fatty acids (34 % palmitic acid and 16% oleic acid) from the poultry manure and by phenolic compounds (phenol and guaiacols) from the lignocellulosic fraction of the bedding material. Nitrogen containing compounds were also detected (4.0% indole, 2.7% hexadecanamide and 2.2 % methyl indole) derived from proteinaceous material of manure.

Olive residue was mainly characterized by oleic acid (22%) and phenolics compounds with guaiacol as the most abundant peak (14%) following by 4-vinyl guaiacol (8.5%), syringol (8.3%) and *trans*-isoeugenol (8.9%)

Spirulina produced bio-oil that contained high percentage of nitrogen containing compounds according to others works [37, 38]. The most abundant compounds are indoles such as indole (25%) and methyl indole (6%) and phenols such as phenol (25%) GC-MS analysis also indicates a striking presence of alkane compounds mainly characterized by heptadecane (24%) probably derived from the decarboxylation of palmitic acids.

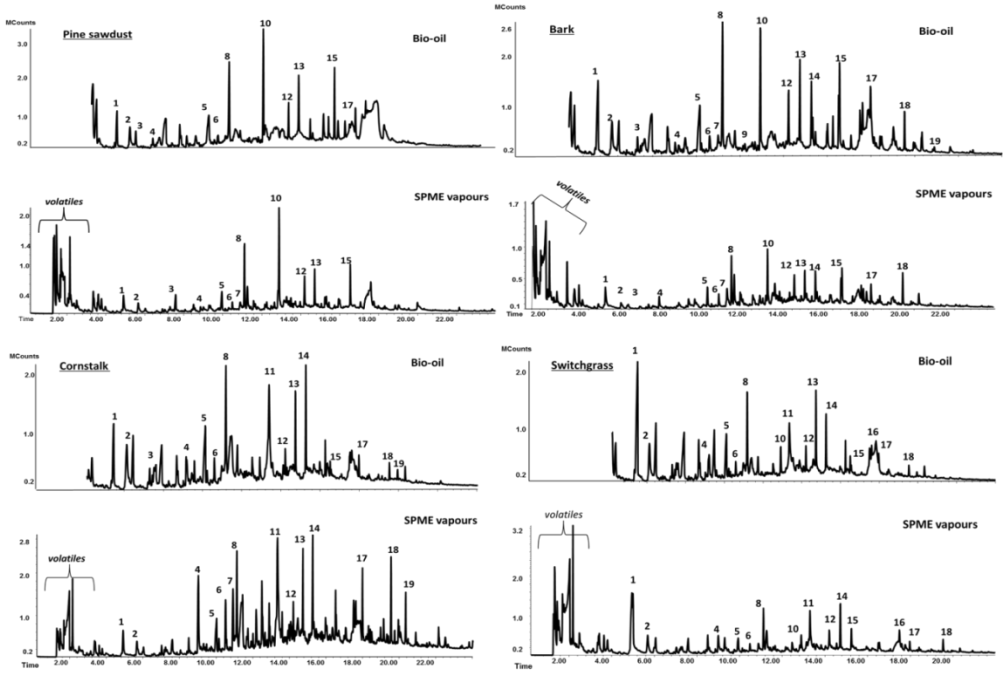

Figure 4.1.2: Total Ion Chromatograms from direct GC-MS analysis of bio-oil and SPME-GC-MS of vapours from preparative pyrolysis with a bench scale reactor of pine sawdust, bark, cornstalk and switchgrass. Numbers correspond to the products in Table 2. In the curly bracket the volatiles products identified: hydroxyacetaldehyde; acetic acid; acetone; hydroxyacetone; 3-pentanone

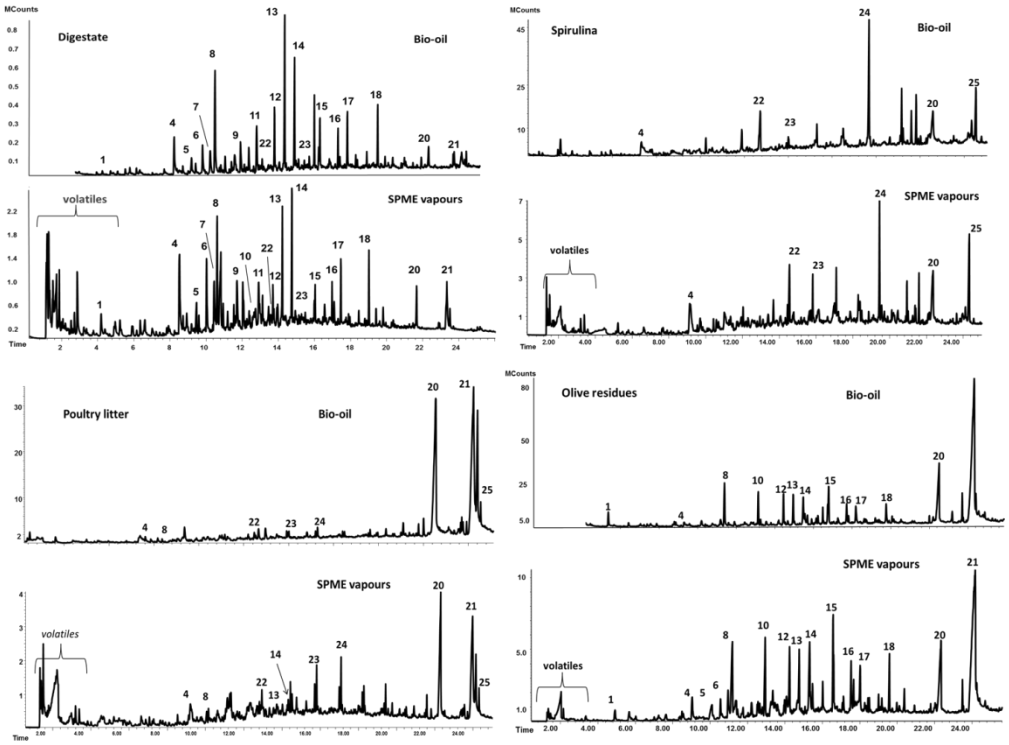

Figure 4.1.3: Total Ion Chromatograms from direct GC-MS analysis of bio-oil and SPME-GC-MS of vapours from preparative pyrolysis with a bench scale reactor of digestate, spirulina, poultry litter and olive residues. Numbers correspond to the products in Table 2. In the curly bracket the volatiles products identified: hydroxyacetaldehyde; acetic acid; acetone; hydroxyacetone; 3-pentanone

Table 4.1.2: Relative distribution (% peak area) of compounds detected into the bio-oil (BO) after pyrolysis at 500°C and after at-line SPME during pyrolysis. In the last row the Pearson correlation coefficient for each biomass is showed.

	Biomass		Pine sawdust		Cornstalk		Switchgrass		Bark		Poultry litter		Olive residues		Spirulina		Digestate	
#	**compound**	**m/z**	**BO**	**SPME**	**BO**	**SPME**	**BO**	**SPME**	**BO**	**SPME**	**BO**	**SPME**	**BO**	**SPME**	**BO**	**SPME**	**BO**	**SPME**
1	Furaldehyde	96	13.5	9.5	11.5	1.1	47.2	24.7	16.9	1.8	–	–	4.3	11.9	–	–	0.40	3.74
2	Hydroxypentenone	98	0.6	2.8	6.0	1.4	6.0	3.7	0.2	3.1	0.6	2.0	0.1	0.1	–	–	0.33	1.10
3	1-methyl cyclopenten-1-one	96	1.4	1.1	1.9	0.8	2.2	0.2	1.5	1.5	–	–	0.5	1.1	–	–	0.50	0.90
4	Phenol	94	2.4	5.0	10.8	18.4	12.3	10.4	3.6	6.9	10.4	19.8	3.3	2.6	23.0	27.3	8.72	18.62
5	3-methyl ciclopentane-1,2 dione	112	16.9	7.9	11.1	4.3	11.6	3.3	11.9	7.5	1.7	4.3	2.3	8.4	–	–	1.85	3.20
6	2-methyl phenol	108	1.2	3.7	2.8	9.1	3.4	3.6	2.7	5.6	4.6	5.3	1.2	1.9	5.6	7.1	2.30	6.93
7	4-methyl phenol	107	2.2	3.7	2.8	9.3	3.4	0.3	2.7	0.6	–	–	3.0	1.9	–	–	3.65	9.99
8	Guaiacol	109	22.3	24.3	10.0	5.8	14.3	10.4	18.2	23.2	5.9	5.5	14.2	12.9	–	–	13.09	13.16
9	4-ethyl phenol	122	0.2	0.5	0.2	1.8	0.2	0.4	0.2	0.4	3.5	14.0	0.0	0.2	–	–	0.66	2.12
10	4-methyl guaiacol	138	1.4	1.8	0.0	0.4	0.1	0.1	0.8	1.3	0.9	1.3	0.2	0.6	–	–	7.10	1.51
11	4-vinyl phenol	120	0.3	1.7	14.3	23.2	12.7	15.9	0.4	1.4	–	–	2.3	0.3	–	–	8.94	6.48
12	4-ethyl guaiacol	137	12.2	14.3	4.1	3.4	6.1	5.0	10.2	10.9	–	–	1.2	7.2	–	–	8.16	4.33
13	4-vinyl guaiacol	150	12.2	10.2	7.5	7.6	10.7	9.2	9.1	9.0	2.8	3.9	8.3	6.4	–	–	14.36	7.68
14	Syringol	154	0.3	1.2	9.9	4.9	9.0	4.4	1.2	5.2	2.3	1.9	8.5	0.8	–	–	10.20	7.80
15	Trans-isoeugenol	164	12.4	10.5	0.5	0.8	1.1	1.4	7.8	8.2	1.7	1.0	8.9	5.5	–	–	3.38	1.72
16	Syringaldehyde	182	0.0	0.5	1.3	1.0	1.8	1.5	3.6	2.6	–	–	7.3	2.6	–	–	3.97	1.72
17	4-vinyl syringol	180	0.6	0.3	2.0	2.0	2.0	2.1	3.7	3.0	–	–	5.3	2.6	–	–	4.80	3.44
18	Methoxyeugenol	194	0.0	0.6	1.4	2.2	1.6	2.5	3.9	3.7	0.7	1.1	6.0	2.8	–	–	4.73	3.12
19	Acetosyringone	181	0.0	0.3	1.5	1.1	1.1	0.5	1.2	0.6	–	–	0.1	0.9	–	–	1.15	1.45
20	Palmitic acid	256	0.0	0.4	0.2	1.2	0.2	0.4	0.1	3.4	34.8	13.8	1.1	0.0	6.2	7.5	0.85	0.98
21	Oleic acid	264	–	–	–	0.2	–	–	–	–	16.0	4.2	21.9	28.8	–	–	0.18	0.00
22	Indole	117	–	–	–	–	–	–	–	–	4.0	0.8	–	–	25.1	24.0	1.40	2.30
23	Methyl indole	131	–	–	–	–	–	–	–	–	2.2	0.8	–	–	6.3	5.7	1.00	1.50
24	Heptadecane	57	–	–	–	–	–	–	–	–	1.0	5.0	–	–	24.2	14.4	–	–
25	Hexadecanamide	72	–	–	–	–	–	–	–	–	2.7	2.4	–	–	9.6	14.1	–	–
26	Cholesterol	386	–	–	–	–	–	–	–	–	3.4	2.0	–	–	–	–	–	–
27	Sitosterol	414	–	–	–	0.3	–	–	–	–	1.0	1.9	–	0.7	–	–	0.72	–
	Pearson correlation coeff		R=+0.92		R= + 0.63		R= +0.92		R= + 0.70		R= +0.56		R= + 0.81		R= +0.86		R= + 0.66	

4.1.3.3 GC-MS analysis (Aqueous phase)

Examples of chromatograms of the aqueous phase are depicted in Figure 4.1.4, while Table 4.1.3 shows the relative distribution (% peak area). Acetic acid was clearly detected in the GC polar column and represented a relatively abundant pyrolysis product of all the aqueous-phase samples. Glyceric acid was also tentatively identified in most of the samples, probably derived from sugar fragmentation in Maillard reaction [39].

In general, the aqueous phase (AP) contained compounds that were also present in the bio-oil (BO) indicating a loss of potential substances, and then a decrease of the relative abundance in the bio-oil compared to pyrolysis vapours detected by SPME. These compounds comprised lignin phenols and sugar derivatives (furaldehydes and cyclopentenones) [40, 41]. A notable exception was the olive residue, in which the aqueous phase seemed poor in organic compounds.

Table 4.1.3: Relative distribution (% peak area) of compounds detected into the aqueous phase (AP) after pyrolysis at 500°C

#	compound	Pine sawdust	Cornstalk	Switchgrass	Bark	Poultry litter	Olive residues	Spirulina	Digestate
1	d-(+)-Glyceric acid	20.7	26.1	16.7	10.3	-	-	-	13.6
2	Acetic acid	24.7	23.4	19.9	45.0	42.5	-	67.4	31.7
3	Furaldehyde	5.6	5.1	15.0	3.9	-	-	-	1.2
4	3-methyl cyclopenten-1-one	1.2	1.5	1.1	0.8	2.4	-	1.9	1.9
5	5-methyl furaldehyde	1.4	0.7	1.8	0.7	-	-	-	0.0
6	Furfuryl alcohol	6.5	8.5	6.4	2.9	38.0	-	-	7.8
7	3-methyl cyclopenten-1,2-dione	5.6	6.1	5.8	3.7	5.4	-	-	9.9
8	Guaiacol	6.0	5.4	5.4	5.0	2.3	-	-	7.5
9	3-ethyl-2-cyclopenten-1-one	1.1	2.1	1.3	0.8	5.1	-	-	3.3
10	4 -methyl guaiacol	6.3	0.9	1.7	5.2	-	-	-	0.6
11	Phenol	1.5	5.1	4.2	1.7	4.3	-	20.0	5.4
12	4-ethyl guaiacol	1.6	1.2	1.8	1.8	-	-	-	0.6
13	2-ethyl phenol	1.3	0.9	1.1	1.0	-	-	-	0.3
14	Vinyl guaiacol	2.5	1.9	2.3	1.0	-	-	-	0.9
15	Syringol	2.4	5.2	5.1	3.6	-	-	-	10.6
16	Trans-Isoeugenol	3.4	1.7	1.9	3.5	-	-	-	1.6
17	5-hydroxymethyl furfural	2.2	1.1	4.0	1.2	-	-	-	-
18	Vanilin	1.7	2.3	2.5	2.0	-	-	-	2.0
19	Propyl guaiacol	2.1	-	0.5	1.4	-	-	-	-
20	Coniferyl alcohol	2.4	0.9	1.1	2.0	-	-	-	1.3
21	4-(ethoxymethyl)-2-guaiacol	-	-	0.6	2.7	-	-	-	-

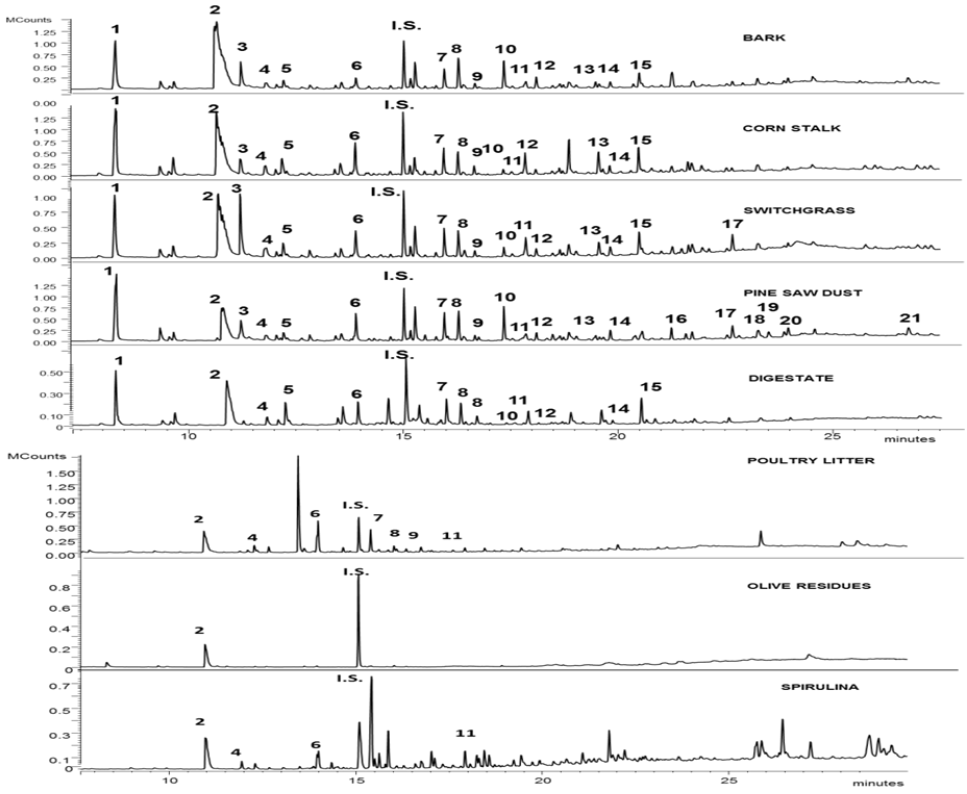

Figure 4.1.4: Total Ion Chromatograms from aqueous phase. Numbers correspond to the products in Total Ion Chromatograms from direct analysis of bio-oil and from SPME of vapours preparative pyrolysis with a bench scale reactor. Numbers correspond to the products in Table 3.

4.1.3.4 SPME-GC-MS

Typical chromatograms from SPME at-line sampling of pyrolysis vapours are depicted in the previous Figure 4.1.2 and Figure 4.1.3. Each SPME chromatogram is place side by side with the corresponding GC-MS of the bio-oil for direct visual comparison. As expected, SPME allowed the detection of highly volatile pyrolysis products that could not be revealed with the direct analysis due to the presence of solvent. Volatile pyrolysis products were tentatively identified by single ion quantitation on the basis of a previous study [15] as methanol (*m/z* 31), acetone (*m/z* 58), acetic acid (*m/z* 60), and hydroxyacetone (*m/z* 43).

Important similarities can be seen in the elution region of the semi-volatiles of the vapours and BO that were featured by the same suite of pyrolysis products. Differences and similarities were investigated on a quantitative basis by the relative distribution expressed as % peak area of selected compounds (Table 4.1.2). Nitrogen containing compounds, fatty acids and sterols were not included because of they were not revealed in most of the biomass pyrolysates.

The relative distribution of the selected compounds in vapour phase sampled by SPME and those condensed in the BO were plotted in Figure 4.1.5 collectively for all the investigated biomass samples.

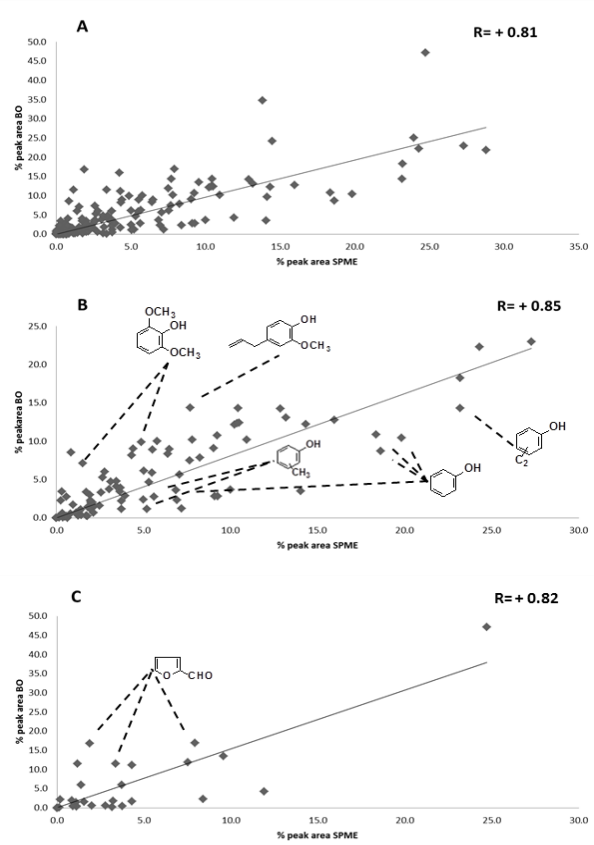

Figure 4.1.5: All-biomass linear correlation between the relative distribution (% peak area) of compounds observed by direct GC-MS analysis bio-oil and from SPME sampling of pyrolysis vapours (*A:* plotting all pyrolysis products; *B:* plotting phenolic fraction*; C:* plotting cellulose derivatives compounds)

A satisfactory linear correlation (R= + 0.81) was found when considering all the compounds. Further correlations, grouping the pyrolysis products on the basis of chemical families, were evaluated. The pyrolysis products have been divided in phenols and cellulose derivatives compounds as the most abundant compounds. The lignin phenols and cellulose derivatives compounds (Fig. 4.1.5) showed a good correlation (with R coefficient respectively of + 0.85 and + 0.82). This finding indicated that the composition of vapours determined by SPME sampling provided a reasonably prediction of the composition of the condensable bio-oil with regard to the semi-volatile fraction. However, the similarity seems to be dependent on the biomass substrate as evident by the linear correlation coefficients resulting from each single biomass (last raw of Table 2). Good linear correlations (R > + 0.8) were found for pine wood, switchgrass, olive residues and spirulina, while less satisfactory (R < + 0.8) were calculated for cornstalk, bark, poultry litter and digestate.

In general, the observed differences could be explained by lower molecular weight compounds (LMW) more abundant in the SPME. This can be due to several factors, a higher affinity of the CAR/PDMS fiber towards LMW compounds which are more effectively sorbed onto the CAR micro-porous structure [42], incomplete trapping of LMW compounds in the cold traps [20], and distribution of polar LMW compounds (e.g. acetic acid) into aqueous phase.

4.1.3.5 Fiber storage capacity

The capacity of the fiber to trap the sorbed pyrolysis products under appropriate conditions was investigated in the case of pyrolysis experiments with digestate. The fiber was stored for 48 and for 96 hours after the sampling before GC-MS analysis. The total peak area of selected compounds (Table 4.1.2) was reported in Figure 4.1.6. Although a decrease in GC detectable compounds was observed with ageing the effect was not significant as intense GC traces could still be obtained that enabled the identification and quantitation of the main compounds (Fig. 4.1.7).The percentage of the compounds retained by the fiber is higher (66%) when the fiber is stored in the vacuum-packed bag for 48 hours, but for longer periods (96 h) or under air atmosphere the percentage is around 45%.

Thus, the analytes remained trapped in the fiber without excessive degradation and volatilisation when stored under air and vacuum-packed bags.

Results obtained are in accordance with those reported by Müller and coworkers [23], who have investigated storage capacity of several SPME fibers at different times from 5 minutes to 24 hours, and at different temperatures (24 °C, 4°C and -70°C) reporting percentages of the analytes retained by the fiber (CAR/PDMS) between 30% and 85% after 24 h of storage at room temperature. However, significant differences from coating to coating were observed.

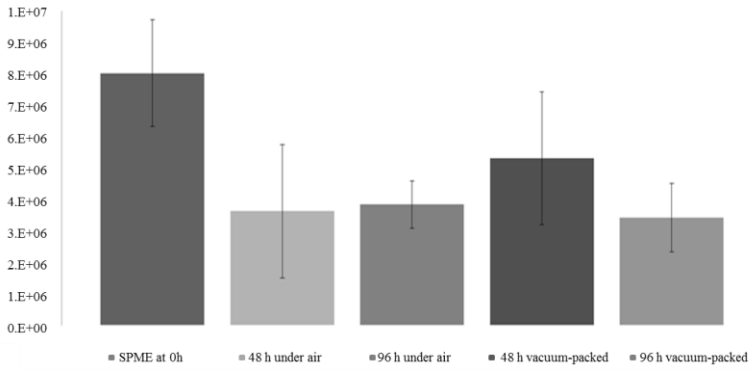

Figure 4.1.6: Total GC-peak areas from SPME of vapours from digestate pyrolysis. GC-MS performed soon after sampling (0 h) and after 48 and 96 hours storage and under air atmosphere and in vacuum packed bag (mean values and standard deviation (n=3))

The relative distribution (Fig.7), although rather similar, generally showed, as expected, a decrease in the relative abundance of pyrolysis products with LMW (more volatiles) such as phenol, 2-methyl phenol and 4-methyl phenol, that decrease by about 40% and 60%, respectively, after 48 and 96 h under air atmosphere and by about 53% and 46% respectively after 48 and 96 h in vacuum-packed bag. However, at 48 h and 96 h storage under air atmosphere, some compounds (above all #1, #3, #8 and #19 which are furaldehyde, 1-methyl cyclopenten-1-one, guaiacol and acetosyringone, respectively) showed relative abundance higher than those after sampling at 0h. We consider that this behavior could be caused by secondary contaminations during the storage under air atmosphere, in accordance with Müller et al., [23], who have affirmed that outer environment can produce some contaminations.
Nevertheless, the feasibility of on-site sampling with a SPME device can be confirmed. In addition, SPME could be applied for a simple online monitoring of a small distributed pyrolysis plant.

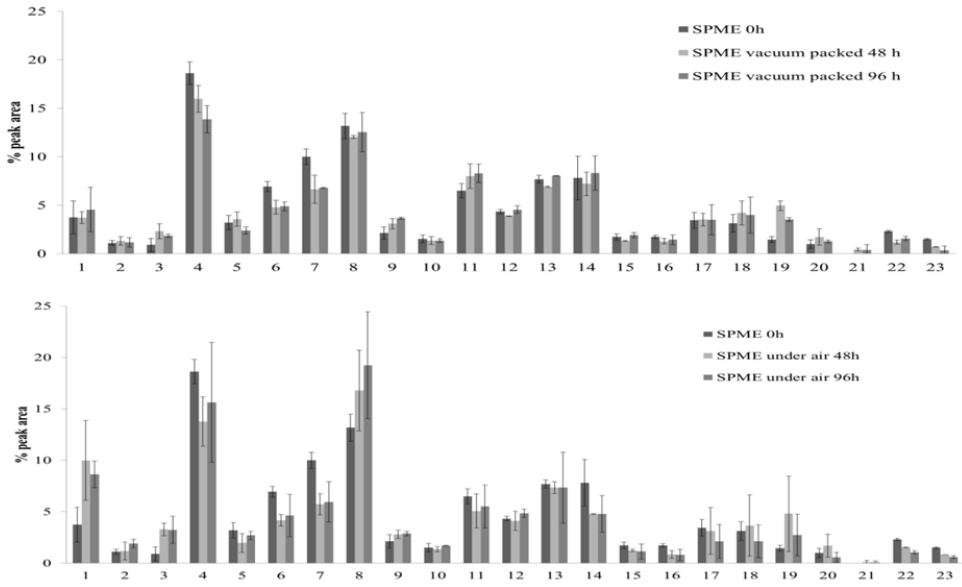

Figure 4.1.7: Products distribution from SPME-GC-MS analysis of digestate soon after sampling (0h) and after storage 48 and 96 hours in vacuum-packed bags (above) and under air atmosphere (below). Numbers in x-axis correspond to the compounds in Table 2

4.1.4 Conclusions

The results of this study conducted on eight different kind of biomass substrates demonstrated that at-line sampling by solid phase microextraction in a bench scale pyrolysis reactor can provide relatively accurate qualitative/semiquantitative analytical information. The chemical composition obtained from at-line sampling by SPME of the vapours evolved during pyrolysis was similar to that of the resulting pyrolysis liquid. SPME provided additional information about the compounds that could be lost by ineffective trapping of the vapours or those distributed into the aqueous phase. The similarity depended on the feedstock and in general was higher for lignocellulosic biomass.

This procedure can be proposed as potentially applicable for the online monitoring of pyrolysis reactors in the production of bio-oil or biochar, or to predict the composition of tars that may contaminate syngas in gasification plants. It was demonstrated that the fiber can be stored in tightly closed plastic bags under vacuum for 4 days before GC-MS analysis. This possibility could be of interest in those situations where the reactor and laboratory are in different places.

Moreover, SPME sampling could represent a helpful tool for bio-oil sampling/analysis that could be employed for monitoring the pyrolysis process avoiding sample collection and sample pre-treatment thus reducing laboratory working time.

References

[1] A.V. Bridgwater, Review of fast pyrolysis of biomass and product upgrading, *Biomass Bioenerg., 38 (2012) 68-94*

[2] Q. Zang, J. Chan, T. Wang, Y. Xu, Review of biomass pyrolysis oil properties and upgrading research, *Energ. Convers. Manage, 48 (2007) 87-92*

[3] P.K. Kanaujia, Y.K. Sharma, U.C. Agrawal, M.O. Garg, Analytical approaches to characterizing pyrolysis oil from biomass, *TrACh 42 (2013) 125-136*

[4] D. Mohan, C. U. Pittman, P. H. Steele, Pyrolysis of wood/biomass for bio-oil: a critical review, *Energ. Fuel., 20 (2006) 848-889*

[5] P. K. Kanaujia, Y. K. Sharma, M. O. Garg, D. Tripathi, R. Singh. Review of analytical strategies in the production and upgrading of bio-oils derived from lignocellulosic biomass, *J. Anal. Appl. Pyrol., 105 (2014) 55-74*

[6] D. Meier, New methods for chemical and physical characterization and round robin testing. In: *A. V., Bridgewater (Eds.), et al., Fast Pyrolysis of Biomass: a handbook, CPL Press: Newbury, U.K., (1999), pp. 92−101*

[7] M. Staš, D. Kubička, J. Chudoba, M. Pospíšil, Overview of analytical methods used for chemical characterization of pyrolysis bio-oil, *Energ. Fuel., 28 (2014) 385-402*

[8] C. Tessini, N. Muller, C. Mardones, D. Meier, A. Berg., D. Von Baer, Chromatographic approaches for determination of low-molecular mass aldehydes in bio-oil, *J. Chromatogr. A, 1219 (2012) 154-160*

[9] C. Torri, E. Soragni, S. Prati, D. Fabbri, Py-SPME-GC-MS with on-fiber derivatization as a new solvent-less technique for the study of polar macromolecules: application to natural gums, *Microchem. J., 110 (2013) 719-725*

[10] A. Oasmaa, E. Kuoppala. Solvent fractionation method with Brix for rapid characterization of wood fast pyrolysis liquids. *Energ Fuel, 22* (2008*) 4245-4248*

[11] C.L. Arthur, J. Pawliszyn., Solid phase microextraction with thermal desorption using fused silica optical fibers, *Anal. Chem., 62 (1990) 2145-2148*

[12] Z. Zang, M.J. Yang, J. Pawliszyn. Solid-phase microextraction. A solvent-free alternative for sample preparation, *Anal. Chem., 66 (1994) 844A-853A*

[13] P. Vesely, L. Lusk, G. Basarova, J. Seabrooks, D. Ryder, Analysis of aldehydes in beer using solid-phase microextraction with on fiber derivatization and gas chromatography/mass spectrometry, *J. Agric. Food Chem., 51 (2003) 6941-6944*

[14] G. Ouyang, D. Vuckovic, J. Pawliszyn, Nondestructive sampling of living systems using in vivo solid-Phase, *Chem. Rev. 111 (2011) 2784-2814*

[15] C. Torri, D. Fabbri, Application of off-line pyrolysis with dynamic solid-phase microextraction to the GC-MS analysis of biomass pyrolysis product, *Microchem. J., 93 (2009) 133-139*

[16] L. Busetto, D. Fabbri, R. Mazzoni, M. Salmi, C. Torri, V. Zanotti, Application of the shvo catalyst in homogeneous hydrogenation of bio-oil obtained from pyrolysis of white poplar: new mild upgrading conditions, *Fuel, 90 (2011) 1197-1207*

[17] J. Deng, Y. Yang, X. Wang, T. Luan, Strategies for coupling solid-phase microextraction with mass spectrometry, *TrACh 55 (2014) 55-67*

[18] J.A Koziel, I. Novak, Sampling and sample-preparation strategies based on solid-phase microextraction for analysis of indoor air, *TrACh 21 (2002) 840-850*

[19] P. J. Woolcock, J.A. Koziel, L. Cai, P.A. Johnston, R. C. Brown, Analysis of trace contaminants in hot gas streams using time-weighted average solid-phase microextraction: Proof of concept, *J. Chromatogr. A, 1281 (2013) 1-8.*

[20] C. Brage, Q. Yu, G. Chen, K. Sjostrom, Use of amino phase adsorbent for biomass tar sampling and separation, *Fuel, 76 (1997) 137-142*

[21] M. Ahmadi, E.E. Svensson, K. Engvall, Application of solid-phase microextraction (SPME) as a tar sampling method, *Energ. Fuel, 27 (2013) 3853-3860*

[22] G. Guehenneux, P. Baussand, M. Brothier, C. Poletiko, G., Boissonnet, Energy production from biomass pyrolysis: a new coefficient of pyrolytic valorization, *Fuel, 34 (2005) 733-73*

[23] L. Müller, T. Górecki, J. Pawliszyn. Optimization of the SPME device design for field applications, *Fresenius J. Anal. Chem., 364 (1999) 610-616*

[24] J.A. Koziel, M. Odziemkowski, J. Pawliszyn, J., Sampling and analysis of airborne particulate matter and aerosols using in-needle trap and SPME fiber devices. *Anal. Chem., 73 (2001) 47-54.*

[25] J. Neumann., S. Binder, A. Apfelbacher, J.R. Gasson, P. Ramírez García, A. Hornung, Production and characterization of a new quality pyrolysis oil, char and syngas from digestate-introducing the thermo-catalytic reforming process, *J. Anal, Appl. Pyrol., 113 (2015) 137-142*

[26] C. Torri, A. Adamiano, D. Fabbri, C. Lindfors, A. Monti, A. Oasmaa, Comparative analysis of pyrolysate from herbaceous and woody energy crops by Py-GC with atomic emission and mass spectrometric detection, *J. Anal. Appl. Pyrol., 88 (2010) 175-180*

[27] D. Fabbri, C. Torri, I. Mancini, Pyrolysis of cellulose catalysed by nanopowder metal oxides: production and characterisation of a chiral hydroxylactone and its role as building block, *Green Chem., 9 (2007) 1374-1379*

[28] A. Oasmaa, E. Kuoppala, E. Y. Solantausta. Fast pyrolysis of forestry residue. 2. Physicochemical composition of product liquid. *Energ. Fuel*, *17* (2003) *433-443*

[29] J. Piskorz, P. Majerski, D. Radlein, D. S. Scott, Conversion of lignins to hydrocarbon fuels, *Energ. Fuel, 3 (1989) 723–726*

[30] A. Hornung, S. Binder, M. Jakuttis, A. Apfelbacher, Patent application 2014041511535400DE, Anlage und verfahren zur thermokatalytischen behandlung von Material und damit hergestelltes pyrolyseöl (2014)

[31] H. Huang, X. Yuan, G. Zeng, J. Wang, H. Li, C. Zhou, X. Pei, Q. You, L. Chen, Thermochemical liquefaction characteristics of microalgae in sub- and supercritical ethanol, *Fuel Process. Technol,. 92 (2011) 147-153*

[32] S-S. Kim, F.A., Agblevor, J., Lim, Fast pyrolysis of chicken litter and turkey litter in a fluidized bed reactor, *J. Ind. Eng. Chem., 15 (2009) 247-252*

[33] B. Scholze, D. Meier. Characterization of the water-insoluble fraction from pyrolysis oil (pyrolytic lignin). Part I. PY–GC/MS, FTIR, and functional groups. *J. Anal Appl. Pyrol., 60 (2001) 41-54*

[34] P. R. Patwardhan, R. C. Brown, B. H., Shanks, Understanding the fast pyrolysis lignin, *Chemsuschem, 4 (2011) 1629-1636*

[35] E. R. E., Van der Hage, M. M., Mulder, J. J., Boon, Structural characterization of lignin polymers by temperature-resolved in-source pyrolysis-mass spectrometry and Curie-point pyrolysis-gas chromatography/mass spectrometry, *J. Anal. Appl. Pyrol., 25 (1993) 149-183*

[36] W. Boerjan, J. Ralph, M. Baucher, Lignin biosynthesis, *Ann. Rev. Plant Biol., 54 (2003) 519–546*

[37] D. R.,Vardon, B.K. Sharma, J. Scott, G., Yu, Z., Wang, L., Schideman, Y., Zhang, T. J., Strathmann, Chemical properties of biocrude oil from the hydrothermal liquefaction of Spirulina algae, swine manure, and digested anaerobic sludge, *Bioresource Technol., 102 (2011) 8295-8303*

[38] P. Biller, A.B. Ross, Potential yields and properties of oil from the hydrothermal liquefaction of microalgae with different biochemical content, *Bioresource Technol., 102 (2011) 215–225*

[39] T. Davídek, F. Robert, S. Devaud, F. Arce Vera, I. Blank, Sugar fragmentation in the Maillard reaction cascade: formation of short-chain carboxylic acids by a new oxidative α-dicarbonyl cleavage pathway, *J. Agric. Food Chem., 54 (2006) 6677-668*4

[40] K. Sipilä, E. Kuoppala, L. Fagernäs, A. Oasmaa, Characterization of biomass-based flash pyrolysis oils, *Biomass Bioenerg., 14 (1998) 103-113*

[41] A. Demirbas, The influence of temperature on the yields of compounds existing in bio-oils obtained from biomass samples via pyrolysis *Fuel Process Technol., 88 (2007) 591-597*

[42] J.A. Koziel, M. Jia, J. Pawliszyn, Air sampling with porous solid-phase microextraction fibers. *Anal. Chem., 72 (2000) 5178-5186*

Chapter 5

Structural investigation of biochar by analytical pyrolysis

5.1 Evaluation of the thermal and environmental stability of switchgrass biochars by Py-GC-MS

5.1.1 Introduction

Biochar is a carbonaceous solid material artificially synthesized from biomass with the purpose to enhance soil properties and carbon sequestration. Explorative studies highlighted a series of advantages in the use of biochar as soil amendment that included increased soil fertilization, valorization of agrochemical byproducts, storage of carbon, reduced greenhouse gas emissions along with possible limitations and drawbacks [1-6]. Because of the growing interest captured by this material, a plethora of analytical techniques have been applied to investigate its chemical structure and undoubtedly GC-MS is the master technique for the determination of individual organic compounds formed during charring and sorbed onto the carbonaceous matrix. GC-MS was applied to the analysis of polycyclic aromatic hydrocarbons (PAHs) [7-10], polychlorinated organic compounds [7], and volatile organic compounds[11-12] in chars obtained from different sources. The chemical information affordable by GC-MS was extended to non-volatile components susceptible to be thermally fragmented into volatile compounds by means of flash pyrolysis (Py) [13-17]. When charcoals were subjected to Py-GC-MS the resulting GC-MS traces (pyrograms) were featured by peaks associated with benzene, toluene, naphthalene, biphenyl, dibenzofuran and benzonitrile [13]. These pyrolysis products were assumed to represent the charred fraction rich of aromatic structures that occur in a thermally labile form in the carbonaceous matrix. In addition, pyrolysis product ratios representing the relative abundance of alkylated and parent compounds (e.g., benzene/toluene peak area ratio) were proposed as indicators for the presence of saturated alkyl bridges between polyaromatic structures and hence a measure of the charring intensity [14]. On a quantitative basis, Py-GC-MS applied to a set of biochar samples produced from the same feedstock at increasing temperatures (thermosequence) showed that the total GC peak areas of the evolved pyrolysis products decreased with increasing charring intensity, whilst the relative peak area (% charred) of products associated with charring (aromatic hydrocarbons, benzofurans, and benzonitriles) increased [15]. Highly polycondensed aromatic moieties cannot be cracked into volatile compounds and pyrolysates of extremely carbonised biochars were barely detectable by GC-MS. In contrast, intense pyrograms featured by pyrolysis products preserving the chemical functionality of

hemicellulose, cellulose and lignin (e.g. pyranones, furaldehydes, methoxyphenols) were revealed in the pyrograms of chars obtained at low temperatures [15]. Therefore, total peak areas and % charred were proposed as indices of the charring intensity in accordance to the results obtained with other analytical techniques applied to the same samples, such as hydrogen pyrolysis (HyPy) with carbon isotope ratio [18], and Fourier transform infrared spectroscopy (FTIR) [16]. The widespread validity of these Py-GC-MS indices (total peak area or pyrolysis product yield, % charred, pyrolysis product ratios) was tested through the analyses of biochars from different feedstock and process conditions [17]. The estimated yield of pyrolysis products was correlated with volatile matter, a parameter proposed for the labile charred fraction [19], while the % charred was inversely correlated with the elemental O/C ratio, a measure of charring and environmental persistence [20]. However, correlations between Py-GC-MS data and the various biochar parameters were not very strong, probably because of the great variability in the biochar sources.

Nevertheless, the knowledge of the thermal behaviour of biochar is of great interest because it may help in predicting the environmental stability of biochar and its ability to store carbon more efficiently than fresh biomass. To this purpose, indices have been proposed based on elemental [20] and thermal analysis [19, 21]. As above illustrated, Py-GC-MS is able to provide molecular indices of the thermal stability, however, a few studies have been published aimed at comparing these indices to those arising from aerobic degradation[17,22]. The CO_2 production from incubation experiments was found to be high for biochars producing pyrograms characterized by the presence of lignocelluloses markers [17]. However, even highly carbonized biochar producing a Py-GC-MS trace characterized by the presence of aromatic hydrocarbons and the lack of lignin/carbohydrate markers can induce respiration when applied to soil [23]. In general, more data are necessary to evaluate the potential and consistency of Py-GC-MS for the characterization of the thermal and environmental stability of biochar using molecular markers. The goal of this study was to provide a comprehensive comparison between molecular analysis by Py-GC-MS and bulk analysis on a large set of biochar samples produced from the same feedstock and the same pyrolysis unit. Different process conditions, charring temperature and residence time, were utilized to obtained biochars with different degrees of charring. Switchgrass (*Panicum virgatum*) was selected as biomass because of its importance in energy crops where pyrolysis to produce bioenergy is coupled with carbon sequestration [24-26].

5.1.2 Experimental

5.1.2.1 Biochar production

Biochar samples were synthesized by pyrolysis of switchgrass (*Panicum virgatum*, air dried at 60 °C, milled and sieved at 2 mm) using a fixed bed tubular quartz reactor (length: 650 mm, internal diameter 37 mm) placed into a refractory furnace. Switchgrass samples (about 3 g of biomass) were uniformly placed onto a sliding quartz boat, under a nitrogen flow of 1500 cm^3 min^{-1}. When the temperature inside the reactor, measured with a thermocouple, reached the selected value, the boat was pushed into the oven. Pyrolyses were performed at different temperatures, in the 400-700°C range, with increments of 50°C. After a given residence time (1, 2, 5, 10 or 20 minutes), the quartz boat was withdrawn from the heated zone and cooled at ambient temperature under nitrogen in order to avoid possible char oxidation. Then, biochar was weighed and kept in closed vials before analysis. Overall, 35 biochar samples were obtained and named according the synthesis conditions. As an example, biochar 500/10, is the biochar synthesized at 500 °C for 10 minutes.

5.1.2.2 Chemical analysis

Elemental composition (HCNS) was determined by combustion using a Thermo Scientific Flash 2000 series analyzer. Ash was determined as the residual mass left after exposure at 600°C for 5 hours. The oxygen content was calculated from the mass balance: %O=100-%(C+H+N+ash)%. A mixture of biochar with deionized water at 1:10 wt/wt ratio was prepared, thoroughly mixed and pH measured at room temperature with a digital pH meter (HI 98103, Checker®, Hanna Instruments). Analyses of PAHs were conducted as described in [10] on about 0.5 g of biochar spiked with 0.1 mL of surrogate PAH mix (Supelco for EPA 525 containing acenaphthene-d_{10}, phenanthrene-d_{10} and chrysene-d_{12} 5 μg mL^{-1} each in acetonitrile) and soxhlet extracted with acetone/cyclohexane (1:1, v/v) for 36 hours. The solution was filtered, added with 1 ml of *n*-nonane (keeper), carefully evaporated by rotatory vacuum evaporation at 40 °C and cleaned up by solid phase extraction onto a silica gel cartridge before analysis with an Agilent HP 6850 GC coupled to a Agilent HP 5975 quadrupole mass spectrometer; GC-MS conditions were those detailed in [10]. Recovery of surrogated PAHs was determined with respect to the internal standard tri-*tert*-butylbenzene.

5.1.2.3 Py-GC-MS

Py-GC-MS analyses were performed using an electrically heated platinum filament CDS 1000 pyroprobe valved interfaced to a Varian 3400 GC equipped with a GC column (HP-5-MS; Agilent Technologies 30 m × 0.25 mm, 0.25 μm) and a mass spectrometer (Saturn 2000 ion trap, Varian Instruments). GC thermal program: 35 °C to 310 °C at 5°C min^{-1}; MS conditions: electron ionisation at 70 eV, full scan acquisition in the 10–450 *m/z* interval. A quartz sample tube containing a weighed amount of sample in the interval of 5 mg (biochars produced at residence times of 5-20 minutes) to 0.5 mg (biochars produced at residence times of 1-2 minutes) was inserted into the Py-GC interface (300 °C) and then pyrolysed at 900 °C (set temperature) for 100 s wit helium as carrier gas (100 ml min^{-1}). The internal standard addition used in [17] failed to provide reliable results, probably because of the different interface used in this study. Single point external calibration (1 μL of 1000 mg L^{-1} ethyl benzoate solution in acetonitrile) was performed to estimate the detector response factor. The yield (μg mg^{-1}) was expressed as the quantity of each pyrolysis product evolved from a weighed amount of analysed biochar and was calculated from the GC peak area in the mass chromatogram at the *m/z* of the characteristic ion in the mass spectrum [17] and the response factor relative to ethyl benzoate. A unitary relative response factor was assumed for all the quantified compounds on the basis that our objective was to determine relative quantities, not the absolute yields of the various pyrolysis products similarly to other studies [14-17].

A set of 34 pyrolysis products were quantified as markers 136 of polysaccharides (holocellulose) (hydroxyacetone,2,5-dimethylfuran, furaldehyde, furfuryl alcohol, 2-cyclopentanedione, 2-hydroxymethylenetetrahydrofuran-3-one, 3-hydroxy-2-methylcyclopentenone, 5-hydroxymethyl-2-furaldehyde);lignin (phenol, 4-methylphenol, guaiacol, 4-ethylphenol, cathecol, 4-vinlylphenol, 4-methylguaiacol, 4-vinylguaiacol, syringol, 4-methylsyringol, *trans*-isoeugenol, 4-vinylsyringol, 4-propenylsyringol); charred biomass (benzene, pyrrole, toluene, ethylbenzene, *m/p*-xylene, styrene, *o*-xylene, benzonitrile, benzofuran, methylbenzofurans (three isomers), naphthalene, phenanthrene [15, 17].

5.1.2.5 Statistical analysis

Reproducibility was determined by triplicate runs of each parameter in different days and assumed to be representative to all the data set. Percent relative standard deviations (% RSD) were the followings: biochar synthesis yields (400/20) ± 5.8 %; Py-GC-MS (biochar 500/20): yields ± 26 %,% charred ± 3.2 %, compound ratios: benzene/toluene± 12 %, toluene/naphthalene ± 7.1 %, *m/p* xylenes/naphthalene ± 23%, benzofuran/naphthalene ± 8.4

%. Recovery of surrogate PAHs was (mean ± %RSD for all the data set): 75% ± 13%, 78% ± 11%, 88% ± 12% for perdeuterated acenaphthene, phenanthrene and chrysene, respectively. PAH analysis was run in duplicates for eight biochar samples, the mean %RSD for total PAHs was 9.8% and 24% for each individual PAH. Two parameters were said to be correlated when the absolute value of the linear (Pearson) correlation coefficient R was larger than 0.45 (the critical value at the level of significance p = 0.01 for two tailed test with 30 degrees of freedom) [17].

5.1.3 Results and discussion

5.1.3.1. Chemical characteristics

In this study, several charring temperatures and residence times were selected in order to obtain chars with a range of chemical characteristics (Table 5.1.1). The degree of carbonization of chars is generally expressed by molar H/C [22] and [27] or O/C ratios [20] and [28]. The H/C ratios here investigated chars ranged from 1.54 (400/1) to 0.25 (700/20) and were strongly correlated with molar O/C ratios (R = +0.97, Table 5.1.2) in accordance to the loss of oxygenated functionalities with increasing carbonization [29]. Because of this strong correlation, the degree of thermal alteration could be expressed by both H/C and O/C ratios. The use of O/C ratios was utilized to differentiate environmental carbonaceous materials, moreover its determination by dispersive X-ray spectrometry coupled with scanning electron microscopy (SEM/EDX) can provide further information on the spatial distribution in particles and a better evaluation of oxygen associated with organic matter through the analysis of metals [28]. In the specific case of biochar, H/C ratio (or H/organic C) was proposed as one of the criteria to assess the basic utility of this material [30] and [31]. Based on this criterion and the fact that the oxygen content was calculated by difference from other parameters, we adopted the H/C ratio as an index of thermal alteration for the purpose of data comparison.

Table 5.1.1: Chemical characterization and Py-GC-MS data (last seven columns) of biochars and their Pearson's coefficients with H/C ratios. Values of the original switchgrass are reported in the first data line.

sample	H/C	O/C	C	N	Yield	ash	PAH	pH	Py yield	cellulose	lignin	charred
°C/min	molar	molar	% wt	% wt	% wt	%	µg g^{-1}		µg/mg	%	%	%
biomass	1.60	0.78	42.5	0.66	n.a.	6.9	n.d.	7.1	15400	33	58	9.1
400/1	1.54	0.80	44.5	0.35	92.0	1.9	0.34	5.7	7000	39	49	12
450/1	1.52	0.71	46.8	0.34	91.0	2.8	0.23	5.6	6200	33	60	7
500/1	1.49	0.73	46.3	0.31	89.1	2.7	0.31	5.6	6500	39	50	11
400/2	1.45	0.72	47.2	0.35	86.0	1.4	0.66	6	5900	36	49	16
550/1	1.33	0.67	48.4	0.32	68.0	2.8	0.37	6.1	4600	35	53	12
450/2	1.26	0.62	50.2	0.32	60.8	2.9	0.58	6.4	5700	33	54	13
600/1	1.22	0.56	52.1	0.36	53.4	3.3	1.8	6.8	3900	36	45	19
500/2	0.96	0.37	60.1	0.40	37.5	5.4	0.82	7	4100	11	60	30
400/5	0.80	0.28	65.5	0.45	31.4	5.5	1.0	7	1300	4.4	74	21
650/1	0.79	0.31	62.2	0.46	26.5	7.8	1.6	8.2	1600	3.3	55	42
400/10	0.71	0.28	63.9	0.44	26.5	8.3	1.4	7	1200	1.2	59	40
450/5	0.69	0.25	67.3	0.51	26.7	6.0	1.0	7.5	1600	0.9	44	55
400/20	0.66	0.24	67.8	0.52	27.7	6.6	1.3	7	1200	0.4	55	44
550/2	0.65	0.27	64.2	0.54	24.5	8.4	0.68	7.5	530	0.9	44	55
700/1	0.64	0.23	66.1	0.46	19.6	9.6	1.7	8.2	1100	0.5	43	57
450/10	0.59	0.26	65.9	0.62	23.8	7.5	0.94	7.8	520	0.1	46	54
450/20	0.58	0.20	68.9	0.53	25.5	8.9	1.1	8.1	650	0.1	46	53
500/5	0.56	0.21	68.5	0.49	22.9	8.8	1.3	8	300	0.0	38	62
600/2	0.54	0.24	67.2	0.51	21.2	7.7	1.6	8.4	470	0.1	24	76
500/10	0.49	0.20	69.1	0.50	22.2	9.6	0.95	8.1	240	0.0	19	81
550/5	0.45	0.21	68.9	0.47	20.6	8.9	0.90	8.2	130	0.0	3.5	96
650/2	0.45	0.19	68.9	0.55	18.6	10.2	1.8	9.5	160	0.0	3.9	96
500/20	0.44	0.21	68.4	0.49	20.4	9.7	1.4	8.6	150	0.0	2.9	97
550/10	0.43	0.22	66.8	0.49	18.8	11.0	1.5	9.2	230	0.0	1.0	99
600/5	0.41	0.17	70.4	0.50	20.4	10.4	1.6	9.2	71	0.0	1.7	98
550/20	0.40	0.21	69.1	0.49	19.0	9.2	1.3	9.3	22	0.0	1.3	98
700/2	0.39	0.15	70.9	0.47	16.7	11.7	1.9	9.2	75	0.0	4.5	96
600/10	0.37	0.16	71.6	0.40	19.8	10.2	1.6	9.4	21	0.0	1.3	99
650/5	0.35	0.25	64.2	0.43	16.7	12.5	1.5	9.6	21	0.0	1.0	99
600/20	0.34	0.15	72.8	0.46	18.8	10.4	1.8	9.5	40	0.3	0.5	99
650/10	0.31	0.16	71.7	0.44	17.5	10.7	1.5	9.4	6.4	1.1	0.7	98
650/20	0.29	0.15	71.8	0.44	17.8	11.8	1.8	9.9	1.6	1.5	1.1	98
700/5	0.28	0.11	75.4	0.40	15.7	11.3	1.9	9.6	4.4	0.9	1.5	98
700/10	0.26	0.18	69.8	0.40	16.8	11.9	2.1	9.8	1.8	0.0	1.8	98
700/20	0.25	0.13	73.4	0.39	17.3	12.3	2.0	10.2	0.4	0.0	0.0	100
R(H/C)	1	0.974	-0.972	-0.623	0.958	-0.960	-0.775	-0.936	0.973	0.932	0.754	-0.931

Table 5.1.2 shows that H/C ratios were inversely correlated with ash (R = −0.96) and concomitantly with pH (R = −0.93). These trends are in line with literature data for similar biomass [27]. The concentrations of PAHs ranged between 0.23 (450/1) and 2.1 µg g^{-1}

(700/10), thus always below the levels recommended by IBI [30] or EBC (4–12 μg g^{-1}) [34]. PAH levels tended to increase with decreasing H/C ratios, however, the correlation was not very strong (R = −0.77), indicating that a multitude of factors could influence the occurrence of PAHs in biochar [32]. In fact, different trends were reported in the literature [7], [9] and [32], such as decreasing or increasing PAH concentrations with increasing pyrolysis time/temperature for slow and fast pyrolysis, respectively [7], or PAH concentrations peaking at 500 °C in grass biochars produced in the 100–700°C pyrolysis interval [9]. In the case of biochar obtained from slow pyrolysis (8 h) of switchgrass, PAH concentrations were reported to decrease from 350 to 800/900°C [7].

The synthesis yields ranged from 16 to 92% (Table 5.1.1). The highest yields were obtained with low temperatures (<600 °C) and low residence times (1–2 min), and were nearly constant with residence times equal or larger than 5 min. An average yields of 21 ± 4% in the whole temperature interval of 400–700 °C was calculated. These data compare reasonably with the results from thermogravimetric analyses of switchgrass reporting that mass loss was complete at 550 °C with a residue of 20% [33].

Table 5.1.2: Correlation matrix of data reported in table 5.1.1. Values from Py-GC-MS are italicized.

	H/C										
O/C	0.975	**O/C**									
C	−0.973	−0.992	**C**								
N	−0.617	−0.686	0.656	**N**							
Char yield	0.959	0.979	−0.953	−0.695	**Char yield**						
Ash	−0.959	−0.913	0.902	0.505	−0.894	**Ash**					
PAHs	−0.777	−0.756	0.75	0.307	−0.760	0.79	**PAH**				
pH	−0.935	−0.867	0.872	0.424	−0.850	0.948	0.844	**pH**			
Py–GC yield	0.974	0.974	−0.960	−0.715	0.97	−0.916	−0.741	−0.868	***Py–GC yield***		
Holocellulose	0.934	0.97	−0.949	−0.774	0.957	−0.869	−0.648	−0.786	0.953	***holocellulose***	
Lignin	0.755	0.622	−0.652	−0.211	0.589	−0.791	−0.645	−0.869	0.656	0.519	***Lignin***
Charred	−0.929	−0.848	0.861	0.468	−0.819	0.929	0.735	0.952	−0.866	−0.785	−0.936

5.1.3.2 Py–GC–MS

Some typical pyrograms resulting from Py–GC–MS of biochar samples are depicted in Fig.5.1.1. Samples with high H/C values produced complex pyrolysates with intense peaks assignable to the pyrolysis products of hemicelluose, cellulose or lignin, on the contrary samples with low H/C ratios produced simple pyrograms with weak peaks of aromatic hydrocarbons.

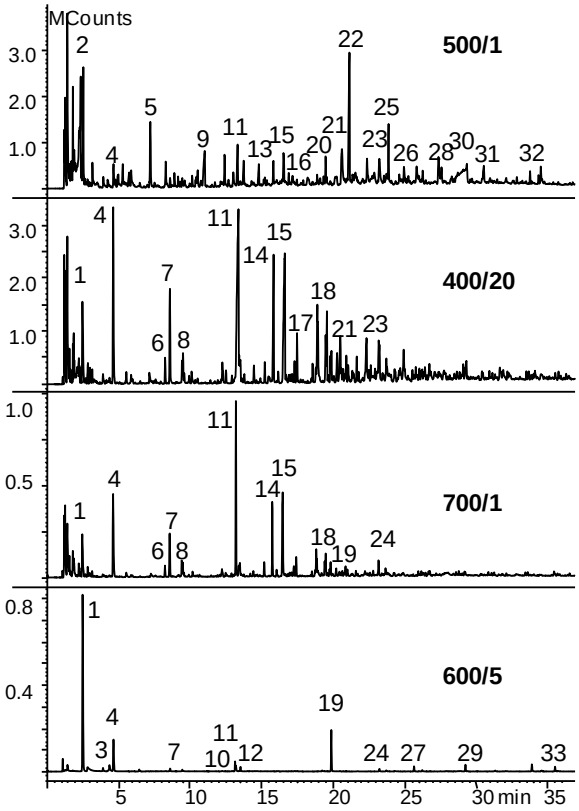

Figure 5.1.1: Total ion chromatograms from Py-GC-MS of biochar 500/1 (0.51 mg), 400/20 (5.37 mg), 700/1 (0.53 mg) and 600/5 (5.21 mg).

Peak attribution: 1: benzene; 2: hydroxyacetone; 3: pyrrole; 4: toluene; 5: furaldehyde; 6: ethyl benzene; 7: *m/p*-xylenes; 8: styrene; 9: 1,2-cyclopentanedione; 10: benzonitrile; 11: phenol; 12: benzofuran; 13: 3-hydroxy-2-methylcylopentenone; 14: *o*-methylphenol; 15: *m/p*-methylphenols; 16: guaiacol; 17: methylbenzofurans; 18: C2-phenols; 19: naphtalene; 20: 4-methylguaiacol; 21: cathecol; 22: 4-vinylphenol; (28); 23: methylcathecols; 24: methylnaphthalenes; 25: 4-vinylguaiacol; 26: syringol; 27: biphenyl; 28: *trans*-isoeugenol; 29: dibenzofuran; 30: levoglucosan; 31: 4-vinylsyringol; 32: 4-propenylsyringol; 33: phenanthrene.

Pyrolysis products selected for quantitation were grouped into three thermolabile class fractions: highly carbonised (charred), weakly carbonised hemi/cellulose and weakly carbonised lignin (see experimental part). The grouping of pyrolysis products into the fraction was specified in Section 5.1.2.3.

Switchgrass hemicellulose is mainly composed of arabinoxylans [34], but anhydropentofuranoses (characteristic ions at m/z 57, 73, 86) which are specific pyrolysis products of hemicellulose [35], could not be unambigously identified in the pyrolysates. Levoglucosan was the only anhydromonosaccharide positively identified in some pyrolysates (Fig. 5.1.1). The set of pyrolysis products of polysaccharides selected in this study could not be assigned specifically to cellulose or hemicellulose, thus this group was generically ascribed to holocellulose. However, the pyrolysis product 2-hydroxymethylenetetrahydrofuran-3-one,

often identified as a hydroxypyrone [38], was indicated as a specific product of xylans [35] and [36].

The quantity of evolved pyrolysis products was expressed in terms of "yield" to give a rough estimate of the mass fraction that was analysed by GC–MS. Table 1 shows that the summed yields covered a large interval ranging from 0.4 μg g^{-1} (700/20) to 7000 μg g^{-1} (400/1).

These orders of magnitudes are in accordance to data obtained under similar conditions from different biochars [17] and indicate that only a very small fraction of biochar could be thermally fragmented and analysed by GC–MS. The Py–GC–MS yields were strongly correlated with H/C and O/C ratios (R = +0.97 in both cases, Table 5.1.2) confirming earlier studies that the quantity of the evolved pyrolysis products is an inverse index of the charring intensity [13], [14] and [15]. Analogously, the %charred fraction was correlated with the content of carbon (R = +0.86), ash (R = +0.93) and inversely correlated with H/C (R = −0.93) and O/C ratios (R = −0.85). A weak positive correlation was found between PAH levels and %charred (R = +0.73).

The molecular compositions of the pyrolysates were found to be significantly different in the investigated biochars. Pyrolysis products associated to cellulose (e.g. 2,5-dimethylfuran) and lignin markers preserving methoxy groups (e.g. guaiacols) became undetectable at H/C < 0.6 as evidenced in Fig. 5.1.2 showing the mass pyrograms of some biochars with decreasing H/C ratios. Less specific markers of lignin (methylphenols) were not detected in biochars with H/C < 0.4, but phenol was revealed in biochars with H/C ratios down to 0.3. Thus, the role of phenols and cathecols as markers of highly or weakly pyrolysed lignin is not that clear as discussed by Kaal et al. [15].

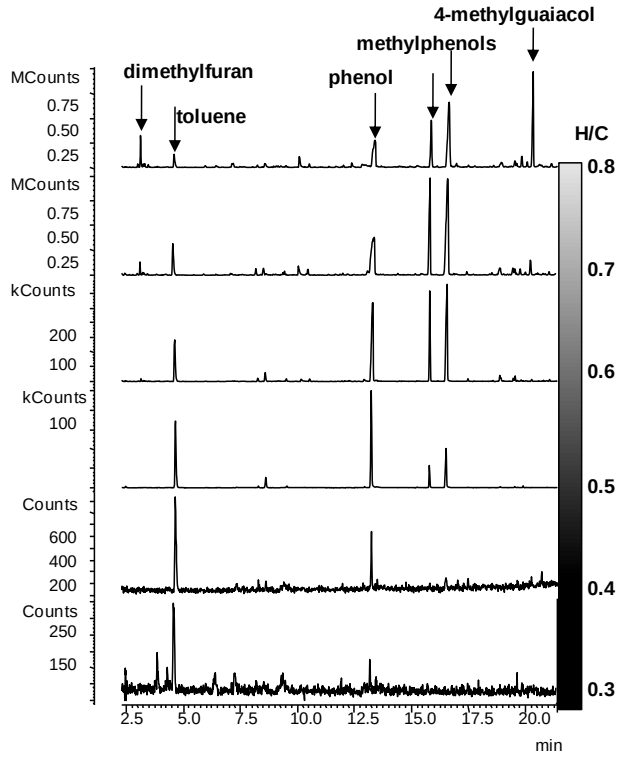

Figure 5.1.2: Mass pyrograms at ions characteristics of toluene/phenol, dimethylfuran, methylphenols and 4-methylguaiacol at *m/z* 65, 96, 108 and 138, respectively. From top to bottom: Py-GC-MS of biochar samples 400/5, 450/5, 450/10, 500/10, 550/20, 700/2 and 650/10 and the corresponding H/C molar ratios.

As far as the presence of markers of the highly carbonized faction is concerned, benzene, toluene, styrene and naphthalene were the only products revealed in the pyrolysates of all the samples, including the most charred biochar (700/20, H/C = 0.25). Benzonitrile, xylenes, benzofuran, pyrrole, ethylbenzene, biphenyl, and phenantrene were the other major pyrolysis products characterising biochars with H/C < 0.4. However, peak integration was difficult for highly carbonised biochars (H/C < 0.3) and artefacts due to cross-contamination may occur (for instance, weak signals of carbohydrate markers were detected in biochars 650/10 and 650/20). The relative content of pyrolysis products indicative of the more thermally altered fraction (% charred, Table 5.1.1) increased from about 10% for weakly charred biomass to 100% and was strongly correlated with the H/C ratio ($R = -0.93$).

Pyrolysis product yield ratios were calculated with respect to benzene, toluene and naphthalene because these were the only quantifiable compounds in the pyrolysates of the most charred biochars. Compound ratios with naphthalene gave better parameter correlations than with benzene or toluene, thus only the results relative to product/naphthalene ratios will be presented and discussed. Table 5.1.3 reports the linear correlation coefficients of pyrolysis product/naphthalene ratios with char characteristics. Significant correlations with H/C ratios were found for benzofuran/naphthalene (R=+0.93), toluene/naphthalene (R=+0.89),

dimethylfuran/naphthalene (R=+0.80) and m/p-xylene/naphthalene (R=+0.78). These specific product/naphthalene ratios were directly correlated with O/C ratios, and inversely correlated with ash, PAH and pH values. The trends of these ratios with H/C were depicted in Fig.5.1.3a. Benzofuran is a marker representative of oxygenated char components formed from the carbonisation of cellulose [37], alkylated benzenes of the labile fraction containing aliphatic domains [15], and naphthalene of polycondensed aromatic structures. Thus, these ratios describe the relative proportion of labile with the respect to recalcitrant fraction and accordingly decrease with increasing charring.

Table 5.1.3: Correlation coefficients of pyrolysis product/naphthalene peak area ratios from Py-GC-MS of switchgrass biochars with data reported in table 1. Grey background: R > 0.45 (p < 0.01).

	Compound / naphthalene ratio									
R	benzene	pyrrole	toluene	*m/p*-xylene	Styrene	benzonitrile	benzofuran	Biphenyl	phenanthrene	dimethylfuran
H/C	0.00	0.08	**0.89**	**0.78**	0.15	**-0.55**	**0.93**	**-0.66**	0.31	**0.80**
O/C	0.15	0.12	**0.80**	**0.66**	0.16	-0.43	**0.87**	**-0.65**	0.24	**0.75**
C	-0.11	-0.06	**-0.81**	**-0.70**	-0.12	0.42	**-0.89**	**0.63**	-0.23	**-0.75**
N	**-0.48**	-0.38	-0.43	-0.32	-0.18	0.17	**-0.51**	0.38	0.15	**-0.60**
Char yield	0.18	0.18	**0.77**	**0.62**	0.18	-0.44	**0.83**	**-0.65**	0.26	**0.73**
Ash	0.06	-0.04	**-0.89**	**-0.80**	-0.19	**0.56**	**-0.91**	**0.62**	-0.40	**-0.80**
PAHs	0.05	0.00	**-0.72**	**-0.63**	-0.19	0.35	**-0.72**	**0.61**	**-0.46**	**-0.60**
pH	0.20	0.02	**-0.92**	**-0.86**	-0.16	**0.59**	**-0.92**	**0.60**	-0.44	**-0.77**
Py-yield	0.12	0.16	**0.80**	**0.69**	0.16	-0.48	**0.87**	**-0.64**	0.19	**0.76**
% holocellulose	0.23	0.20	**0.72**	**0.57**	0.17	-0.41	**0.80**	**-0.61**	0.21	**0.73**
% lignin	-0.34	-0.04	**0.92**	**0.97**	-0.02	**-0.59**	**0.88**	-0.43	0.38	**0.74**
% charred	0.15	-0.05	**-0.96**	**-0.94**	-0.06	**0.59**	**-0.97**	**0.56**	-0.36	**-0.84**

A closer inspection to the pyrolysis product ratios vs. H/C showed that the linear relationships become stronger for biochars with H/C in the 0.8–0.4 interval, as exemplified in Fig. 5.1.3b. When calculated for these biochars, correlation coefficients increased to R > +0.90 (n = 27) for the pyrolysis product ratios of toluene, m/p-xylene and benzofuran with naphthalene. The dimethylfuran/naphthalene ratios decreased almost linearly with decreasing H/C ratios down to 0.6 where cellulose markers were not detected in the pyrograms. The benzene/toluene ratio utilised in other studies [15] and [17] was loosely correlated with H/C (R = −0.45), while the toluene/benzene ratio was better correlated (R = +0.66). Pyrolysis ratios of nitrogen-containing compounds, pyrrole and benzonitrile, with naphthalene were not correlated with the content of nitrogen; however, the benzonitrile/naphthalene ratio was weakly correlated with H/C, pH and ash.

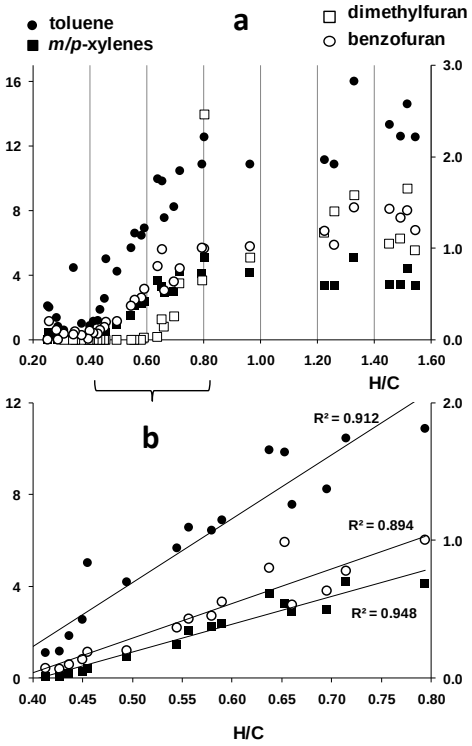

Figure 5.1.3: Py-GC-MS yield ratios of selected pyrolysis products with naphthalene (a) in the whole and (b) in a selected H/C molar ratio interval.

5.1.4 Conclusions

The results of this study conducted on a large set of samples produced from the same feedstock and reactor unit demonstrated that the GC–MS analysis of the tiny fraction produced by analytical flash pyrolysis can provide molecular indices useful for the interpretation of the thermal and environmental stability of biochar. The quantity of evolved pyrolysis products, the relative abundance of pyrolysis products associated to charring, and selected pyrolysis product ratios were strongly correlated with H/C and O/C ratios. The pyrolysates of biochars with H/C ratios above 0.8 were characterized by typical pyrolysis products of holocellulose (dimethylfuran) and lignin (methoxyphenols) and the dimethylfuran/naphthalene ratio was linearly correlated with H/C ratios. The toluene/naphthalene, benzofuran/naphthalene and m/p-xylene/naphthalene ratios were linearly correlated with H/C ratios in the 0.8–0.4 H/C ratio interval. This finding suggested that alkylbenzenes and benzofuran are proxies of aliphatic and oxygenated structures composing the most degradable fraction of biochar, while naphthalene is representative of polycondensed units that are more resistant to thermal degradation.

At lower H/C ratios, the intensity of pyrolysates of biochars was weak and few pyrolysis products could be detected.

In summary, the thermally labile fraction of biochar could be classified into three categories (obviously the reported values are not clear cut boundaries):

- weakly charred, thermochemical alteration minimal, molecular markers of holocellulose and lignin (methoxyphenols) clearly detected, % charred < 30% (biochar with H/C > 0.8);
- moderately charred, holocellulose markers not detected, methylphenols detected, % charred 40–80% (biochar with 0.4 < H/C < 0.8);
- highly charred, pyrolysates dominated by markers of charring (>90%) (biochar with H/C < 0.4; with H/C < 0.3 the biochar could not be fragmented into GC–MS analyzable products by flash pyrolysis).

Biochars with a degree of carbonization consistent with environmental recalcitrance could be obtained at relatively mild synthesis conditions that are low charring temperatures or short residence times. The optimal process conditions could be rapidly investigated by Py–GC–MS utilizing the appropriate molecular proxies. The proxies proposed in this study emerged from the analysis of a single substrate (switchgrass) and pyrolysis system, further research is needed to attest their general validity and elucidate relationships across different feedstock and pyrolysis units.

References

[1] J.Lehman. Bio-energy in the black. Front. Ecol. Environ. 5 (2007) 381–387.

[2] S.P. Sohi, E. Krull, E. Lopez-Capel, R. Bol, A review of biochar and its use and function in soil, Advances in Agronomy 105 (2010) 47–82.

[3] S. Jeffery, F.G.A. Verheijen, M. van der Velde, A.C. Bastos. A quantitative review of the effects of biochar application to soils on crop productivity using meta-analysis. Agriculture, Ecosystems and Environment 144 (2011) 175–187.

[4] K.A.Spokas, K.B.Cantrell, J.M. Novak, D.W. Archer, J.A. Ippolito, H.P. Collins, A.A. Boateng, I. M. Lima, M.C. Lamb, A.J. McAloon, R.D. Lentz, K.A. Nichols Biochar: A Synthesis of Its Agronomic Impact beyond Carbon Sequestration. J. Environ. Qual. 41 (2012) 973-989.

[5] C.J. Barrow Biochar: Potential for countering land degradation and for improving agriculture Applied Geography 34 (2012) 21-28.

[6] I.Stavi, R.Lal Agroforestry and biochar to offset climate change: a review Agron. Sustain. Dev. 33 (2013) 81–96.

[7] S.E. Hale, J. Lehmann, D. Rutherford, A.R. Zimmerman, R.T. Bachmann, V. Shitumbanuma, A. O'Toole, K.L. Sundqvist, H. Hans Peter, H.P.H. Arp, G. Cornelissen, Quantifying the total and bioavailable polycyclic aromatic hydrocarbons and dioxins in biochars, Environ.Sci.Technol. 46 (2012) 2830–2838.

[8] I. Hilber, F. Blum, J. Leifeld, H.-P. Schmidt, T.D. Bucheli, Quantitative determination of PAHs in biochar: a prerequisite to ensure its quality and safe application, J. Agr. Food Chem. (2012) 3042–3050.

[9] M. Keiluweit, M. Kleber, M.A. Sparrow, B.R.T. Simoneit, F.G. Prahl, Solvent extractable polycyclic aromatic hydrocarbons in biochar: influence of pyrolysis temperature and feedstock, Environ. Sci. Technol. 46 (2012) 9333–9341.

[10] D. Fabbri, A.G. Rombolà, C. Torri, K.A. Spokas, Determination of polycyclic aromatic hydrocarbons in biochar and biochar amended soil, J. Anal. Appl. Pyrol. 103 (2013) 60-67.

[11] K.A. Spokas, J.M. Novak, C.E. Stewart, K.B. C.M. Uchimiya, M.G. DuSaire, K.S. Ro, 445 Qualitative analysis of volatile organic compounds on biochar. Chemosphere 85 (2011) 869–882.

[12] R.Becker , U.Dorgerloh, M.Helmis, J.Mumme, M.Diakité, I.Nehls. Hydrothermally carbonized plant materials: Patterns of volatile organic compounds detected by gas chromatography. Bioresource Technology 130 (2013) 621–628.

[13] J. Kaal, A.M. Cortizas, K.G.J. Nierop, Characterisation of aged charcoal using a coil probe pyrolysis–GC/MS method optimized for black carbon, J. Anal. Appl. Pyrolysis 85 (2009) 408–416.

[14] J. Kaal, C. Rumpel, Can pyrolysis–GC/MS be used to estimate the degree of

thermal alteration of black carbon? Org. Geochem. 40 (2009) 1179–1187.

[15] J.Kaal, M.P.W. Schneider, M.W.I. Schmidt. Rapid molecular screening of black carbon (biochar) thermosequences obtained from chestnut wood and rice straw: A pyrolysis-GC/MS study. Biomass Bioenergy 45(2012)115-129.

[16] J.Kaal, A.M.Cortizas, O.Reyes, M.Solino. Molecular characterization of Ulex europaeus biochar obtained from laboratory heat treatment experiments – A pyrolysis–GC/MS study. J.Anal. Appl.Pyrolysis 95 (2012) 205–212.

[17] D. Fabbri, C. Torri, K.A. Spokas, Analytical pyrolysis of synthetic chars derived from biomass with potential agronomic application (biochar). Relationships with impacts on microbial carbon dioxide production, J. Anal. Appl. Pyrol. 93 (2012) 77–84.

[18] C.M. Wurster, G.Saiz, M.P.W. Schneider, M.W.I. Schmidt, M.I. Bird. Quantifying pyrogenic carbon from thermosequences of wood and grass using hydrogen pyrolysis, Organic Geochemistry 62 (2013) 28–32.

[19] A.R. Zimmerman. Abiotic and Microbial Oxidation of Laboratory-Produced Black Carbon (Biochar). Environ. Sci. Technol. 44(2010)1295–1301.

[20] K.A. Spokas, Review of the stability of biochar in soils: predictability of O:C molar ratios, Carbon Manag. 1 (2010) 289–303.

[21] O.R. Harvey, L.J. Kuo, A.R. Zimmerman, P.Louchouarn, E. Amonette, B.E. Herbert. An Index-Based Approach to Assessing Recalcitrance and Soil Carbon Sequestration Potential of 481 Engineered Black Carbons (Biochars). Environ. Sci. Technol. 2012, 46, 1415−1421.

[22] R. Calvelo Pereira, J. Kaal, M. Camps Arbestain, R. Pardo Lorenzo, W. Aitkenhead, M.Hedley, F.Macías, J. Hindmarsh, J.A.Maciá-Agulló. Contribution to characterisation of biochar to estimate the labile fraction of carbon. Organic Geochemistry 42 (2011) 1331–1342.

[23] C.E. Stewart, J.Y Zheng, J.Botte, M.F.Cotrufo. Co-generated fast pyrolysis biochar mitigates greenhouse gas emissions and increases carbon sequestration in temperate soils, GCB Bioenergy (2013) 5, 153–164.

[24] G.Pilon, J.M. Lavoie, C.E. Stewart, J.Y Zheng, J. Botte, M.F. Cotrufo. Co-generated fast pyrolysis biochar mitigates greenhouse gas emissions and increases carbon sequestration in temperate soils, GCB Bioenergy (2013) 5, 153–164. Bioresource.com 8 (2011) 4824-4839.

[25] C.E.Brewer, R.Unger, K.Schmidt-Rohr, R.C. Brown. Criteria to Select Biochars for Field Studies based on Biochar Chemical Properties. Bioenerg. Res. 4 (2011) 312–323.

[26] A.A. Boateng, C.A. Mullen. Fast pyrolysis of biomass thermally pretreated by torrefaction. J. Anal. Appl. Pyrolysis 100 (2013) 95-02.

[27]A. Enders, K. Hanley, T. Whitman, S. Joseph, J. Lehmann. Characterization of biochars to evaluate recalcitrance and agronomic performance. Bioresource Technology 114 (2012) 644 653.

[28] Brodowski, S., Amelung, W., Haumaier, L., Abetz, C., Zech, W., 2005. Morphological and chemical properties of black carbon in physical soil fractions as revealed by scanning electron microscopy and energy-dispersive X-ray spectroscopy. Geoderma 128, 116-129.

[29] E.S. Krull, J. Baldock, J.O. Skjemstad, R.J. Smernik, Ch.4 Characteristics of biochar: organo chemical properties. In Biochar for Environmental Management: Science and Technology Edited by J.Lehmann, S.Jospeh., 2009, 53-65, London, Earthscan.

[30] International Biochar Initiative (IBI). Standardized Product Definition and Product Testing Guidelines for Biochar that Is Used in Soil. May 15, 2012. IBI-STD-01 http://www.biochar-international.org/characterizationstandard. Version 1. accessed on 17th March, 2014.

[31] European Biochar Certified (EBC). Version 4.5 of 19th January 2013 by H.PSchmidt, S.Abiven, C.Kammann, B. Glaser,T.Bucheli, J. Leifeld, www.european-biochar.org, accessed on 17th March, 2014.

[32] S.Schimmelpfennig, B.Glaser. One Step Forward toward Characterization: Some Important Material Properties to Distinguish Biochars. J.Envon.Qual. 41 (2012) 1001-1013.

[33] S.-B. Lee, O.Fasina. TG-FTIR analysis of switchgrass pyrolysisJ. Anal. Appl. Pyrolysis 86 (2009) 39–43.

[34] K.Mazumder, W.S. York.Structural analysis of arabinoxylans isolated from ball538 milledswitchgrass biomass. Carbohydrate Research 345 (2010) 2183–2193.

[35] A.D.Pouwels, A.Tom, J.B.Eijkel, J.J.Boon. Characterisation of beechwood and its holocelluloseand xylan fractions by pyrolysis-gas chromatography-mass spectrometry. 11 (1987) 417-436.

[36] T. Hosoya, H. Kawamoto, S. Saka. Cellulose–hemicellulose and cellulose–lignin interactions inwood pyrolysis at gasification temperature. J. Anal. Appl. Pyrolysis 80 (2007) 118–125

[37] H.Knicker, A.Hilscher, F.J.Gonzalez-Vila, G.Almendros. A new conceptual model forthe structural properties of char producedduring vegetation fires. Org. Geochem. 39(2008) 935–939.

5.2 Py-GC-MS and thermogravimetric analysis (TGA) to evaluate labile fraction and molecular composition of biochar derived from different biomass

5.2.1 Introduction

Biochar is the porous material produced by pyrolysis of biomass. It is a secondary by-product that must be economically valorized to increase the attractiveness of pyrolysis process. Nowadays, there is high interest in economic and environmental sustainable application of biochar as soil amendment and fertilizer [1, 2], sink of carbon [3, 4] or filter/adsorbent material [5, 6, 7].

Biochar usage could not withstand from a deeper chemical-physical characterisation and environmental behavior of this material [8].

Many authors have investigated the characteristics of biochars produced at different temperature and from several type of biomass [9, 10, 11, 12]. For a given biomass the thermal conditions of pyrolysis are important to determine the type and the amount of products [13]. The crystalline structure of biochar is developed during pyrolysis from small quantities of aromatic units randomly arranged in an amorphous matrix to a highly ordered graphitic structure [14].

The biochar matrix is often characterize by the presence of thermally labile fraction given by the incomplete carbonization of the biomass, and it is related to the matter that could be removed through a complete pyrolytic process. Volatile matter constitutes the less stable fraction of biochar made up of heteroatoms and functional groups that can contribute to the reactivity of biochar [15]. Therefore, this labile fraction has been the subject of several studies with different thermal analytical techniques, such as thermogravimetry (TGA) and analytical pyrolysis (Py-GC-MS).

TG is an analytical technique in which sample weight is measured as a function of temperature. The sample is loaded on a high-precision thermo-balance within the furnace and weighed continuously during the course of the heating program. This is a simple and economic technique that is used for determining the intrinsic labile fraction of carbon in biochar [16].

TGA can give quantitative information on volatile matter (VM), which is a useful index to evaluating biochar stability [17]. However, a qualitative-support analysis is required to know the chemical composition of VM to better understand the role of labile fraction on biochar properties [16].

Py-GC-MS is a reliable method to gather information on the molecular structure of complex organic materials which was applied to the characterization of natural black carbon and charcoal [16, 18-24]

Kaal et al. used Py-GC-MS to assess the molecular composition of old charcoals [19-22]. The results suggested that the high peak intensities of benzene, toluene, benzonitrile and PAHs can be considered indicative of a carbonized material [19-22]

These pyrolysis products were assumed to represent the charred fraction rich of aromatic structures that occur in a thermally labile form in the carbonaceous matrix [16, 18].

Fabbri et al., [18] used Py-GC-MS to investigate a set of 20 synthetic biochars from different feedstock. The study shows a detailed comparison between quantitative Py-GC-MS, physic-chemical properties and the production of greenhouse gas (CO_2).

Pyrolysis products were grouped into four principal families according to the their origin (charred compounds, lignin, sugar and proteins), were quantified and correlated with the volatile matter (VM) and with the CO_2 production. The approach was further applied to a set of 35 biochars produced from the same biomass (switchgrass) and pyrolysis apparatus, but under different process conditions (temperature and time) as to produce biochar with different degree of charring [24]. The ratio of the relative abundance of selected pyrolysis products (e.g. toluene/benzene, naphthalene/toluene, benzofuran/naphthalene) were determined as molecular indicator (or proxies) of the charring degree. The ratios were intended to compare products with/without methyl groups, oxygen, polyaromatic rings on the ground that with increasing carbonization alkylated, oxygenated and monoaromatic structures become less important over dealkylated polyaromatic ones [18, 22].

These studies showed that good correlation between pyrolysis product ratios and the atomic hydrogen/carbon ratio (H/C).

However, they were conducted on a single substrate (switchgrass), the reliability of the compound ratio approach for comparing biochars produced from different substrates under the same pyrolysis conditions was not evaluated. Moreover, the results arising from TGA and Py-GC-MS were seldom compared in the literature. In particular, the concept that Py-GC-MS is capable to provide molecular information on VM has not been fully investigated yet.

The aim of this study was to investigate cornstalk biochars obtained at different pyrolysis conditions and biochars obtained from different feedstock but pyrolysed at same conditions in order to investigate both the effect of synthesis conditions and feedstock source on biochar structure by means of TGA and Py-GC-MS analysis.

TGA was applied to proximate analysis of biomass and biochar to analyze the correlation between composition of raw material and biochar yield. Furthermore the labile and stabile carbon content have been investigated in solid residue under different thermal treatments.
Py-GC-MS was conducted to characterize different biochar by means of molecular markers. Application of molecular markers is also aimed to validate the results obtained in a previous study [24].

5.2.2. Experimental

5.2.2.1 Biomass feedstock

In this study 11 different feedstock divided in 4 groups were investigated (the short name utilized in this study is reported in parenthesis): i) woody biomass: Pine sawdust (Pine), Poplar chips (Poplar) and hardwood bark (Bark); ii) herbaceous biomass: Corn stalks (Corn), *Panicum virgatum* (Switchgrass) and *Mischantus* (Mischantus); iii) 2 Algal biomass: *Desmodesmus communis* (*D. communis*) and *Arthrospira platensis* (Spiruline); iv) agro industrial residual biomass represented by mushroom litter (Litter), olive pomace (Olive) and chicken manure (Manure). The all feedstock are provided by Interdipartimental Center for Research in Environmental Science of University of Bologna.

5.2.2.2 Biomass pyrolysis

Biomass was processed in a laboratory-scale quartz tube fixed bed reactor following a published procedure [24]. Approximately, 3.0±0.1 g of biomass was pyrolysed under N_2 flow of 1500 cm^3 min^{-1}, at a specified temperature and time, here indicated as °C/min (for instance, biochar 500/20 corresponds to biochar obtained from pyrolysis at 500 °C for 20 minutes). All the substrates were pyrolysed at 500 °C for 20 min., because these parameters show the optimal synthesis conditions in terms of H/C and O/C ratios and environmental stability in accordance to a previous work [24].
In addition, cornstalk biochars at different temperature (T°C) and time (min) conditions (450*5; 450*20; 500*1; 550*5; 550*20; 650*5; 650*10; 650*20; 700*1) were obtained.

5.2.2.3 Ultimate and proximate analysis

The determination of C, H, N and S was performed using the elemental analyzer Flash 2000 series (Thermo Scientific). A quantity of 4-5 mg of biomass or biochar was introduced into a tin crucible mixed with 10 mg of vanadium pentoxide (Thermo Scientific) that is necessary

for the best identification of S. The oxygen content was calculated by mass difference: O=100-(C+H+N+S+ash).

Proximate analysis of biomass and biochar was carried out according to ASTM D7582 method with slight modification. The method determines relative moisture (M), volatiles (VM), fixed carbon (FC) content during different condition steps of analysis. Ash content (ASH) was calculated by difference of all these fractions. Before analysis, samples were crushed in an agate mortar to a fine powder.

For each analysis about 3-5 mg of sample was introduced in aluminum oxide crucible (volume of 70 µl) and covered with the specific lid. Then the crucible is inserted in the thermogravimetric analyzer (Mettler Toledo TGA /SDTA 851e).

5.2.2.4 Py-GC-MS

Py-GC–MS analyses were performed using an electrically heated platinum filament CDS 5250 pyroprobe interfaced to a Varian 3400 GC equipped with a GC column (HP-5-MS; Agilent Technologies 30 m × 0.25 mm, 0.25 µm,) and a mass spectrometer Saturn 2000 ion trap, Varian Instruments. The GC– MS conditions used were reported elsewhere (Conti et al., 2014). Internal standard (1 µL of 1000 mgL^{-1} iso-eugenol solution in acetonitrile) was added to the sample for quantitative analysis.

A set of 32 pyrolysis products were quantified as markers of *polysaccharides (holocellulose)* (hydroxyacetone,2,5-dimethyl-furan, furaldehyde, furfuryl alcohol, 2-cyclopentanedione, 3-hydroxy-2-methyl-cyclopentenone, 5-hydroxymethyl-2-furaldehyde, Levoglucosan); *lignin* (phenol, 4-methyl phenol, guaiacol, 4-ethyl phenol, cathecol, 4-vinyl phenol,4-methyl guaiacol, 4-vinyl guaiacol, syringol, 4-methyl syringol, trans-isoeugenol, 4-vinyl syringol, 4-propenyl syringol); *charred biomass* (benzene, pyrrole, toluene, ethyl benzene, m/p-xylene, benzonitrile, benzofuran, methyl benzofurans (three isomers), naphthalene, 1-methylnaphthalene, dibenzofuran.

5.2.3. Results and discussion

5.2.3.1 Biomass characterization

The results of proximate and ultimate analysis of biomass were summarized in Table 5.2.1. Carbon, hydrogen and oxygen concentrations are similar in lignocellulosic biomass.

Table 5.2.1: Proximate and ultimate analysis of different biomass samples. Standard deviations are reported in brackets (db: on dry basis; FC: fixed carbon; TC: total carbon)

BIOMASS	M%	VM% db	FC% db	Ash% db	N	TC	H	S	O	H/C	O/C
Bark	6.11(±0.02)	81.8(±0.3)	15.4(±1.1)	2.85(±0.79)	0.25	45	5.6	n.d	46	1.5	0.76
Corn	5.51(±0.01)	71.2(±0.6)	17.1(±1.27)	11,7(±0.7)	1	40	5.4	n.d	43	1.6	0.80
Desmodesmus	5.18(±1.05)	77.4(±1.9)	7.69(±3.32)	14.9(±1.6)	5.7	45	6.6	0.29	34	1.8	0.57
Litter	5.26(±0.78)	61.8(±4.7)	0.64(±8.04)	37.6(±9.6)	2.1	23	3.0	2.0	35	1.5	1.1
Manure	9.55(±2.48)	75.6(±6.3)	1.32(±3.79)	23.9(±5.8)	4.1	34	4.8	1.3	31	1.7	0.70
Miscanthus	6.08(±1.17)	86.1(±0.5)	9.52(±0.55)	4.36(±0.05)	0.57	43	5.6	n.d	47	1.5	0.81
Olive	4.86(±0.35)	83.8(±1.0)	12.9(±0.4)	3.31(±1.43)	1.4	50	6.4	n.d	41	1.5	0.61
Pine	5.27(±0.59)	84.5(±1.3)	13.0(±0.9)	2.40(±0.27)	n.d	47	5.9	n.d	47	1.5	0.76
Poplar	5.91(±1.32)	81.2(±1.6)	14.1(±1.5)	4.69(±1.15)	0.56	45	5.6	n.d	48	1.5	0.80
Spiruline	7.79(±1.40)	82.6(±2.6)	9.17(±2.44)	8.44(±0.86)	9.7	46	6.4	0.52	26	1.7	0.42
Switchgrass	5.63(±0.20)	81.9(±1.5)	13.7(±0.9)	4.39(±0.54)	0.66	43	5.7	n.d	44	1.6	0.78

The elemental composition of other kind of feedstock are quite different. Algal samples have a similar C and H content but the amount of N and S is higher than soft/hardwood biomass.
The manure and litter have a minor content of C, H, N due to the higher content of ash. For all the biomass H/C ratio is similar whereas O/C varies from 0.42 of spiruline to 1.1 of litter.
Overall, the volatile matter in biomass ranged from 61.8 % of litter to 86.1 % of miscanthus and the fixed carbon content varies from 0.64 % of litter to 17.1 % of Corn. litter and manure, which are characterized by the lower carbon content, reports the higher ash content, which is over than 20 %. Also the algae feedstock, spiruline and *D. communis* report remarkable ash content of 8.44 and 14.9 %, respectively.
The reproducibility of analysis is reported in table as standard deviation (SD) of two or more analyses. All the biomass showed a low variability (SD lesser than 2 %). Only two exceptions are manure and litter and in a measure *D. communis*; in these samples, in particular the determinations of fixed carbon (FC) are effected by a high standard deviation, probably linked to high ash content that influence the aromatic structure formation. In the oxidative phase the loss of weight caused by combustion of organic material is lower that the gain of weigh linked to the oxygen adsorption by high quantity of metals in biomass. This behavior determines an overestimate and lesser reproducible FC values.

In Figure 5.2.1 the TGA thermograms are reported relative to volatiles evolution recorded for each biomass sample. For all the biomasses, the pyrolysis of the major part of material takes place between 200-500 °C. In this range of temperature, more than 60 % of weight of volatile material, almost 40 % for manure and litter is lost, due to the degradation of organic material. In particular the degradation of holocellulose takes place in this range of temperature and the lignin starts degradation at 300 °C [13]. The elevated content of ash in manure and litter influences clearly the minor pyrolysis yield of these biomasses. Furthermore for all the samples the higher increasing of conversion rate was determined between 300 °C – 400 °C.

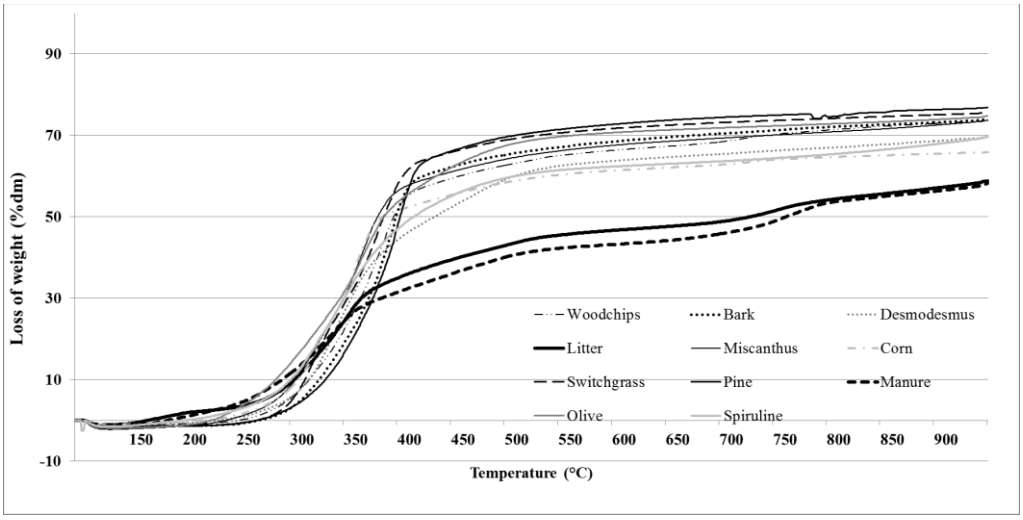

Figure 5.2.1: Pyrolytic evolution of biomass from 100 °C to 950 °C

The fixed carbon content depends on biomass characteristics but it may change during pyrolytic process depending on speed of heating. The heating ramp influences was investigated to evaluate the contribution of fixed carbon arranged during the TGA analysis. In Table 5.2.2 results of the proximate analysis, carried out using different heating speeds of 5, 20, 40, 60 e 100 °C/min, are reported for olive, spiruline and manure samples .

Thermogravimetric analysis performed changing the pyrolysis heating rate from 5 to 100 °C/min show slight variation in volatile matter, fixed carbon and ash percentages determination. In particular from 20 to 60 °C/min the variation of results are minor then SD error of standard condition analysis (40 °C/min).

Table 5.2.2: Proximate and ultimate analysis of different biochars produced from different biomass under the same conditions (500 °C, 20 min). Standard deviations are reported in brackets. (db: on dry basis; FC: fixed carbon; TC: total carbon)

BIOMASS	BC yield % (db)	M (%)	VM % (db)	FC % (db)	ASH % (db)	N	TC	H	S	O	H/C	O/C
Bark	24.2	3.07(±0.53)	21.0(±2.7)	71.6(±3.2)	7.37(±0.42)	0.69	78	3.1	n.d.	11	0.50	0.10
Corn	35.5	4.12(±0.55)	25.9(±0.7)	43.7(±0.6)	30.4(±0.1)	1.1	57	2.7	n.d.	5	0.57	0.06
Desmodesmus	34.2	2.73(±0.27)	22.5(±1.5)	40.7(±1.6)	36.8(±0.2)	7	51	3	0.07	14	0.70	0.21
Litter	54.4	2.43(±0.65)	34.7(±0.3)	15.5(±1.0)	49.8(±0.8)	1.3	24	0.95	0.19	14	0.48	0.43
Manure	44.1	3.16(±0.64)	32.0(±2.0)	16.4(±1.0)	51.6(±1.8)	1.8	21	0.78	n.d.	17	0.45	0.61
Miscanthus	25.6	5.73(±0.88)	32.2(±2.7)	58.1(±2.0)	9.60(±0.71)	1.2	67	3.2	n.d.	15	0.57	0.17
Olive	26.2	2.26(±0.35)	19.9(±0.9)	76.3(±0.3)	3.85(±0.62)	1.7	79	3.3	n.d.	12	0.50	0.12
Pine	20.0	3.80(±0.31)	27.5(±1.4)	69.1(±1.2)	3.37(±0.13)	0.03	80	3.5	n.d.	16	0.53	0.15
Poplar	23.0	3.17(±1.42)	28.1(±0.8)	63.3(±1.2)	8.60(±2.1)	0.36	75	3.2	n.d.	13	0.51	0.13
Spiruline	24.8	5.29(±2.61)	28.2(±1.3)	42.2(±1.3)	29.5(±0.5)	7.7	51	2.5	n.d.	18	0.58	0.27
Switchgrass	25.0	3.10(±0.13)	22.2(±1.6)	65.7(±1.4)	12.1(±2.9)	0.95	69	3.2	n.d.	14	0.56	0.15

5.2.3.2 TGA: Biomass and biochar comparison

Thermogravimetric analysis describes biomass behavior under thermal treatment from 105 to 950 °C in intermediate pyrolysis plants. The weight loss during the thermal treatment under nitrogen flow is a direct measure of biomass pyrolytic conversion into oil or gas.

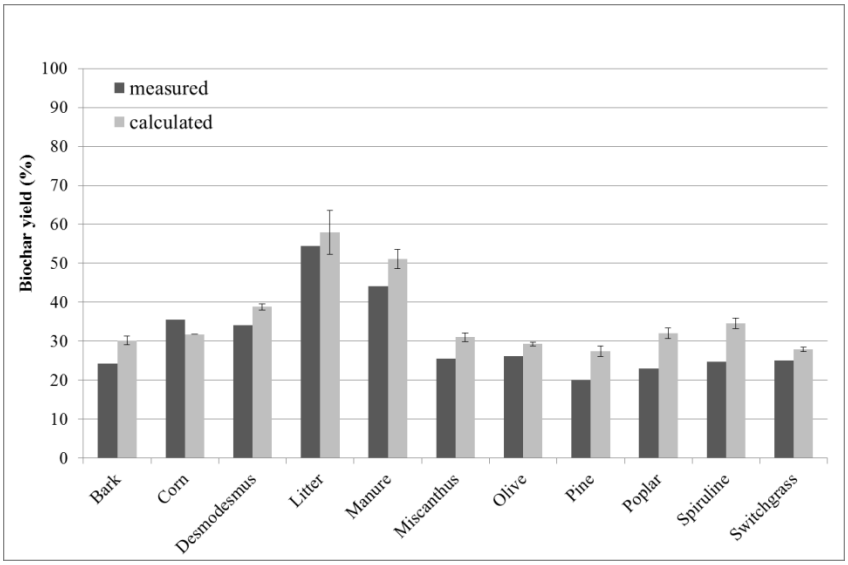

Figure 5.2.2: Comparison between biochar yields measured in the laboratory-scale fixed bed reactor and calculated from TGA biomass analysis (mean values and SD from 3 analyses .

Figure 5.2.2 reports the comparison between the yield measured after the pyrolysis of biomasses at 500 °C processed in the laboratory-scale fixed bed reactor and the yield inferred from thermogravimetric analysis of biomass.

To calculate the theoretical yield, the amount of volatiles released from 35 to 500 °C (pyrolysis temperature) during TGA was measured. The two pyrolytic processes (TGA and reactor) took place under different conditions of nitrogen flow, mass transfer, heat conduction, biomass size and quantity. Neverthelss, yields calculated from TGA were rather similar to those obtained from the experiments with the pyrolysis reactor. In general, TGA tended to overestimate yields.

The TGA of feedstock could be also useful to predict the biochar proximate VM, FC and Ash contribution (Fig. 5.2.3).

The theoretical composition of biochar was obtained from TGA analysis of biomass considering the calculated yield. These data and was compared with the analytical results of proximate analysis of the biochar produced from fixed-bed reactor.

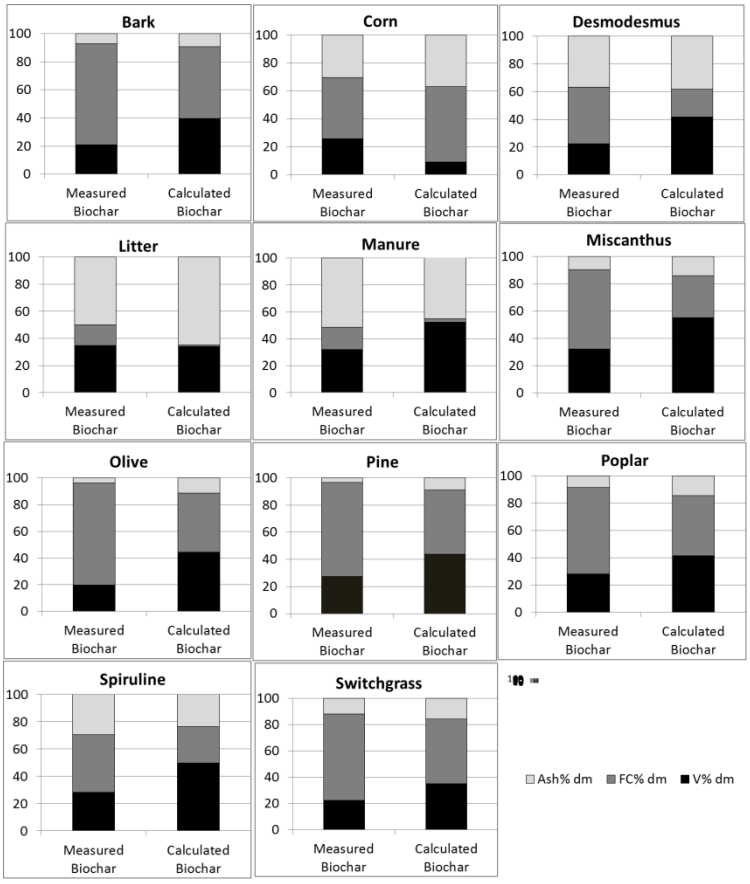

Figure 5.2.3: VM, FC and Ash content measured on biochars derived from pyrolysis and the same parameters calculated from proximate analysis of biomasses considering theoretical pyrolysis yield.

As the study on different speed of heating showed in the previous paragraph, these data confirm that fixed carbon and ash content depend mostly on the feedstock proprieties [14]. Indeed, the comparison of experimental and extracted data from feedstock TGA shows similar data. Significant difference may be caused by different conditions in pyrolytic process in fix-

bed reactor and in a little crucible that influencing heating transfer may interfere with the carbonization process [13]. Some differences are also correlated with analytical variability in laboratory plant.

5.2.3.3 Py-GC-MS of cornstalk biochars obtained under different pyrolysis conditions

Pyrograms resulting from Py-GC-MS of cornstalk biochars obtained under different synthesis conditions are depicted in Fig. 5.2.4. The samples with H/C molar ratio ≥ 0.7 (Table 5.2.3) produced pyrolysates characterized by intense peaks relative to pyrolysis products of hemicellulose, cellulose and lignin, such as dimethyl furan, furaldehyde and phenols. On the other hand, samples with low H/C values were mainly characterized by aromatic hydrocarbons.

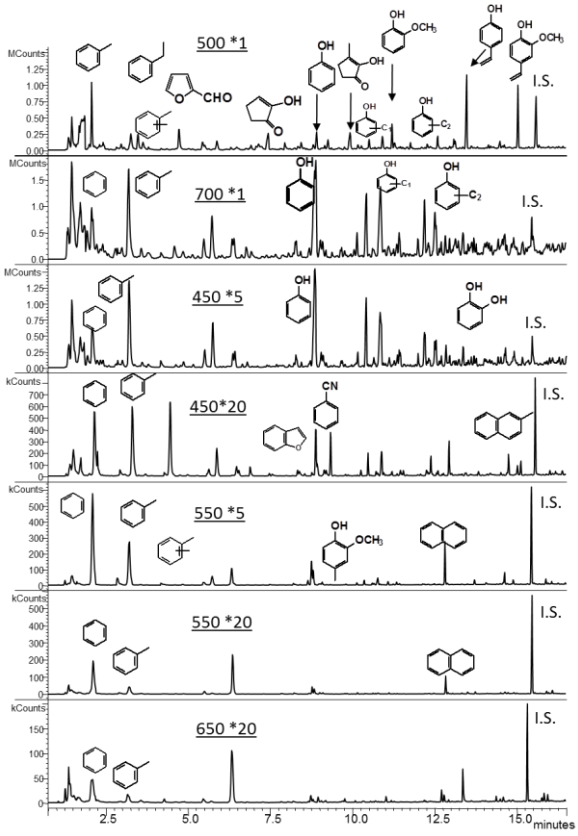

Figure 5.2.4 : Pyrograms of cornstalk biochar

The quantity of evolved pyrolysis products (Py-yield) was calculated dividing GC peak area by sample amount (area/µg). Yields calculated by internal calibration with isoeugenol presented a higher variability due to the variability of the internal standard peak area (RSD 56%). This variability can be ascribed to greater absorption of internal standard into the highly charred biochars. As reported in Table 5.2.3, Py-yields (area/µg) ranged from 6873 (500*1; H/C: 1.54) to 50 (650 *20; H/C: 0.3) showing the influence of high temperature and

residence time on the thermally labile fraction of different biochars. In addition, the large range of three orders of magnitudes herein observed is in accordance with previous works [18, 22, 24].

Table 5.2.3: Cornstalk biochars at different pyrolysis conditions: Characterization by Py-GC-MS (Py-yield and molecular ratios) and TGA (volatile matter (VM) and fixed carbon (FC).

			Py-GC-MS					TGA	
Sample	BC Yield (%)	H/C	Py yield (Area/µg)	T/B	T/NAP	BF/NAP	MetNAP/NAP	VM (%)	FC (%)
700*1	38	0.82	3065 ± 98	2.08 ± 0.30	11.3 ± 0.6	0.84 ± 0.02	0.63 ± 0.03	35	40
450*5	37	0.74	2446 ± 274	1.85 ± 0.05	10.5 ± 1.5	0.61 ± 0.08	0.35 ± 0.01	30	41
450*20	32	0.61	775 ± 151	0.95 ± 0.03	5.1 ± 0.6	0.19 ± 0.00	0.27 ± 0.10	25	42
550*5	29	0.55	604 ± 43	0.45 ± 0.01	2.78 ± 0.04	0.06 ± 0.00	0.12 ± 0.05	25	32
550*20	30	0.45	180 ± 15	0.22 ± 0.08	1.2 ± 0.4	0.06 ± 0.01	0.04 ± 0.01	21	30
650*5	30	0.38	124 ± 20	0.13 ± 0.02	0.7 ± 0.1	0.04 ± 0.01	0.02 ± 0.00	18	45
650*20	28	0.33	50 ± 3	0.29 ± 0.06	2.7 ± 0.2	0.12 ± 0.01	0.07 ± 0.01	16	44
650*10	27	0.33	55 ± 10	0.16 ± 0.03	1.2 ± 0.2	0.07 ± 0.02	0.04 ± 0.01	17	50
500*1	92	1.54	6873±2647	4.23± 0.89	15.4± 1.7	0.92 ± 0.14	0.64 ± 0.01	67	12

Py-yield showed a good correlation (R=+0.94) with H/C (Fig. 5.2.5) according to Kaal et al., [21] who affirms that total pyrolysis area can reflects increasing proportion of polycondensed aromatics. In addition, Py-yield trends obtained in a previous study on switchgrass biochars [24] have been confirmed.

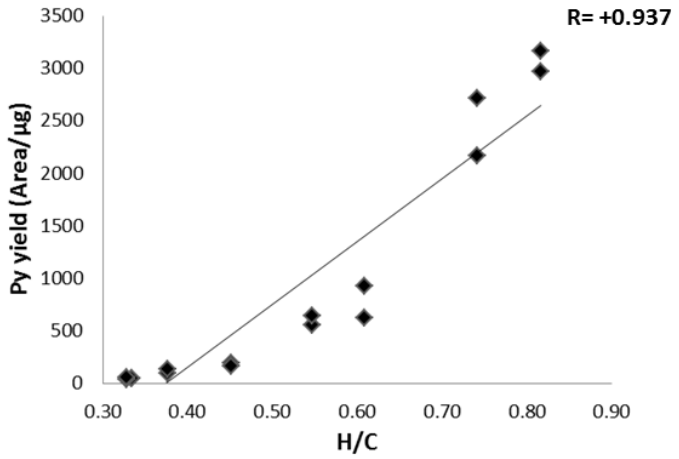

Figure 5.2.5: Linear correlation between pyrolysis yield (Area/µg) and H/C molar ratio of cornstalk biochars

Furthermore, Py-yield showed a strong correlation (R=+0.95) with respect to the volatile matter (VM) detected by thermo gravimetric analysis (Fig. 5.2.6). The correlations founded show that Py-GC-MS is a good tool able to evaluate the degree of carbonization of biochars.

Nevertheless, the correlation Py-yields-H/C showed that Py-GC-MS is not able enough to determine the degree of carbonization in biochars with H/C ratio < 0.3 because of the low yields of the pyrolysis products. The same trend has also been observed in the correlation with the volatile matter (VM) in which values around 15% of VM correspond to Py-yield (Area/µg) value close to zero.

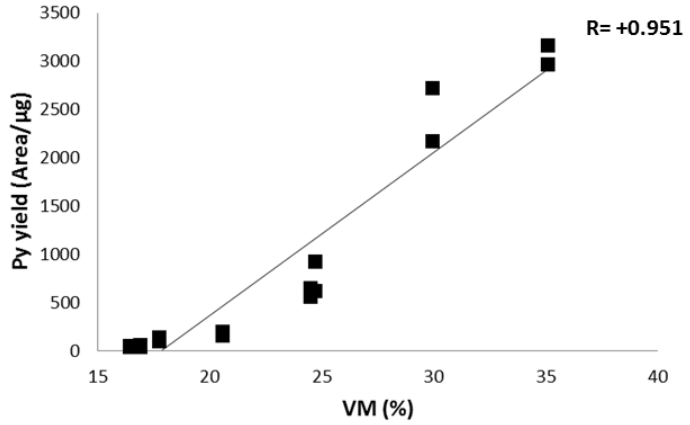

Figure 5.2.6: Linear correlation between Pyrolysis Yield and VM % obtained by TGA analysis of cornstalk biochars

Finally, H/C was also strongly correlated (R=+0.99) with the VM (Fig. 5.2.7) indicating TGA as a helpful and fast tool to predicting biochar charring intensity.

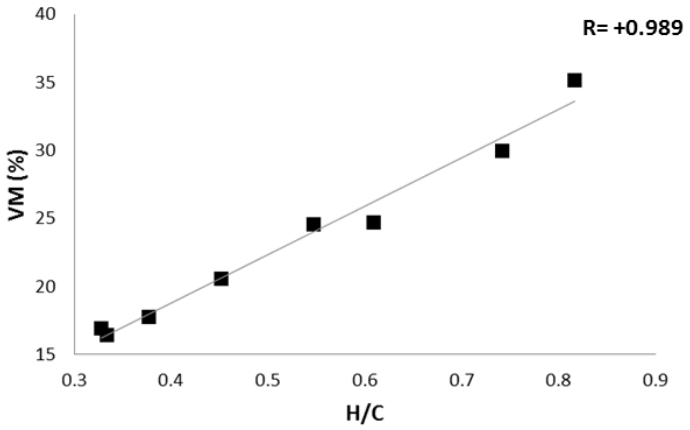

Figure 5.2.7: Linear correlation between pyrolysis yield (Area/µg) and H/C molar ratio of cornstalk biochars

H/C molar ratio has also been calculated with respect to some molecular ratios (toluene/benzene (T/B), toluene/naphthalene (T/NAP), benzofuran/naphthalene (BF/NAP) and 1-methylnaphthalene/naphthalene (MetNAP/NAP)) that have been utilized in earlier studies as indicative of the degree of carbonization [21, 22, 24].

Molecular proxies above-mentioned indicate the proportion between the labile fraction and recalcitrant fraction decreasing with increasing charring intensity.

According to Kaal et al., [22] the decrease in toluene/benzene and methylnaphthalene/naphthalene ratios can be representative of dealkylation reflecting polycondensation process. Indeed, benzofuran is a marker of oxygenated components due to the carbonization of cellulose [24, 25]

In the earlier study [24], compound ratios with naphthalene by Py-GC-MS were proposed as a rapid investigation method of pyrolysis process. However, the proxies had been validated on a single substrate (Switchgrass).

Following, the results obtained on cornstalk biochar using the same proxies are showed (Fig 5.2.8).

H/C were highly correlated with toluene/naphthalene ratio (R=+0.94). Even the other molecular ratios T/B, MetNAP/NAP and BF/NAP have arisen good correlation with value of R=+0.92, R=+0.90 and R=+0.87 respectively. Thus, these product/naphthalene ratios reflected thermal rearrangement of alkylated and oxygenated in more resistant structures [21]. Toluene/benzene and methylnaphthalene/naphthalene were found as indicative of dealkylation process according to Kaal et al., [20].

Finally, this overall result confirmed the good correlation showed in the previous work [24]. Product/naphthalene ratios such as T/NAP, metNAP/NAP and BF/NAP were linearly correlated with H/C demonstrating onto a different feedstock the validity of a rapid investigation of pyrolysis process conditions by Py-GC-MS using molecular proxies.

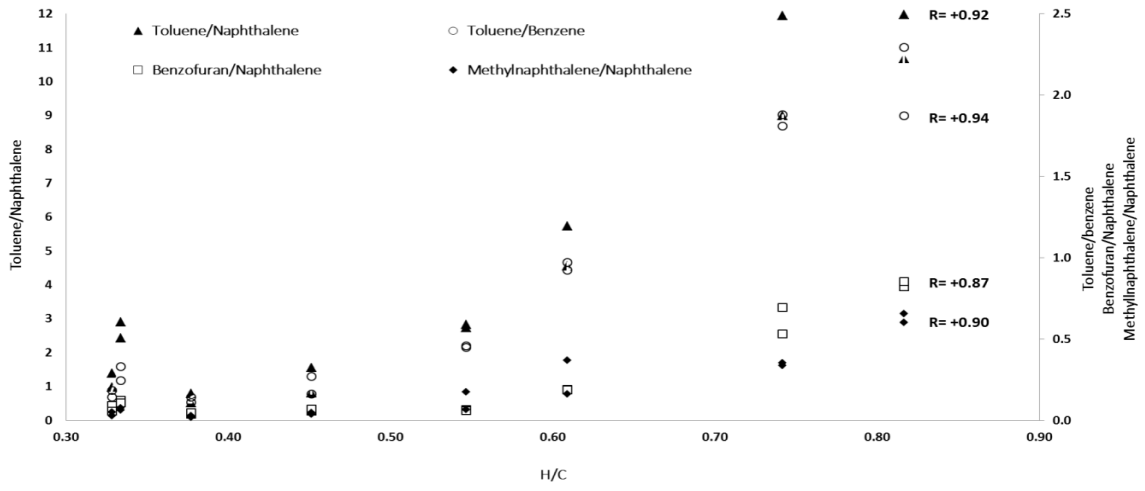

Figure 5.2.8: Linear correlation between H/C molar ratio and molecular markers (toluene/naphthalene; toluene/benzene; benzofuran/naphthalene; methylnaphthalene/naphthalene) of cornstalk biochars

5.2.3.4 *Py-GC-MS of biochars obtained from different biomass*

Pyrolysates of different biochars obtained from pyrolysis at 500°C for 20 min have been also investigated. Feedstock consisted of lignocellulosic biomass divided into woody (e.g.: pine sawdust) and herbaceous (e.g.: mischantus), agricultural wastes (e.g.: manure) and algal biomass (e.g.: *D. communis*).

As above-mentioned in section 5.2.3.3, Py-yield in term of Area/μg_{sample} was calculated and molecular proxies were applied in order to evaluate achievable correlations with H/C (Table 5.2.4)

The H/C molar ratios ranged between 0.45 and 0.71. Averaged for all the biochars, H/C ratio was 0.53 with a RSD of 12% (Table 5.2.4). The lower H/C ratios (~ 0.45) were observed for litter and manure characterized form the highest content of ash presumably containing some inorganic carbon, the highest value for *D. communis* (0.70). TGA data of these biochars are reported in Table 5.2.2. The volatile matter ranged from 19.9 to 34.7, on average 27.

Table 5.2.4 : Characterization by Py-GC-MS (Py-yield and molecular ratios) and H/C molar ratio from biochars derived from different feedstock

Feedstock	**Py yield (Area/µg)**	**H/C**	**MetNAP/NAP**	**T/B**	**T/NAP**	**BF/NAP**
switchgrass	261	0.56	0.29	1.06	5.0	0.19
cornstalk	1482	0.57	0.60	1.92	8.0	0.24
mischantus	401	0.57	0.41	0.85	6.1	0.30
pine	568	0.53	0.33	0.70	4.8	0.39
poplar	222	0.51	0.50	1.21	5.7	0.49
bark	235	0.48	0.46	1.24	5.6	0.51
olive	242	0.50	0.49	1.60	9.3	0.19
litter	126	0.48	0.36	1.11	6.9	0.15
manure	137	0.45	0.46	1.23	13.2	0.18
spirulina	413	0.59	0.54	2.46	34.2	0.27
D. communis	360	0.71	0.53	2.47	22.6	0.23

Table 5.2.5: mean value and standard deviation of molecular ratios and H/C ratio from different feedstock-derived biochars

Ratio	Mean	SD	RSD%
H/C	0.54	0.07	13
VM	27	5	18
MetNAP/NAP	0.45	0.09	21
T/B	1.44	0.60	42
T/NAP	11.1	9.30	84
BF/NAP	0.29	0.12	43

Table 5.2.5 shows that %RSD of some molecular ratios determined by Py-GC-MS were much higher (40-84%) than those of H/C (13%) and VM (18%). It can be seen that toluene/naphthalene (T/NAP) ratio showed the highest variability with RSD 84%. This was mainly due to the high T/NAP values found spiruline, *D. communis*, manure and olive (Fig 5.2.9). Indeed, *D.communis* and spiruline showed T/NAP values of 23 and 34, respectively, while manure and olive, even if lower than microalgae, showed a value of 13 and 9, respectively. On the other hand, T/NAP ratio in lignocellulosic feedstock is in the range between 3 and 5. Although mushroom litter does not belong to lignocellulosic group its ratio is around 5. The high T/NAP values could be associated to the presence of proteins.

Indeed, avoiding proteinaceous biomass from the dataset, % RSD showed a lower value around 21% demonstrating the variability is caused by different feedstock source.

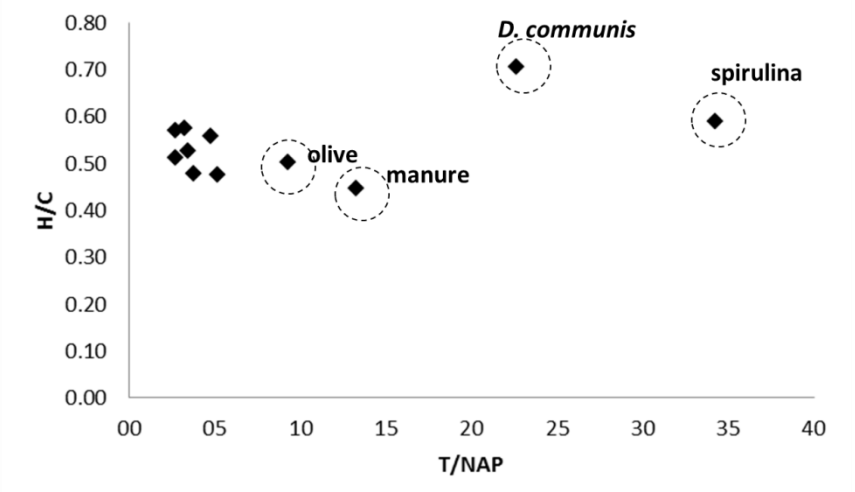

Figure 5.2.9: H/C ratio (elemental analysis) and toluene/naphthalene (Py-GC-MS) ratio of biochars produced at 500 °C from different feedstock.

The high T/NAP ratio characterized the pyrograms of biochars from protein-containing biomass could be explained by a larger production of toluene. Generation of toluene in proteinaceous biomass is associated with the presence of aromatic amino acids such as tyrosine and phenylalanine [25] and high percentage of toluene was recently observed Py-GC-MS of microalgae [26, 27] and by GC-MS analysis of microalgae bio-oil [28].

Thus, we can suppose that protein-derived toluene amount could be the main reason of the outlier behavior of proteinaceous biomass approximately expressed by the C/N ratio (inverse trend). The C/N ratios increased in the order *D.communis* (8.5), spiruline (8.7), manure (14), litter (13), olive (54), lignocellulosic biomass (> 60). The trend (inverse) is similar to that of T/NAP (Figure 5.2.9) for microalgae and manure, but not for olive pomace-derived biochar. For this biomass the presence of lipids could explain the higher T/NAP ratio. Indeed, olive pomace is mainly composed by water (60-70%), lignin (13-15%), holocellulose (18-20%) and oils retained in the pulp (2.5-3%) while protein amount is about 1% [29]. In addition the calculated C/N ratio is similar to that reported in others study that showed values ranged between 43 and 51 [30, 31].

Some data of table 5.2.4 are presented in graphical form in Figure 5.2.10 to facilitate the comparison.

Toluene/benzene (T/B) showed a great variability probably for the reasons discussed above for T/NAP ratio (RSD 42%). The benzofuran/naphthalene (BF/NAP) ratios presented large differences, less evident in the figure because the absolute value is low. The variability was probably due to the fact that BF is a very minor product in the pyrograms of biochar with this H/C ratios (see Figure 5.2.8)

On the other hand, methylnaphthalene/naphthalene showed a mean value of 0.45 with SD of 0.09 (RSD 21%).

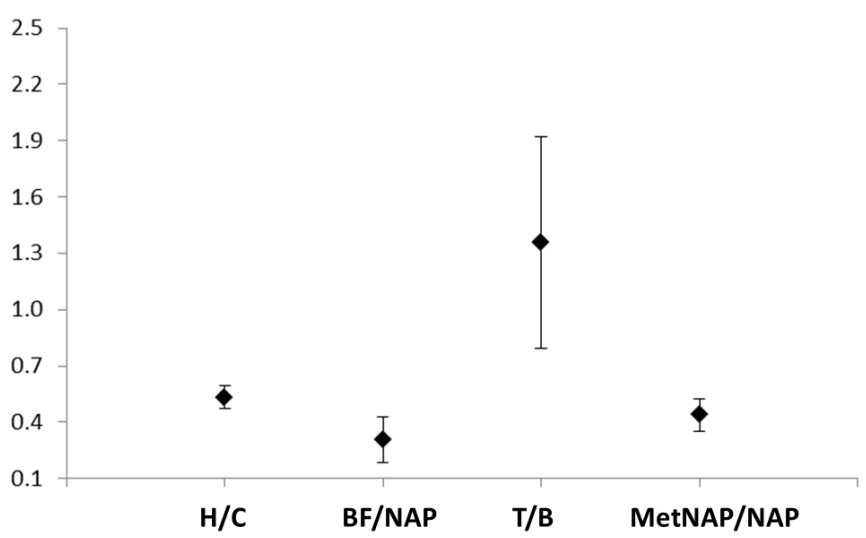

Figure 5.2.10: molecular proxies and H/C molar ratio of different feedstock-derived biochars: mean value and standard deviation (SD) (BF: benzofuran; NAP: naphthalene; T: toluene; B: benzene; MetNAP:1-methylnaphthalene)

The MetNAP/NAP showed a range sufficiently homogenous and then applicable as molecular proxy of degree of carbonization on different feedstock-derived biochars.

Thus, we can assume that although toluene/benzene or toluene/naphthalene were used by Kaal et al., [20-22] and in our previous work [24] as representative of dealkylation between aromatic moieties and then indicative of polycondensation process with increasing of pyrolysis temperature, they are not applicable comparing biochar obtained from different feedstock because of the protein-based origin of toluene. Similarly, benzofuran/naphthalene as marker of oxygenated components derived from the carbonization of cellulose [32] is not successfully applicable to different feedstock-derived biochars because of the presence of biomass with different levels of cellulose or polysaccharides.

MetNAP/NAP seems to be a molecular proxy less sensitive to the original biomass substrates. However, the ratio becomes too small to be adopted as marker to differentiate highly carbonized biochars (see Table 5.2.3).

5.2.4. Conclusions

Py-GC-MS was applied both on 11 different biochar obtained from cornstalk pyrolysis under
The quantity of compounds evolved from Py-GC-MS (Py-yield) of biochars obtained from the same biomass (cornstalk) under different pyrolysis conditions were linearly correlated withvolatile matter (VM) determined by TGA. This finding supports the idea that Py-GC-MS furnishes quantitative information on the biochar fraction concurring to VM, that is thermally degradable. VM and Py-yields were correlated with H/C ratios. These chemical (H/C from elemental composition, Py-yields from Py-GC-MS) and physical (VM from TGA) parameters provide consistent evaluation on the extent of charring of biochars derived from the same feedstock. Further indices can be obtained from Py-GC-MS utilizing molecular ratios indicative of de-functionalisation/de-alkylation/polycondensation degree. The methylnaphthalene/naphthalene, toluene/naphthalene, toluene/benzene and benzofuran/naphthalene ratios were correlated with H/C for the thermo sequence of cornstalk biochars confirming the previous results obtained onto switchgrass biochars and other biomass types. However, these ratios cannot be used to compare biochar derived from different feedstock as the values resulted dependent on the composition of the original biomass. Biochars from proteinaceous substrates such as microalgae were characterized by higher values of toluene in comparison to lignocellulosic substrates.

Instead, methylnaphthalene/naphthalene ratio was less influenced by the feedstock and showed good similarity with H/C. The molecular pattern resulting from Py-GC-MS could be utilized to infer information on the nature of the initial substrate and differentiate biochars with the same H/C and VM values

References

[1] Graber, E. R., Elad, Y., (2013). Biochar impact on plant resistance to disease. Ladygina, N., Rineau, F. (Eds.). *Biochar and soil biota. CRC Press., pp. 41-68*

[2] Wiedner, K., Naisse, C., Rumpel, C., Pozzi, A., Wieczorek, P., Glaser, B. (2013). Chemical modification of biomass residues during hydrothermal carbonization–What makes the difference, temperature or feedstock?. *Organic Geochemistry, 54, 91-100.*

[3] Zimmerman, A. R., Gao, B. (2013). The stability of biochar in the environment. Ladygina, N., Rineau, F. (Eds.). *Biochar and soil biota. CRC Press, pp 1-40*

[4] Lehmann, J. (2007). A handful of carbon. *Nature, 447, 143-144.*

[5] Gomez-Eyles, J. L., Beesley, L., Moreno-Jimenez, E., Ghosh, U., Sizmur, T. (2013), The potential of biochar amendments to remediate contaminated soils. Ladygina, N., Rineau, F. (Eds.). *Biochar and soil biota. CRC Press, pp 100-133*

[6] Beesley, L., Marmiroli, M. (2011), The immobilisation and retention of soluble arsenic, cadmium and zinc by biochar. *Environ. Pollut., 159, 474-480.*

[7] Day, D., Evans, R. J., Lee, J. W., Reicosky, D. (2005). Economical CO_2, SO_x, and NO_x capture from fossil-fuel utilization with combined renewable hydrogen production and large-scale carbon sequestration. *Energy, 30, 2558-2579.*

[8] Lehmann J., Riling M.C., Thies J., Masiello C.A., Hockaday W.C., Crowley D., (2011), Biochar effects on soil biota-A review, *Soil Biol. Biochem. 43, 1812-1836.*

[9] Raveendran K., Ganesh A., Khilar K.C., (1996) Pyrolysis characteristics of biomass and biomass components, *Fuel 75, 987-998*

[10] A. Gani and I. Naruse. (2007), Effect of cellulose and lignin content on pyrolysis and combustion characteristics for several types of biomass, *Renew. Energy, 32, 649-661*

[11] Yuan, Jin-Hua, Ren-Kou Xu, and Hong Zhang. (2011), The forms of alkalis in the biochar produced from crop residues at different temperatures, *Biores. Technol., 102, 3488-3497.*

[12] Enders A., Hanley K., Withman T., Joseph S., Lehmann J., (2012), Characterization of biochars to evaluate recalcitrance and agronomic performance, *Biores. Technol., 114, 644-653*

[13] Haykiri-Acma H., Yaman S., Kucukbayrak S., (2010), Comparison of the thermal reactivities of isolated lignin and holocellulose during pyrolysis, *Fuel Process. Technol., 91, 759-764*

[14] Keiluweit M., Nico P.S., Johnson M.G., Kleber M., (2010), Dynami molecular structure of plant biomass-derived black carbon (biochar), *Environ. Sci. Technol., 44, 1247-1253*

[15] Amonette, J. E., Joseph, S. (2009). Characteristics of biochar: Microchemical properties. *Biochar for environmental management: Science and technology, 33*

[16] Pereira, R. C., Kaal, J., Arbestain, M. C., Lorenzo, R. P., Aitkenhead, W., Hedley, M., Maciá-Agulló, J. A. (2011). Contribution to characterisation of biochar to estimate the labile fraction of carbon. *Org. Geochem., 42, 1331-1342.*

[17] Zimmerman A.R., (2010) Abiotic and microbial oxidation of laboratory-produced black carbon (biochar). *Environ. Sci. Technol., 44, 1295-1301*

[18] Fabbri D., Torri C., Spokas K.A., (2012) Analytical pyrolysis of synthetic chars derived from biomass with potential agronomic application (biochar). Relationship with impacts on microbial carbon dioxide production. *J. Anal. Appl. Pyrol., 93, 77-84*

[19] Kaal J., Cortizas A.M., Nierop K.G.J., (2009) Characterisation of aged black carbon using a coil pyroprobe pyrolysis-GC/MS method optimized for black carbon. *J. Anal. Appl. Pyrol., 85, 408-416*

[20] Kaal J., Rumpel C., (2009) Can pyrolysis-GC/MS be used to estimate the degree of thermal alteration of black carbon?, *Org. Geochem., 40, 1179-1187*

[21] Kaal J., Schneider M.P.W., Schmidt M.W.I, (2012), Rapid molecular screening of black carbon (biochar) thermosequences obtained from chestnut wood and rice straw: A pyrolysis-GC/MS study. *Biomass Bioenerg., 45,115–129.*

[22] Kaal J., Cortizas A.M., Reyes O., Solino M., (2012), Molecular characterization of *Ulex europaeus* biochar obtained from laboratory heat treatment experiment - A pyrolysis-GC/MS study. *J. Anal. Appl. Pyrol., 95, 205-212*

[23] Gonzalez-Perez J.A., Almendros G., de la Rosa J.M., Gonzalez-Vila F.J., (2014), Appraisal of polycyclic aromatic hydrocarbons (PAHs) in environmental matrices by analytical pyrolysis (Py-GC-MS), *J. Anal. Appl. Pyrol., 109, 1-8.*

[24] Conti R., Rombolà A.G., Modelli A., Torri C., Fabbri D., (2014).Evaluation of the thermal and environmental stability of switchgrass biochars by Py-GC-MS. *J. Anal. Appl. Pyrol.,110, 239–247*

[25] Moldoveanu C.S, Analytical pyrolysis of natural organic polymers (1998). Elsevier

[26] Kebelmann K., Hornung A., Karsten U.,Griffiths G., (2013), Intermediate pyrolysis and product identification by TGA and Py-GC-MS of green microalgae and their extracted protein and lipid components, *Biomass Bioenerg., 49, 38-48*

[27] Biller P. and Ross A.B., (2014), Pyrolysis GC-MS as a novel analysis technique to determine the biochemical composition of microalgae, *Algal Res., 6-A, 91-97*

[28] Wang K., Brown R.C., Homsy S., Martinez L., Sidhu S.S., (2013), Fast pyrolysis of microalgae remnants in a fluidized bed reactor for bio-oil and biochar production, *Biores. Technol, 127, 494-499.*

[29] Borja R., MartìnA., Rincòn B., Raposo F., (2003). Kinetics fro substrate utilization and methane production during mesophilic anaerobic digestion of two phases olive pomace (TPOP). *J. Agric. Food Chem., 51, 3390-3395*

[30] Brunetti G., Plaza C., Senesi N., (2005). Olive pomace amendment in mediterranean conditions: effect on soil and humic acid properties and wheat (*Triticum turgidum L.*) yield. *J. Agric Food Chem., 53, 6730-6737*

[31] Canet R., Pomares F., Cabot B., Chaves C., Ferrer E., Ribò M., Albiach M.R.. (2008). Composting olive mill pomace and other residues from rural southeastern Spain. Waste Manag., 28, 2585-2592.

[32] Knicker H., Hilscher A., Gonzalez-Vila F.J., Almendros G., (2008), A new conceptual model for structural properties of char produced during vegetation fires, *Org. Geochem., 39, 935-939*

Chapter 6

Conclusions

In this dissertation, pyrolysis of lignocellulosic and protein-rich biomass was investigated focusing on chemical characterization both of bio-oil and biochar.

This thesis was focused on the use of analytical techniques such as Py-GC-MS and solid phase microextraction (SPME) as methods to gather information on the pyrolysis process and on the thermal behavior of biomass at a molecular level.

Concerning bio-oil, catalytic cracking was studied on analytical scale by Py-GC-MS.

Then, catalytic pyrolysis experiments have been carried out with a bench scale pyrolysis reactor in order to compare analytical and lab scale results.

Py-GC-MS was applied as screening method to study the effect of different catalysts and biomass-catalyst weight ratio on aromatic hydrocarbons production.

As catalyst, zeolite HZSM-5 and Ti- or Sn-containing MCM 41 mesoporous materials have been tested using different biomass-catalyst ratios (1:5, 1:10, 1:20).

The preliminary study was conducted on microalgae *Desmodesmus communis*, selected because of its resistance and growth rate.

The obtained results demonstrated that Py-GC-MS enable the selection of pyrolysis conditions. Zeolite confirmed to be the catalyst with the best performance in terms of hydrocarbon production. In addition, the chemical composition observed by Py-GC-MS significantly reflects that obtained on larger scale.

However, some difference has been found. Indeed, formation of high molecular weight PAHs (3-4 aromatic rings) have been observed only on bench scale.

High molecular weight PAHs can be due to secondary reaction occurred during the condensation step or reaction on the catalyst surface.

In addition, nitrogen-containing compounds and oxygenated compounds exhibited some difference related to condensation step have been observed. Indeed, lower amount of N-compounds was observed in bio-oil with respect to Py-GC-MS and it was attributed to the preferential distribution of N- and O- compounds into the aqueous fraction.

Furthermore, amount of nitrogen-containing compounds detected by Py-GC-MS increase when increasing protein percentage in biomass increase.

Moreover, comparing different protein-rich biomass (seaweed, fish and microalgae) with respect to lignocellulosic feedstock (pine sawdust) no significant difference in terms of aromatic hydrocarbons among the different feedstock was observed.

Py-GC-MS was applied to the chemical characterization of biochars. Structural investigation on biochars obtained under different pyrolysis conditions (i.e.: different temperatures and residence time) and on biochars from different feedstock was carried out.

Py-GC-MS can provide molecular indices by quantitative analysis of pyrolysis products useful to gather information on biochar thermal stability.

Selected pyrolysis product ratios were strongly correlated with H/C molar ratio suggesting their reliability to predicting the biochar carbonization degree.

Instead, most of those molecular ratios (i.e.: toluene/naphthalene, toluene/benzene) are not useful predictors of thermal behavior when applied onto biochar from different feedstock because of the manifold origin of some pyrolysis products. However, methylnaphthalene/naphthalene ratio was less influenced by the feedstock source and it showed good similarity with H/C. The molecular pattern resulting from Py-GC-MS could be utilized to infer information on the nature of the initial substrate and differentiate biochars with the same H/C.

Further analytical technique based on solid phase microextraction method (SPME) for chemical characterization of bio-oil was investigated.

As previously explained, bio-oil chemical characterization is quite complex because implies use of an appropriate solvent depending on polarity of bio-oil constituents. In addition, after pyrolysis two different liquid fractions are obtained with resulting distribution of pyrolysis products in two different fractions. Moreover, often some problems during condensation step can be found (e.g.: difficult to catching highly volatile compounds) with a subsequent loss of qualitative and quantitative information.

Therefore, SPME as at-line monitoring technique during the process capable of hot gas phase analysis was proposed to this purpose.

The obtained results, conducted on eight different feedstock, showed a strong similarity both in terms of qualitative and semiquantitative aspects between GC-MS analysis of hot vapours and bio-oil from condensation traps. Furthermore, the storage feasibility of SPME fiber till 96 hours before GC-MS analysis without significant loss of information was demonstrated.

This could allow SPME usage for hot vapours monitoring in small scale pyrolysis plant to predict bio-oil composition or in gasification plant for tars contamination in the syngas produces in gasification plants.

Acknowledgements

Research was partially supported by the Italian Ministry of Economic Development of the program agreement MiSE-CNR ‘‘Ricerca di Sistema Elettrico” and by the Interdepartmental Center for Industrial Research-Energy and Environment (C.I.R.I.-EA) of University of Bologna with the cooperation of Emilia Romagna High Technology Network within CIPE funding and by the collaboration agreement between University of Bologna and Fraunhofer UMSICHT.

I would like to thanks all the professors and colleagues who contributed to the work presented in this thesis:
Prof. Rossella Pistocchi, Dr. Giulia Samorì, Dr. Laura Pezzolesi and Dr. Franca Guerrini from ALGOLAB (CIRSA, University of Bologna) for providing the algae samples, Prof. Jale Yanik from Ege University (Izmir, Turkey) and Chiara Lorenzetti for their contribution in the experimental part of catalytic pyrolysis described into the paragraph *3.2*, Dr. Cristian Torri for helping me with SPME experiments and for all precious suggestions gave me during my studies, Dr. Alessandro Girolamo Rombolà for PAHs analysis on biochars, Prof. Ivano Vassura and Laura Ferroni for providing TGA analysis on biochar samples
I would like to acknowledge all the people who supported me during my PhD: thanks to Beatrice, Chiara, Danilo, Michele, and Alisar.
A special thanks to “*Mom&Dad Research Funding*” granted in the first year.
Last but not least, I would like to express all my gratitude to my supervisor Prof. Daniele Fabbri for giving me scientific and humane support for a period much more longer than PhD.